

**THE ROLE OF ADENOSINE IN REGULATING URINARY BLADDER
FUNCTION AND A₁AR-MEDIATED MEMBRANE TRAFFICKING IN UMBRELLA
CELLS**

by

Herman Sandeep Prakasam

B.Sc Zoology, Loyola College, Chennai, 2006

M.Sc Molecular Biology, University of Madras, Chennai, 2008

Submitted to the Graduate Faculty of
The School of Medicine in partial fulfillment
of the requirements for the degree of
Doctor of Philosophy

University of Pittsburgh

2013

UNIVERSITY OF PITTSBURGH

SCHOOL OF MEDICINE

This dissertation was presented

by

Herman Sandeep Prakasam

It was defended on

October 4th, 2013

and approved by

Dr. Jeffrey Hildebrand, PhD., Associate Professor, Department of Biological Sciences

Dr. Edwin K. Jackson, Professor, PhD., Department of Pharmacology and Chemical Biology

Dr. Ora Weisz, PhD., Professor, Department of Medicine

Dr. Susan Amara, PhD., Professor, Department of Neurobiology

Dissertation Advisor: Dr. Gerard Apodaca, PhD., Professor, Department of Medicine

Copyright © by Herman Sandeep Prakasam

2013

**THE ROLE OF ADENOSINE IN REGULATING URINARY BLADDER
FUNCTION AND A₁AR-MEDIATED MEMBRANE TRAFFICKING IN UMBRELLA
CELLS**

Herman Sandeep Prakasam, PhD

University of Pittsburgh, 2013

ABSTRACT

The uroepithelium lines the urinary bladder, urethra and the lower renal pelvis. It provides a tight blood-urine barrier that prevents the unregulated movement of solutes, ions and metabolites present in the urine. Apart from forming a robust barrier, a growing body of evidence supports the role of the uroepithelium as a sensory transducer that is sensitive to extracellular biochemical and mechanical stimuli. One of the mediators that is released from the uroepithelium and impacts bladder activity is adenosine. Adenosine is a well-known stress relieving hormone in other organ systems and the bladder lumen is a region of constant stress due to cyclical filling and voiding of urine, therefore I hypothesized that *adenosine has an impact on urinary bladder function under stress*. First I assessed the mechanism of adenosine turnover and how luminal adenosine affects bladder function. I report that adenosine is released from the mucosal and serosal surfaces of the uroepithelium when the tissue is maximally stretched. The released adenosine is actively turned over by distinct pathways at either surfaces of the uroepithelium. Further, enriching the luminal adenosine concentration by blocking its routes of turnover or by specific activation of apically localized A₁AR by using CCPA, bladder function was modulated by decreasing the threshold pressure of bladder voiding. In the second study, I looked at the impact of adenosine on exocytosis and membrane trafficking in umbrella cells. I report that activation of A₁AR at the

apical surface of umbrella cells increased apical exocytosis in umbrella cells. The apical exocytosis was similar to late phase stress-mediated exocytosis and required transactivation of EGFR. The pathway involved G_i - $G_{\beta\gamma}$ -PLC-PKC and ADAM17 which in-turn cleaved and released HB-EGF leading to EGFR transactivation and downstream ERK1/2 MAPK. Further, Ser811 in the cytoplasmic tail of ADAM17 was important for A_1AR -mediated activation of the protein. Finally, ADAM17 was also involved in late-phase stretch-mediated apical exocytosis in rats but not in rabbits. In conclusion, my studies show that adenosine plays a protective role in the bladder both at the organ and cellular level. At the organ level, adenosine alleviates luminal stress by reducing the threshold pressure for voiding and at the cellular level, it triggers apical exocytosis and increase in membrane surface area of umbrella cells thus mitigating the stress induced by mechanical stretching associated with bladder filling.

TABLE OF CONTENTS

ABSTRACT.....	II
PREFACE.....	XV
1.0 INTRODUCTION.....	1
1.1 OVERVIEW OF THE UROEPITHELIUM.....	1
1.1.1 The uroepithelium	1
1.1.2 The Ussing stretch chamber apparatus	5
1.1.3 Determining tissue capacitance	8
1.1.4 Note on using C_T to determine the apical membrane surface area of umbrella cells.....	10
1.1.5 Apical membrane trafficking in umbrella cells	13
1.1.6 Stretch-mediated apical exocytosis	13
1.1.6.1 Stretch-mediated exocytosis is biphasic	13
1.1.6.2 Regulation of stretch-mediated exocytosis.....	17
1.1.7 Endocytosis.....	19
1.1.8 Exocytosis in the absence of stretch	20
1.2 THE UROEPITHELIAL SENSORY WEB.....	21
1.2.1 Introduction	21
1.2.2 The neural circuitry of the urinary bladder:	21

1.2.3	Receptors and ion channels expressed on the apical and basolateral surfaces of the umbrella cells:	25
1.2.4	Release of hormones, neurotransmitters and signaling molecules from the uroepithelium:	26
1.2.5	Conclusion	28
1.3	ADENOSINE RECEPTORS	28
1.3.1	Introduction	28
1.3.2	Extracellular adenosine.....	29
1.3.3	A brief overview of G-protein coupled receptors (GPCRs).....	31
1.3.4	Types of adenosine receptors.....	32
1.3.5	A ₁ adenosine receptors (A ₁ AR)	33
1.3.6	A ₂ and A ₃ adenosine receptors (A ₂ AR and A ₃ AR)	35
1.3.7	Positive and negative impact of adenosine signaling.....	38
1.3.8	Role of adenosine in membrane trafficking and EGFR transactivation..	39
1.4	GPCR-MEDIATED EGFR TRANSACTIVATION	40
1.4.1	Introduction	40
1.4.2	EGFR	41
1.4.3	Transactivation	42
1.5	A DISINTEGRIN AND A METALLOPROTEINASE (ADAM)	45
1.5.1	Introduction	45
1.5.2	Subcellular localization, domain architecture and functional regulation of ADAMs.....	45
1.5.3	ADAM17.....	46

1.5.4	Molecular structure and regulation of ADAM17 activity	49
1.5.5	Regulation of ADAM17 activity	50
1.5.6	Role of ADAM17 in EGFR transactivation	53
1.6	EGFR TRANSACTIVATION IN MEMBRANE TRAFFICKING.....	55
1.6.1	Overview of the physiological importance of EGFR transactivation	55
1.6.2	EGFR transactivation in secretion and membrane trafficking.....	55
1.7	GOALS OF THIS DISSERTATION	57
1.7.1	Broad focus of this dissertation	57
1.7.2	Goal 1: To study the mechanism behind adenosine release and turnover in the bladder and understand the physiological relevance of the same	57
1.7.3	Goal 2: To understand how activation of apically localized A ₁ AR triggered apical exocytosis in umbrella cells	58
1.7.4	Summary	59
2.0	MODULATION OF BLADDER FUNCTION BY LUMINAL ADENOSINE TURNOVER AND A ₁ RECEPTOR ACTIVATION	60
2.1	ABSTRACT.....	60
2.2	INTRODUCTION	61
2.3	RESULTS.....	67
2.3.1	Distinct pathways for adenosine biogenesis are found at the mucosal and serosal surfaces of the rabbit uroepithelium	67
2.3.2	Adenosine release from the mucosal surface of filled rat bladders is sensitive to inhibitors of adenosine deaminase and concentrative nucleoside transporters	74

2.3.3	Stimulation of luminal A ₁ receptors decreases the threshold pressure of bladders during cystometry	75
2.3.4	Blocking pathways for adenosine turnover reveals an adenosine and A ₁ receptor-like response.....	79
2.3.5	A ₁ receptor activation stimulates bladder activity in bladders with cyclophosphamide-induced cystitis	82
2.4	DISCUSSION.....	85
2.4.1	Distinct mechanisms of adenosine turnover at either surface of the uroepithelium	85
2.4.2	Luminal adenosine, acting through A ₁ receptors, modulates threshold pressure	92
2.4.3	Adenosine as a stimulatory factor in bladder function.....	93
3.0	ADENOSINE PROMOTES UMBRELLA CELL EXOCYTOSIS VIA A PROTEIN-KINASE C-STIMULATED, ADAM17-MEDIATED, EGF RECEPTOR TRANSACTIVATION PATHWAY	96
3.1	ABSTRACT.....	96
3.2	INTRODUCTION	97
3.3	RESULTS.....	100
3.3.1	A ₁ AR-stimulated apical exocytosis occurs through transactivation of the EGFR	100
3.3.2	ADAM17 is localized to the apical surface of umbrella cells where it stimulates CCPA-induced EGFR transactivation and exocytosis	108

3.3.3	ADAM17 is also critical for stretch-mediated apical exocytosis in rat, but not rabbit uroepithelium	112
3.3.4	G_i , phospholipase C, and PKC act upstream of ADAM17 to promote A_1AR -mediated EGFR transactivation.....	116
3.4	DISCUSSION.....	123
3.4.1	Adenosine, like stretch, stimulates apical exocytosis via EGFR transactivation	124
3.4.2	ADAM17 mediates adenosine-dependent EGFR transactivation.....	125
3.4.3	A $G_i \rightarrow G_{\beta\gamma} \rightarrow PLC \rightarrow DAG \rightarrow PKC$ pathway promotes ADAM17 activation 126	
4.0	CONCLUSION.....	132
4.1	INTRODUCTION	132
4.2	SUMMARY OF RESULTS	133
4.2.1	Impact of adenosine on bladder function	133
4.2.2	The network of signals that coordinate umbrella cell function.....	134
4.2.3	Conclusion of my studies.....	135
4.3	FUTURE DIRECTIONS.....	136
4.4	CLOSING COMMENTS.....	141
5.0	MATERIALS AND METHODS	142
5.1	CHAPTER 2 MATERIALS AND METHODS	142
5.1.1	Reagents.....	142
5.1.2	Animals	143
5.1.3	Mounting the uroepithelium in Ussing stretch chambers.....	143

5.1.4	Measurement of adenosine, AMP, and inosine.....	144
5.1.5	Cystometry analysis.....	145
5.1.6	Cyclophosphamide treatment.....	147
5.1.7	Immunofluorescence labeling and image acquisition.....	147
5.1.8	Western blot analysis.....	148
5.1.9	Statistical analysis.....	148
5.2	CHAPTER 3 MATERIALS AND METHODS	149
5.2.1	Reagents and antibodies.....	149
5.2.2	Animals	150
5.2.3	Cell Culture	150
5.2.4	Immunofluorescence labeling and image acquisition.....	151
5.2.5	Mounting rabbit uroepithelium or rat bladders in Ussing stretch chambers	152
5.2.6	Western blot analysis.....	153
5.2.7	Reverse transcriptase PCR.....	154
5.2.8	Generation of adenoviruses encoding ADAM17 shRNA	155
5.2.9	In situ adenoviral transduction and detection of human growth hormone (hGH) release.....	157
5.2.10	WGA-FITC labeling experiment	158
5.2.11	Generation of shRNA resistant-ADAM17 and S811A and S811D point mutants.....	158
5.2.12	Statistical analysis.....	159
5.3	ADDITIONAL MATERIALS AND METHODS	159

5.3.1	Generation of lentiviral vectors encoding A ₁ AR shRNA	159
5.3.2	DNA and plasmids	160
5.3.3	Procedure	160
5.3.3.1	Lentiviral infection in HEK293 cells	160
5.3.3.2	Lentiviral infection in rats.....	161
5.3.4	Western blot	161
APPENDIX A		162
APPENDIX B		164
APPENDIX C		166
BIBLIOGRAPHY		168

LIST OF FIGURES

Figure 1 The urinary bladder mucosa	2
Figure 2 The Ussing chamber apparatus.....	7
Figure 3 Equivalent circuit of the epithelial cells	12
Figure 4 Early and late phase exocytosis	16
Figure 5 The neural circuitry of the urinary bladder.....	24
Figure 6 The sensory web of the umbrella cell.....	27
Figure 7 Extracellular adenosine synthesis and turnover	30
Figure 8 EGFR transactivation	44
Figure 9 ADAM17 domain architecture	48
Figure 10 Adenosine turnover at the mucosal surface of the uroepithelium	64
Figure 11 Adenosine turnover at the serosal surface of the uroepithelium	68
Figure 12 Effect of EHNA, NBTI, or IDT on adenosine release in the rat bladder	72
Figure 13 Adenosine does not alter bladder function	76
Figure 14 Activation of apical A1 receptors with CCPA lowers the threshold pressure for voiding	80
Figure 15 Inhibitors of adenosine turnover lower the threshold pressure for voiding.....	83
Figure 16 Cyclophosphamide treatment induces urinary bladder cystitis	86

Figure 17 CCPA exacerbates the hyperactive bladder phenotype.....	90
Figure 18 Activation of A ₁ AR triggers apical exocytosis in umbrella cells	102
Figure 19 A ₁ ar-mediated apical exocytosis occurs through transactivation of EGFR.....	105
Figure 20 ADAM17 is localized to the apical surface of Umbrella cells	109
Figure 21 In situ knockdown of ADAM17 impairs A ₁ ar- and stretch-mediated apical exocytosis:	113
Figure 22 PKC mediates A ₁ ar-induced ADAM17 activation	118
Figure 23 Ser811 in the c-tail of ADAM17 is required for A ₁ AR-mediated apical exocytosis .	120
Figure 24 Schematic of A ₁ AR-mediated EGFR transactivation.....	130
Figure 25 A ₁ AR knockdown using lentiviral vectors	163

PREFACE

I am grateful to a number of people for their guidance, support and friendship through the course of my PhD. First and foremost, I would like to thank Dr. Gerry Apodaca for being a great mentor and friend. I thank him for not only guiding me through my thesis but for also making a scientist out of me. His passion for science has always inspired me to keep going forward and continue exploring. The skills and values that I have acquired under his mentorship are priceless and I am deeply indebted to him for that. I would like to thank my committee members Dr. Jeff Hildebrand, Dr. Ora Weisz, Dr. Ed Jackson and Dr. Susan Amara. Their valuable advice and critical analysis of my research has helped me greatly in shaping my thesis. I would also like to thank each one of them individually for taking time from their busy schedules to guide me and give their expert advice during committee meetings and whenever I wanted to meet them.

I would like to thank the members of my lab who have been my family for the past five years. I thank Luciana for her guidance and advice on experimental design and trouble shooting. I also thank her for being a constant source of cheerfulness and laughter. I thank Gio for his help and his wise advice on matters pertaining to research and life in general. I thank Dennis for his help with my experiments and for teaching me art and graphic design. I enjoyed learning from him and I gained valuable skills in making effective presentations and creative scientific drawings. I thank Shalini for being a great friend and moral support. I would like to thank the

previous members of the lab, especially Dr. Puneet Khandelwal and Dr. Heather Herrington for their scientific guidance, help and friendship.

I would like to thank the members of the Renal Electrolyte Division at the University of Pittsburgh for their help and guidance. Especially, I would like to thank Dr. Marcelo Carattino for guiding me in my work and providing critical feedback. I also thank him for involving me in his projects and widening my knowledge and skill base. I would like to thank the members of the Weisz lab for their help and scientific input.

I thank Ms. Vasumathi Sundaram my high school biology teacher, Dr. G. Jayaraman who introduced me to molecular biology and made me realize my love for the subject and Dr. Madhulika Dixit who mentored me during my Master's thesis. They inspired me to pursue scientific research as a career option and motivated me to do a PhD.

I thank all my friends for always being there for me. They helped during times of adversity, they made me part of their family and they made sure I succeeded in my PhD. I am forever indebted to them. Though there are many, I would like to especially thank Ms. Anjana Shanmugavel, Ms. Chitra Gautam, Dr. Reety Arora and Mr. Samrat Sarovar. They have been a great source of moral support and strength. I wish them all the best in their lives.

I thank the PIMB program. They gave me the opportunity of a lifetime and if not for the program I doubt if I would have ever done a PhD. I thank all my friends and fellow PIMBers for being such great people and for making me feel at home. I would like to thank the PIMB faculty members for their expert advice and guidance. The five years I have spent in the program and the people I have interacted with have influenced me as a scientist and as a person in a very positive way. I would also like to thank Ms. Jen Walker and Ms. Susanna Godwin for making sure my paperwork and official documents are in order.

I would like to thank my parents Dr. Vinod Prakasam and Ms. Anita Vinod for their prayers and constant support. The hardships that they went through to bring me to where I am today will always be a driving force for me to go forward in life. I would like to thank my sister Ms. Therese Deepika for being supportive and understanding. Her creative skills inspire me and I am forever proud of her.

I would like to thank my family in the United States for taking care of me and making sure I never felt homesick. I thank them for being a great source of moral support and strength. They have high aspirations for me and I promise to always strive to meet their expectations. Finally, all this would not have been possible without the grace of the almighty. I will continue to walk in the path that he has paved for me.

1.0 INTRODUCTION

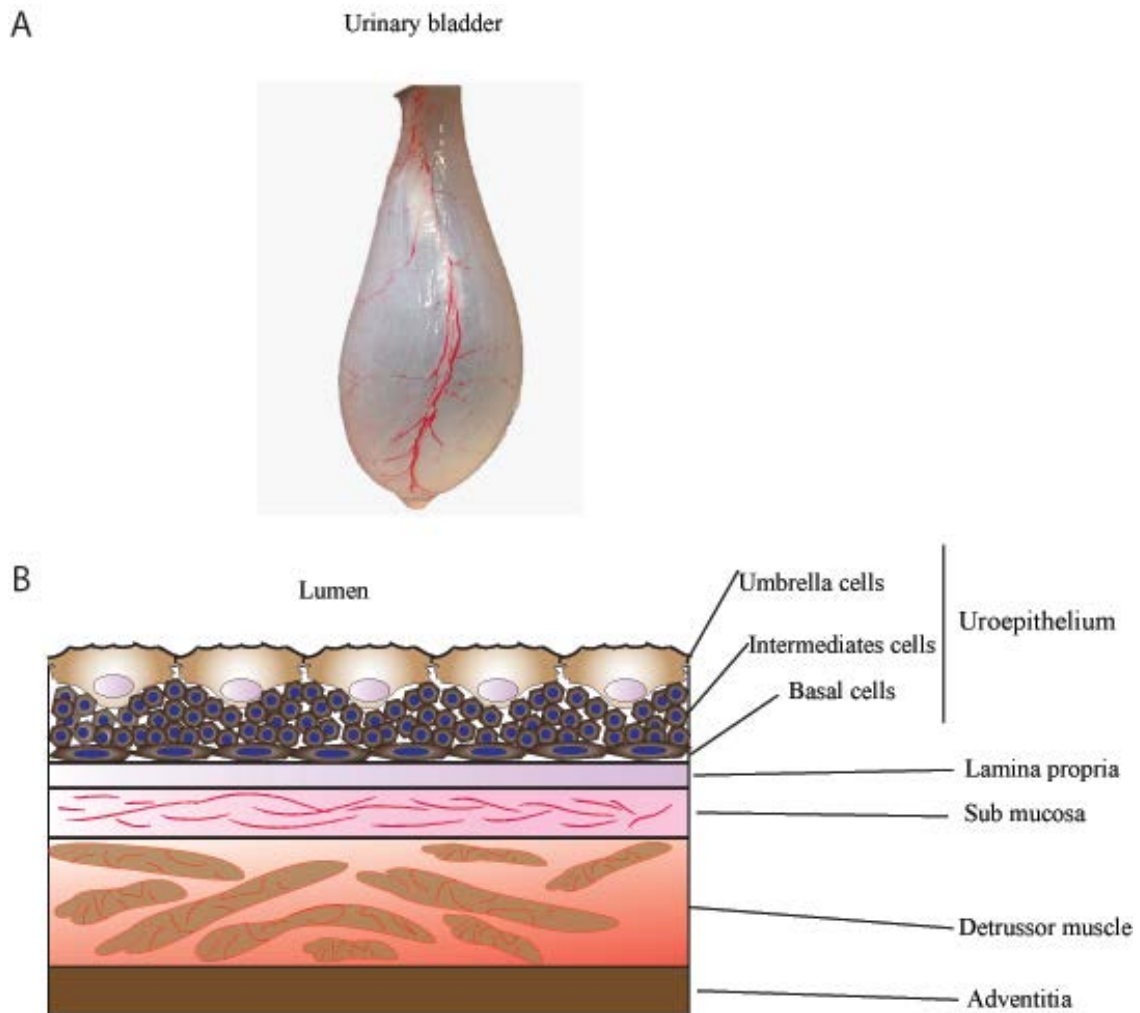
1.1 OVERVIEW OF THE UROEPITHELIUM

1.1.1 The uroepithelium

The uroepithelium is the epithelial lining of the urinary bladder, urethra and the renal pelvis. It is a stratified tissue that consists of the outermost umbrella cells, followed by 1-5 layers of intermediate cells and finally a single layer of basal cells (Figure 1) (1). The umbrella cells are polarized epithelial cells with distinct apical and basolateral surfaces. The apical surface directly interfaces with urine in the bladder lumen while the basolateral surface faces the intermediate cells.

The primary functions of the uroepithelium are to provide a robust blood-urine barrier that prevents the leakage of urine into the underlying tissue and regulates the movement of water, ions and solutes across the mucosal surface (1-3). The outer umbrella cells are highly specialized to perform these tasks. Some of the key features of the umbrella cells are their specialized apical surface, high transepithelial resistance and the presence of numerous discoidal-and fusiform-shaped vesicles (DFVs) beneath their apical surface

Figure 1 The urinary bladder mucosa



A., an image of a rabbit bladder that has been filled with buffer and held by the neck is depicted.

B. The multiple layers of the bladder mucosa are presented. The uroepithelium consists of the outer umbrella cells, the intermediate cells and the basal cells. Beneath the uroepithelium is the lamina propria which is followed by the submucosa. The Submucosa is followed by the three layers of smooth muscles called detrusors. Finally, the organ is enveloped by the adventitia layer.

Specialized apical surface of the umbrella cells

The most immediately identifiable feature of the umbrella cells when examined under the microscope is the scalloped nature of the apical surface, characterized by plaques and intervening hinge regions (1,4,5). Closer observation of the ultrastructure of the plaque regions under scanning and transmission electron microscopes reveals that the outer plasma membrane leaflet is thicker than the inner leaflet, and forms what is known as the asymmetric unit membrane (AUM) (5-7). The AUM consists of crystalline arrays of particles, each of which is made up of 6 proteins arranged in two tiers of three each. These proteins belong to the family of membrane-bound proteins called uropodins (UP), namely UPIa, UPIb, UPII, UPIIIa and UPIIIb (6-8). The UPs form the most abundant protein population of the apical surface of umbrella cells as the plaques cover almost 70-90% of the apical surface (9,10). The plaques contribute to the permeability barrier of the apical surface of umbrella cells. UPIIIa^{-/-} mice have greatly diminished plaque assemblies at the apical surface and have significantly higher permeability to water and urea across the umbrella cells (3,11).

The apical surface is also highly detergent resistant. This is due to the unusual lipid composition of the apical surface, which is rich in cholesterol, phosphatidylcholine, phosphatidylethanolamine and cerebroside (9). Curiously, the lipid composition is similar to the composition of lipids in the myelin sheaths that envelope nerve fibers (9,12). The AUMs and the lipid composition of the apical surface together maintain a tight permeability barrier that regulates the exchange of water and solutes across the apical surface.

High transepithelial resistance

The second feature of the umbrella cells are their exceptionally high transepithelial resistance. The umbrella cells are fused at the outer margin by a ring of high-resistance tight

junctions. The tight junctions regulate the flux of water, ions and solutes across the paracellular space. They are formed by the close positioning of anastomosing filamentous strands of plasma membrane from neighboring cells. The junctional complex in umbrella cells is made up of zona occludin-1, occludin, and claudins 4, 8, and 12 (13). The specialized apical membrane and the tight junction together contribute to the exceptionally high-resistance barrier formed by the umbrella cells (transepithelial resistance ranging from 20000-75000 Ωcm^2) (14,15). In addition, the apical surface of the umbrella cells is covered by a thick layer of heparin proteoglycans and mucin (16,17). This might provide additional protection by separating the urine from the underlying tissues.

DFVs

The third feature of these cells is the presence of numerous DFVs beneath the apical surface (18). The presence of the DFVs give the umbrella cells the ability to regulate the components and area of their apical surface without compromising on their barrier function (9,18). The plaques (described above) form the major component of the DFVs. The DFVs play a critical role in the dynamic maintenance of the apical surface. They are inserted into the apical surface and removed to modulate the apical surface area.

While UPs form the major constituent of the DFVs, they are also the carriers of receptors, ion channels, and other surface proteins that populate the apical surface of the umbrella cells. Although not the focus of this dissertation, the identification of the other components of the DFVs would greatly enhance our knowledge of their function and regulation. In this study, I have used the expression of UPIIIa a marker for vesicles that populate the apical pole of umbrella cells.

In summary the specialized apical surface, the tight junctions and the DFV allow the umbrella cells to form the tight barrier that can accommodate large changes in the urine volume. However, the traditional view that the bladder is a passive sac that retains urine until voided does not hold true anymore. The uroepithelium is dynamically involved in regulating bladder function. The first line of evidence in support of this is: when the bladder fills with urine and the bladder mucosa unfurls to accommodate the increasing urine volume, the apical surface of the umbrella cells also unfurls, and intriguingly, increases the apical surface area by exocytosis of DFVs. Fresh membrane is inserted into the apical surface, and this contributes to the increase in luminal volume. When the bladder voids, the reverse occurs, the apical membrane is recaptured via endocytosis thus resulting in decrease in apical surface area.

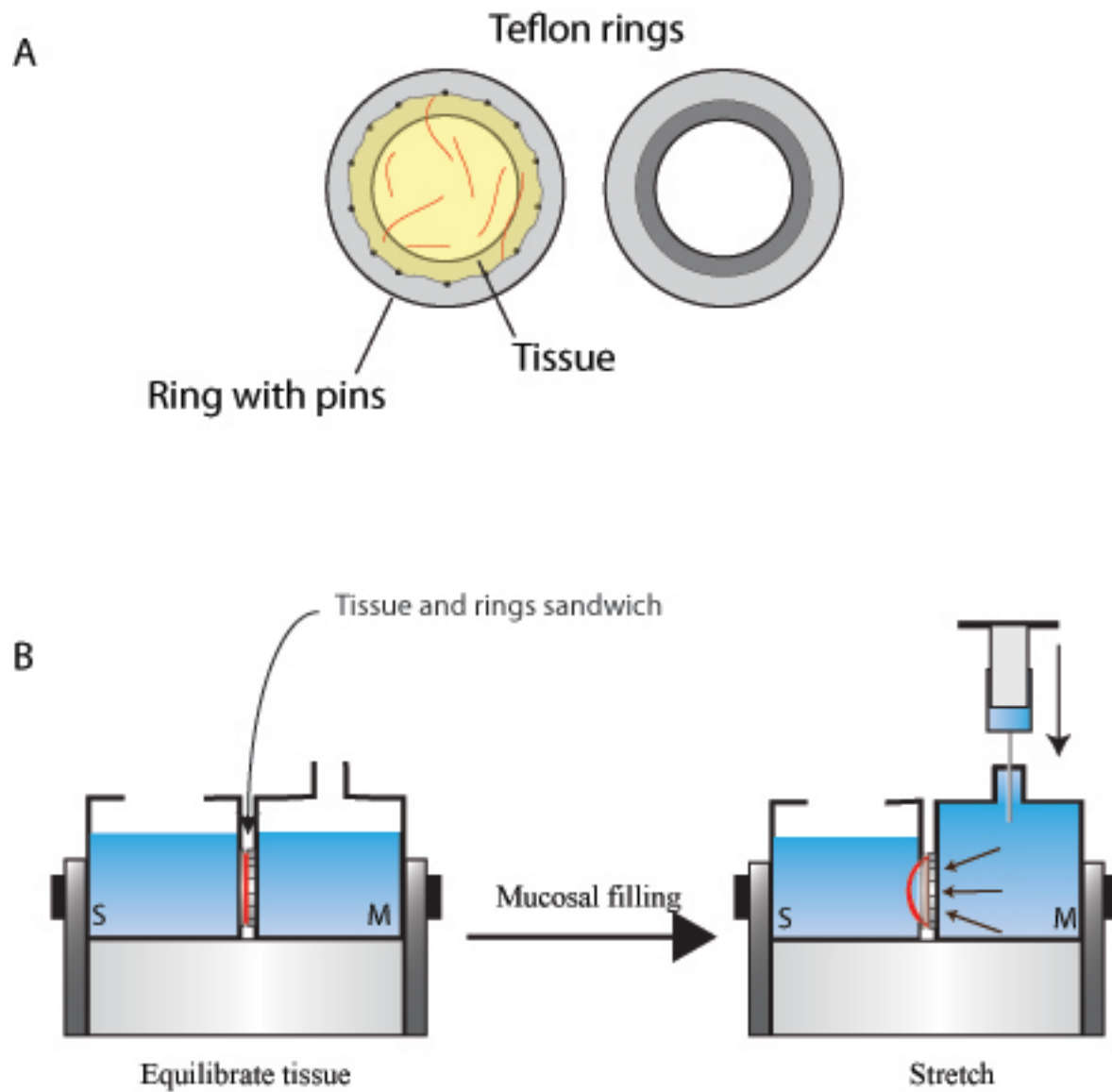
The dynamics of apical exocytosis and endocytosis has been studied in cell culture (19,20), *in situ* (21-23), and in isolated tissue using Ussing chambers (22,24-29). Many of the experiments that I performed in this dissertation were done on isolated rabbit uroepithelium or rat bladders that were mounted on Ussing stretch chamber apparatus. Therefore before introducing the apical membrane trafficking events in umbrella cells, a brief description of the apparatus and the electrophysiological technique used to determine apical membrane surface area is warranted.

1.1.2 The Ussing stretch chamber apparatus

The Ussing stretch chamber is a convenient way to study membrane trafficking events or release of mediators into the bladder lumen in isolated uroepithelial tissues. The apparatus consists of a serosal and mucosal hemichamber and a pair of Teflon rings that are sandwiched between the two chambers (28). One of the Teflon rings has stainless steel pins on its outer edge that holds

the tissue. Isolated uroepithelial tissue is held between the pins of the Teflon ring and is mated with the other ring. This sandwich is inserted between the mucosal and serosal hemichambers and clamped in position on a base with the help of adjustable screws. The chambers are filled with warm Krebs buffer simultaneously until the tissue is completely bathed in the buffer. The mucosal and serosal hemichambers allows the uroepithelium to be treated with specific agonist, drugs or other compounds on either of the surfaces. In addition, bladder filling can be simulated by filling buffer in the mucosal chamber which results in bowing out of the tissue (Figure 2) (28).

Figure 2 The Ussing chamber apparatus



A, The top views of the Teflon rings are presented with the tissue held between the pins of the ring. B, The serosal and the mucosal hemichamber with the tissue rings in between them is represented. The tissue in B is marked in red. Filling buffer in the mucosal chamber causes bowing out of the tissue. Once the chamber is filled to capacity, additional buffer is added to mechanically stretch and stress the tissue.

1.1.3 Determining tissue capacitance

Changes in exocytosis and endocytosis at the apical surface of umbrella cells can be studied by measuring the apical surface area of the cells (26,30). In my studies, I measured the changes in apical surface area by determining the transepithelial capacitance (C_T) of the apical membrane. Capacitance is the amount of charge stored between two parallel plates separated by a dielectric. The capacitance is represented using the formula:

$$C = \frac{\epsilon A}{d} \frac{1}{4\pi k}$$

Where C is capacitance; ϵ is the dielectric constant; A is area of each plate; d is the distance between the plates; k is a constant ($9.0 \times 10^{11} \text{ cm/F}$) and π has the usual value. The lipid bilayer of the plasma membrane in essence works like a parallel plate capacitor. It has a ϵ value of ~ 5 and a very small distance between the two leaves of the bilayer (3.5-7 nm) (31). Further, from the formula, it is clear that the capacitance of the membrane is directly proportional to surface area of the membrane (28). Epithelial tissue can be described as a simple circuit where the apical and basolateral plasma membrane are modeled as capacitors and resistors in parallel (Figure 3). The resistive pathway is the flow of ions via ion channels and the capacitive component is the ability of the plasma membrane to store charge. Because the tight junctions have no surface area, but conduct paracellular ion transport, they are modeled just as a resistor (R_{TJ}) (32).

Capacitance in series is added inversely. therefore

$$\frac{1}{C_T} = \frac{1}{C_a} + \frac{1}{C_{bl}}$$

Rearranging the formula:

$$C_T = \frac{C_a}{\left(\frac{C_a}{C_{bl}}\right) + 1}$$

Where, C_T is transepithelial capacitance; C_a is apical capacitance; and C_{bl} is basolateral capacitance. In the quiescent state, C_a is much less than the C_{bl} , therefore $C_T \sim C_a$ (25). In the umbrella cells the C_a/C_{bl} ratio is approximately 1:5, therefore the C_T is an underestimation of the C_a by $\sim 20\%$ (33).

To determine C_T a pair of Ag/AgCl electrodes is inserted into the mucosal and serosal hemichambers of the Ussing apparatus and a pulse of square current waveform (I , 0.001A) is applied. The voltage response is recorded and the curve is fitted in the formula:

$$V_T = V_{max} \cdot e^{-1/\tau}$$

Where V_T is the voltage, V_{max} is the maximum voltage, τ is the time constant, which is the length of time it takes for the voltage to reach 63% of the maximum or decay to 37% from the V_{max} . The value of τ is calculated from the formula.

The resistance (R_T) is calculated using Ohm's law:

$$R_T = \frac{V_{max}}{I}$$

From the R_T and τ values, C_T of the membrane is calculated using the formula:

$$C_T = \frac{\tau}{R_T}$$

1.1.4 Note on using C_T to determine the apical membrane surface area of umbrella cells

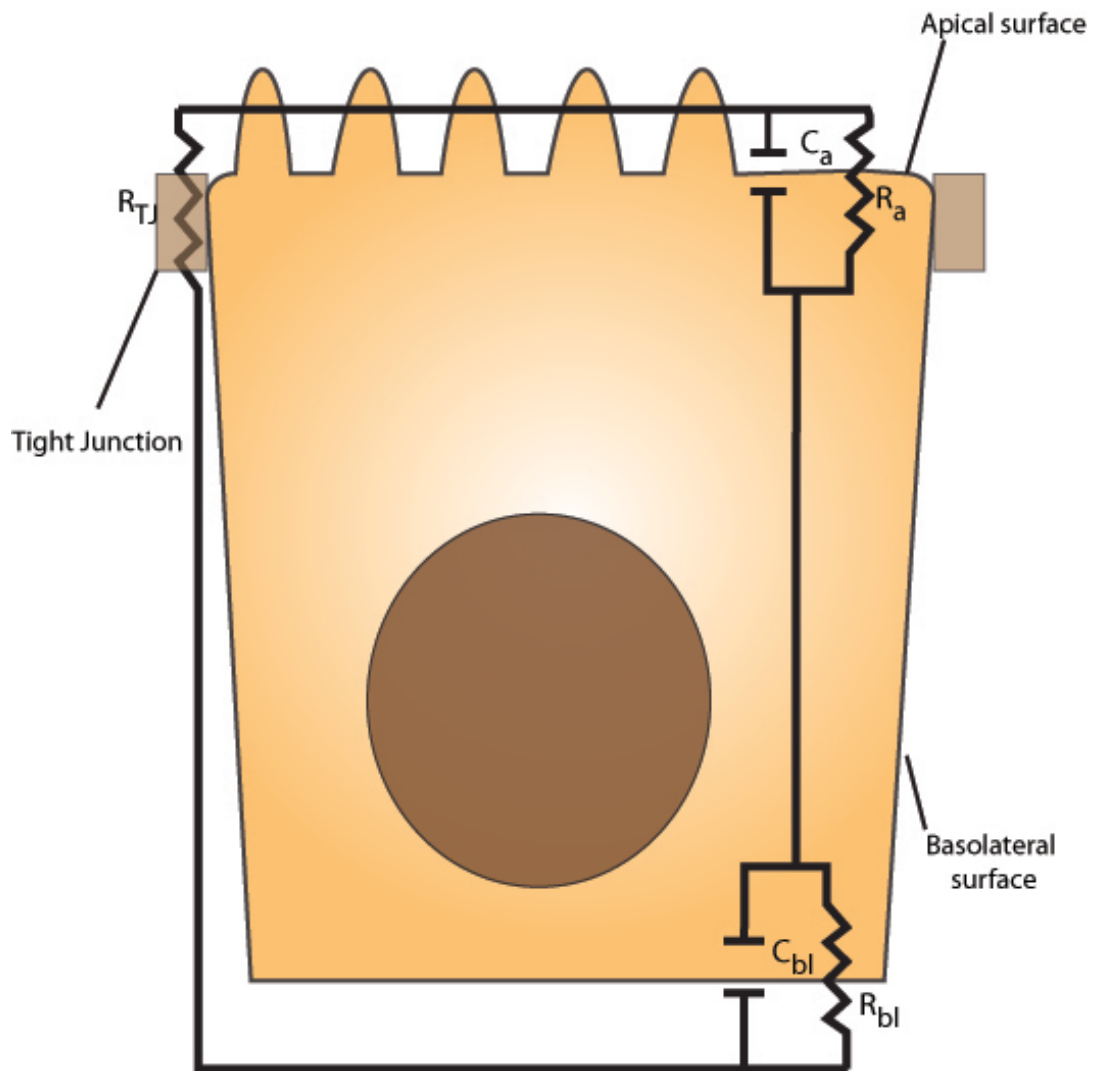
The uroepithelium consists of the outer umbrella cells, the intermediate cells and the basal cells. The C_T is measured by inserting the electrodes on either sides of the uroepithelium. Then the question arises, will the presence of the intermediate and basal cells between the two electrodes interfere with the C_T measurements?

To measure membrane capacitance, the biological membrane in question must be able to separate charge across the membrane. In the uroepithelium, the intermediate and basal cells do not impede the flow of ions or in other words lack resistance and hence cannot separate the charge. Therefore, the R_T of the uroepithelium is essentially the resistance provided by the umbrella cells. This was confirmed by Lewis *et. al.* in experiments where a single electrode was carefully advanced in steps through the rabbit uroepithelium from the mucosal solution to the serosal solution and the fraction of transepithelial voltage was measured at each step. This fraction equals the fraction of transepithelial resistance at each position. This analysis showed that the transepithelial resistance is entirely concentrated at the umbrella cell layer of the uroepithelium and is negligible for the intermediate and basal cells. Furthermore, unlike other epithelia like frog skin, no detectable transverse coupling was observed in the rabbit uroepithelium.

From these two observations, it can be argued that the R_T calculated using the Ussing chamber apparatus is the resistance across the umbrella cell layer. Therefore, the capacitance, which is measured using this R_T value, is a true representation of the capacitance of the umbrella cell layer with no interference from the intermediate or the basal cells (14,15,34). This model of resistance-dependent measurement of C_T is suited for tight epithelia such as the uroepithelium. The capacitance signal is lost when the umbrella cells are permeabilized, thus allowing

unimpeded flow of ions. Other more complex cellular circuit models to calculate membrane capacitance are available for epithelia with low impedance such as the epithelial lining of the gut and gall bladder (35-37).

Figure 3 Equivalent circuit of the epithelial cells



A polarized epithelial cell with the apical and basolateral surfaces and the tight junction is presented. Superimposed on this cell is an equivalent electrical circuit showing the junctional resistor (R_{TJ}), the apical resistor (R_a) and capacitor (C_a) and the basolateral resistor (R_{bl}) and capacitor (C_{bl}).

1.1.5 Apical membrane trafficking in umbrella cells

The bladder is capable of modulating its surface area to accommodate a wide range of urine volumes. This is accomplished by membrane trafficking events that occur at the apical surface of the umbrella cells. These membrane trafficking events ensure that the integrity of the uroepithelium is maintained as the mucosa is subjected to mechanical stress as the bladder fills and voids. In addition, the exocytosis and endocytosis also ensures the turnover of UPs, receptors, ion channels and lipids that are expressed at the apical surface of the umbrella cells.

1.1.6 Stretch-mediated apical exocytosis

The idea that the mechanically stretching the uroepithelium triggers apical exocytosis was first suggested two sets of evidence: First, stereological analysis of electron micrographs revealed that the umbrella cells from full bladders had fewer DFVs in their cytoplasm than contracted bladders (38); and second, C_T measurements showed that mechanical stretching or osmotic stress triggered increased in apical surface area of umbrella cells (26). Numerous studies have since shown that mechanical stretching triggers apical exocytosis of DFVs (25,27,28,39,40).

1.1.6.1 Stretch-mediated exocytosis is biphasic

Studies done so far indicate that stretch-mediated apical exocytosis is a biphasic event comprising of an “early phase” and a “late phase” (Figure 4). The two phases are triggered by distinct signals and are controlled by distinct cellular pathways. Studies performed in Ussing chamber apparatus revealed that the rate of early phase exocytosis was directly proportional to

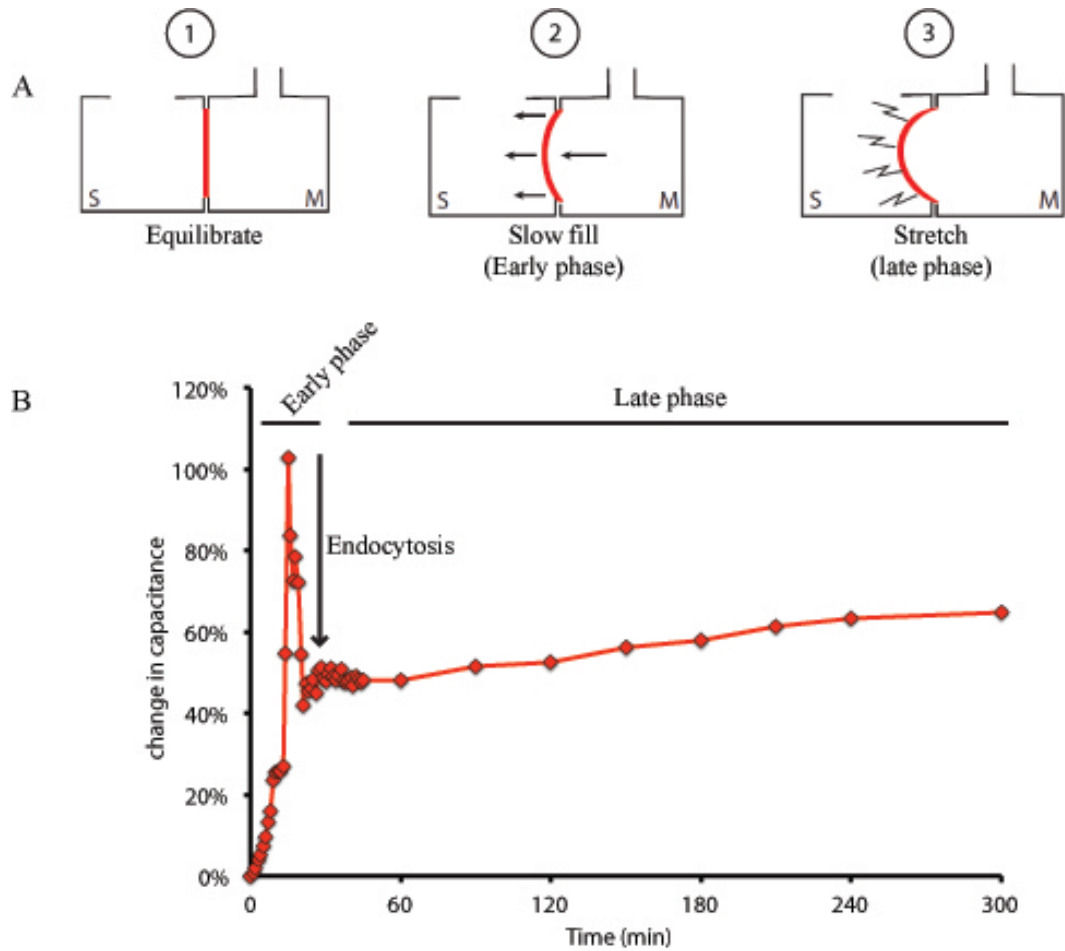
the rate of filling of the mucosal chamber (41). The rate of exocytosis increased if the rate of filling was increased. The exocytic event was triggered by mechanical stretch and was not dependent on changes in luminal pressure. The signal transduction mechanism that triggered this response was independent of protein synthesis, temperature and inhibitors of secretion. Further, the data indicated that a Ca^{2+} wave, likely initiated by opening of mechanosensors such as epithelial sodium channels (ENaC) and non-selective cationic channels (NSCC) was responsible for the exocytosis. The Ca^{2+} -induced intracellular Ca^{2+} wave was released from IP3-dependent stores inside the cell and removal of Ca^{2+} from the buffer inhibited the early phase exocytosis (41).

In experiments that I performed, the early phase response resulted in a large increase in C_T to ~120% of the starting value. The early phase response could reflect the physiological bladder filling where increase in bladder volume causes mechanical stretching of the mucosa and triggers the exocytosis of a pre-existing pool of DFVs to increase the surface area. Following the early-phase exocytosis is a rapid phase of stretch induced endocytosis, where >60% of the exocytosed membrane is recaptured. It is likely to be regulated by the same mechanism that triggers compensatory endocytosis (42). However, further investigation is required to decipher the molecular signals that trigger the endocytic response.

The late-phase response is governed by a very different signal transduction pathway and is independent of NSCC and ENaC. The exocytosis is slow, resulting in the gradual increase in the apical surface area over many hours. Work done by Balestreire et al. indicated that stress induced by stretching the uroepithelium to its maximum capacity triggered late-phase exocytosis (43). The exocytosis was sensitive to metalloproteinase inhibitors, diphtheria toxin (a specific inhibitor of HB-EGF), required the transactivation of EGFR and activation of MAPK signaling.

Significantly, the exocytic response was sensitive to treatment with inhibitors of protein synthesis and secretion. However, the metalloproteinase involved in the pathway was not identified. Further, the identity of the protein(s) that were synthesized downstream of EGFR activation are not known (discussed in the Chapter 4).

Figure 4 Early and late phase exocytosis



A. The three stages of membrane stretching are depicted. 1. The quiescent phase where the tissue is not exposed to mechanical stimuli by stretch. There is no appreciable change in C_T . 2. The tissue is bowed out by filling buffer in the mucosal chamber. This results in the stretch-mediated early phase response. 3. The tissue is subjected to stretch-mediated stress. The mucosal chamber is filled to capacity and then additional buffer is added to stretch the tissue. This triggers the stretch-mediated late phase exocytosis. B. A representative C_T curve clearly showing the early phase response, the endocytosis that follows and the late phase response.

1.1.6.2 Regulation of stretch-mediated exocytosis

The vital cellular components and signaling molecules involved in exocytosis of DFVs include the cytoskeleton, Ca^{2+} signaling, cAMP, and the cellular machinery involved in membrane fusion such as SNAREs (soluble N-ethylmaleimide-sensitive factor attachment protein receptors)

Cytoskeleton

The involvement of the cytoskeleton in membrane trafficking events has been well documented in polarized epithelial cells. Because the cells have a distinct apical and basolateral surfaces, the cytoskeleton plays an important role in the spatial segregation of membrane trafficking complexes and directed membrane fusion. In other secretory cells such as acinar cells, the actin network forms a dense mesh at the apical surface called the terminal web. The secretory granules have to traverse this actin barrier (44). Thus it is suggested as a regulatory component of granular secretion. The umbrella cells have a cortical actin network at the apical pole that plays a role in regulated apical exocytosis (24,26). Preventing actin polymerization by treating the tissue with cytochalasin D blocked stretch-mediated increase in C_T (41). Further, Khandelwal et al. reported that the actin motor myosin5b works in association with the small GTPases Rab11a and Rab8a to promote apical exocytosis in umbrella cells. Though the mechanism is not clear, the motor protein can aid in the transit of DFVs across the apical cortical actin network (24).

Ca^{2+} signaling

The role of Ca^{2+} -mediated signaling in exocytosis has been well-studied in numerous cells types. In the uroepithelium, treatment with calcium ionophores triggered apical exocytosis even in the absence of stretch. Both extracellular Ca^{2+} and Ca^{2+} released from inositol-3-

phosphate-dependent ERs stores promoted apical exocytosis (28). Work done by Yu et al. indicated that tissue bowing triggered Ca^{2+} entry into the umbrella cells possibly via opening of ENaC, NCSS and other mechosensory channels. Further, removal of Ca^{2+} from the media blocked stretch-mediated exocytosis (41).

cAMP signaling

Another important signal that promotes stretch-mediated apical exocytosis is cAMP. Mechanical stimulation leads to increased cAMP levels in many mechanically sensitive tissues (45,46). In the uroepithelium, mechanical stretching triggered more than 2-fold increase in the cAMP levels. Further, activating cAMP with an analog of adenylyl cyclase, forskolin dramatically potentiated stretch-mediated apical exocytosis. Though the signaling pathway is not fully known, cAMP possibly acts via PKA-mediated signaling in promoting exocytosis (27).

SNAREs

Finally, an indispensable protein complex involved in membrane fusion is the SNAREs (47). Briefly, fusion of vesicles to its target membrane is mediated by the formation of a trans-complex between the SNARE proteins on the vesicle (v-SNAREs) to its cognate SNARE partner found on the membrane (t-SNARE). The complex forms a four-helix bundle that zippers towards the fusion pore, thus bringing the vesicle and the target membrane close enough to promote fusion. The formation of the SNARE complex is regulated by Ca^{2+} signaling and other associated SNARE regulatory proteins. In umbrella cells v-SNAREs synaptobrevin and t-SNAREs syntaxin-1 and SNAP-23 have been reported (48). They were found to colocalize with UPIIIa and the apical plasma membrane. These SNAREs are important for the fusion of DFVs to the apical surface. Though the SNARE regulatory proteins such as synaptotagmin and Sec-

1/Munc-18-like proteins have not been reported so far in the umbrella cells, further investigation is required to identify how the SNARE machinery is regulating DFV exocytosis.

Other proteins involved in membrane trafficking

Aside from the cytoskeleton, Ca^{2+} signals and SNAREs, the signaling proteins such as the Rab family of small GTPases play a vital role in DFV exocytosis in umbrella cells. The uroepithelium expresses multiple Rab family proteins including Rab4, Rab5, Rab8, Rab11a, Rab13, Rab15, Rab25, Rab27, Rab28 and Rab32 (4). Rab 8, Rab11a and Rab27b are especially interesting because they are expressed in the umbrella cells and colocalize with DFVs. Blocking activity of Rab8 or Rab11a by expressing a dominant negative version of the protein in the umbrella cells impairs stretch-mediated apical exocytosis (22,49). Rabs function as adaptor proteins that tether DFVs to the cell's cytoskeleton via molecular motors such as myosin5B and aid in the intracellular trafficking of the DFVs.

At least one other proteins called myelin-and-lymphocyte (MAL), is known to be involved in apical membrane fusion. In experiments performed in MDCK cells, MAL did not affect apical sorting of UPs but impaired the rate apical incorporation of the protein (50).

The coordinated function of these signaling proteins and complexes mediated stretch-induced apical exocytosis in umbrella cells.

1.1.7 Endocytosis

The added membrane at the apical surface are reinternalized via endocytosis. Endocytosis upon voiding was first visualized by Minsky et al. who discovered the formation of new vesicles

upon removal of stretch (38). The rapid internalization of membrane upon release of stretch is called compensatory endocytosis (CE) (44,51). Studies done by Khandelwal et al. elucidated the signaling events that govern CE (42). The endocytosis was initiated by increased tension at the basolateral surface as the umbrella cell expands, and resulted in the activation of β 1-integrins. The endocytosis was triggered by a β 1-integrin-dynamin-actin- and RhoA-associated pathway. The DFVs were internalized via a clathrin, caveolin and flotillin independent bulk endocytosis pathway and were destined to the lysosome for degradation. Interestingly, CE in umbrella cells is similar to the endocytosis that follows the exocytic release of neurotransmitters from neurons and neuroendocrine cells such as insulin secreting cells, further highlighting the sensory nature of the cells (51,52).

1.1.8 Exocytosis in the absence of stretch

Intriguingly, DFVs are also trafficked when certain apically localized cell-surface receptors are activated. For instance, activation of apically localized epidermal growth factor receptors (EGFR), ATP receptors or adenosine receptors (AR) trigger apical membrane trafficking (23,43,53). However, the physiological significance of this receptor-induced membrane trafficking and the cellular machinery that regulates it is poorly understood. The focus of my work was to better understand how umbrella cells respond to extracellular stimuli such as activation of apically localized A₁ adenosine receptors.

To fully understand how umbrella cells respond to extracellular biochemical stimuli and how this might trigger membrane trafficking, an understanding of the sensory web of the uroepithelium, the receptors expressed on the umbrella cells and the neuronal circuitry of the

bladder are required. In the next section, I will introduce the sensory signaling web of the uroepithelium.

1.2 THE UROEPITHELIAL SENSORY WEB

1.2.1 Introduction

The uroepithelium was long viewed a passive barrier that merely holds urine until voiding. This has changed over the years because of four critical observations: 1. Data showing that the uroepithelium is innervated; 2. Umbrella cells express numerous receptors that are associated with neuroendocrine cells and nerves; 3. The uroepithelium releases factors such as hormones and neurotransmitters that could potentially modulate bladder function by stimulating underlying muscles and nerve processes and 4. Adding substances such as ATP into the bladder lumen triggers bladder contraction.

1.2.2 The neural circuitry of the urinary bladder:

The efferent nerves:

Bladder function is regulated by three sets of nerves: the sympathetic thoracolumbar (hypogastric) nerve, the parasympathetic sacral (pelvic) nerve and the sacral somatic

motorneuron (pudandal) nerves (Figure 5). The sympathetic innervations of the bladder arise from the thoracolumbar region (T11-L2). It is divided into two groups: those fibers that innervate the main bladder and those that innervate the bladder neck and the urethra (54). During bladder filling, the sympathetic fibers release norepinephrine (NE) that binds to β -adrenergic receptors in the smooth muscles and cause bladder relaxation. At the neck of the bladder and urethra, the NE released from the sympathetic fibers bind α -adrenergic receptors and trigger muscle constriction and closing of the inner urethral sphincter (54,55).

The parasympathetic nerve processes arise from the sacral spinal cord (S₂-S₄) and innervate the bladder walls. These nerves release acetylcholine (ach) and ATP that bind to M₃ muscarinic receptor and P_{2X} receptors respectively on the smooth muscles and trigger bladder contraction. The parasympathetic nerves also innervate the inner urethral sphincter, where it releases NO leading to relaxation of the smooth muscle and opening of the outlet (54).

Bladder voiding in higher mammals is controlled by the group of cells located in the pontine medial tegmentum region of the brain, also called the pontine micturition center (PMC). PMC is the ultimate efferent nucleus that controls bladder voiding. Neurons arising from the PMC end in the S₂-S₄ sacral region, where they meet the parasympathetic nerves that innervate the bladder. Micturition is initiated in the PMC, travels down the spinal cord to the sacral region and trigger the parasympathetic neurons to release Ach and NO leading to bladder voiding (56-58).

The somatic nerves innervate the striated muscles of the outer urethral sphincter and regulate its function. During bladder filling they release ach that bind to nicotinic receptors on the striated muscles (54). During bladder voiding, PMC trigger inhibitory GABAergic and glycinergic neuron which mediate relaxation of the striated muscles (59). Thus the PMC

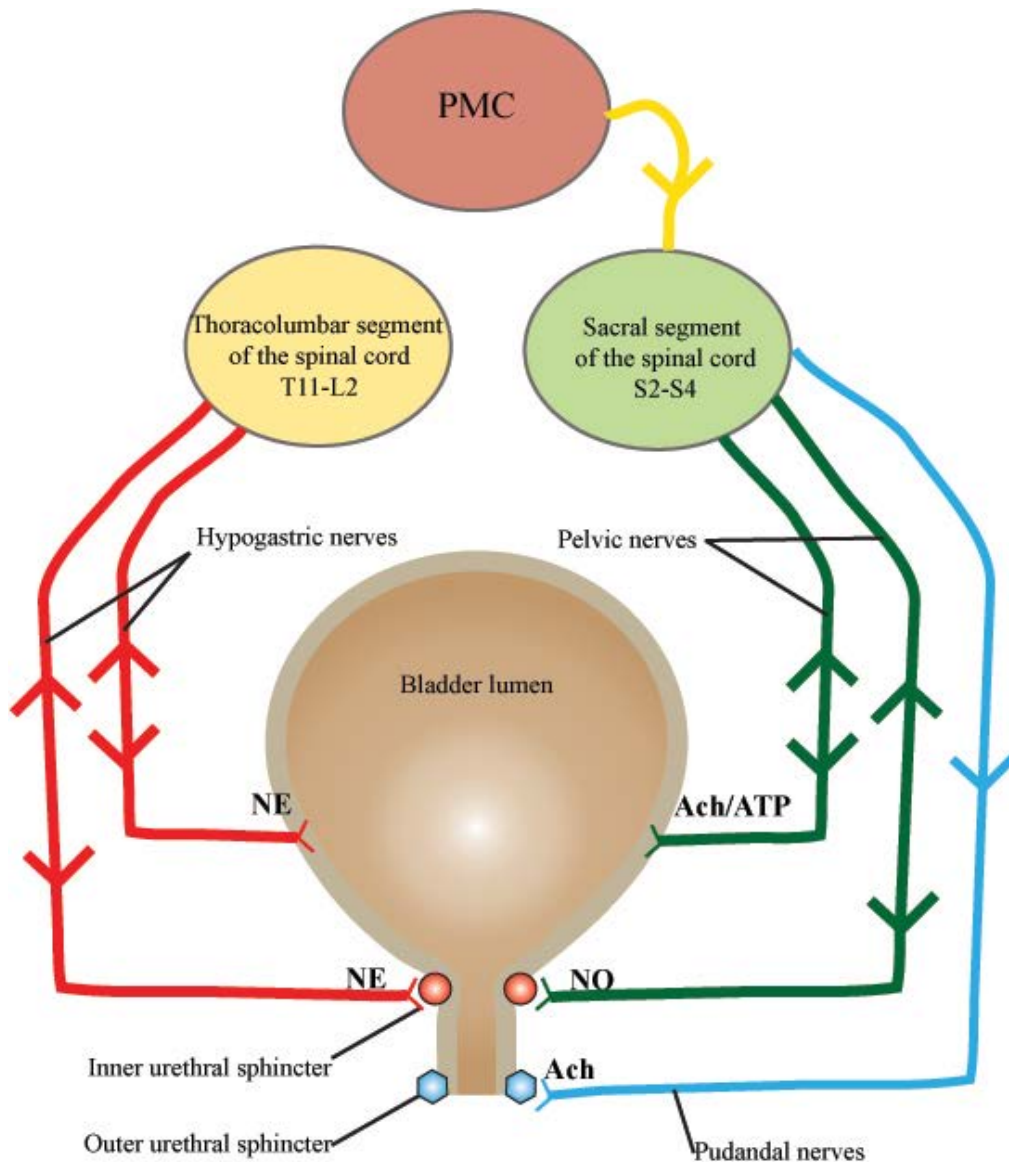
coordinates the contraction of the smooth muscles on the bladder walls and the relaxation of the striated muscles on the outer urethral sphincter resulting in the expulsion of urine.

Afferent nerves:

Sensory information from the bladder is conveyed to the spinal cord via the afferent pelvic and hypogastric nerves. The afferent component of the bladder consists of the myelinated A δ fibers and the un-myelinated C-fibers. The A δ fibers communicate mechanosensory information such as bladder fullness and interluminal volume change. The C-fibers on the other hand respond to noxious stimuli such as urethral infection and irritation and are the chief pain receptors of the bladder (55,60,61).

Interestingly, ultrastructural and biochemical studies in humans have revealed that the afferent nerve processes that innervate the bladder namely the small myelinated A δ or unmyelinated C fibers extend their dendritic processes deep into the uroepithelium, and rest close the basolateral surface of umbrella cells (62,63). Further, in animal studies, mechanical stretching of the bladder mucosa resulted in excitation of the afferent nerves which in-turn resulted in activation of the sympathetic fibers that innervate the bladder walls and urethral sphincter (64). However, the precise modulatory compound released by the uroepithelium on mechanical stretching is unknown, and whether these compounds activate the A δ and C-fibers is not well understood. Nevertheless, these studies add weightage to the mechanosensory role of the uroepithelium. A likely scenario is that changes in mechanical forces such as stretching or release of neuro-modulatory factors such as ATP, adenosine and Ach from the uroepithelium are likely to directly bind and excite afferent nerve process leading to modulation of bladder function.

Figure 5 The neural circuitry of the urinary bladder



The efferent pathway is depicted by the downward facing arrow heads. NE released from the hypogastric nerves (red) bind β -adrenergic receptors on the bladder walls and α -adrenergic receptors present on the inner urethral sphincter. Ach is released from the Pelvic nerves (green) that innervates the bladder walls and bind M3 receptors. NO is released from the Pelvic nerves that innervate the inner urethral sphincter. The pudandal nerves (blue) release Ach that bind to nicotinic receptors present on the striated muscles of the outer urethral sphincter. The afferent pathway is depicted by the upward facing arrow heads.

1.2.3 Receptors and ion channels expressed on the apical and basolateral surfaces of the umbrella cells:

The repertoire of receptors and ion channels expressed on the apical and basolateral surfaces of the umbrella cells are curiously similar to that found on nociceptive and mechanosensory cells. The sensory receptors and ion channels identified on these cells till date includes ATP receptors ($P2_{X1-7}$ and $P2_Y 1,2,4$) (65-67), adenosine (A_1, A_{2a}, A_{2b} and A_3) (53), EGFR (ErbB1-3) (43), norepinephrine (α and β), acetylcholine (muscarinic, M1-5 and nicotinic) (68,69), protease-activated receptors (PARs), amiloride- and mechanosensitive epithelial sodium channels (ENaC) (28), bradykinin receptors (B1 and B2) (70), and various TRP channels including TRPV1, TRPV2, TRPV4, TRPM8 and TRPA₁ (63,71).

Though the physiological importance of these receptors in regulating bladder function is not fully understood, it is possible that the presence of these receptors enables the umbrella cells to sense extracellular biochemical stimuli and modulate bladder function accordingly. For example EGF and HB-EGF present in the urine or released from the uroepithelium can bind to EGFR expressed on the umbrella cells, whereas mechanosensory cues such as mechanical stretch during bladder filling can act on mechanosensors such as ENaC and NSCC (41,72). The downstream result of receptor activation is twofold, it alters the membrane trafficking events in the umbrella cells (via early and late phase exocytosis) and releases neurotransmitters and sensory compounds such as neurotrophins, vascular endothelial growth factor (VEGF), corticotrophin releasing factor (CRF1 and CRF2) and estrogens (ER α and ER β), and peptides such as substance P, pituitary adenylate cyclase-activating peptide (PACAP) and calcitonin gene-related peptide that can bind efferent and afferent nerve process and regulate bladder function by modulating sensory transmission from the spinal cord (60,71,73,74).

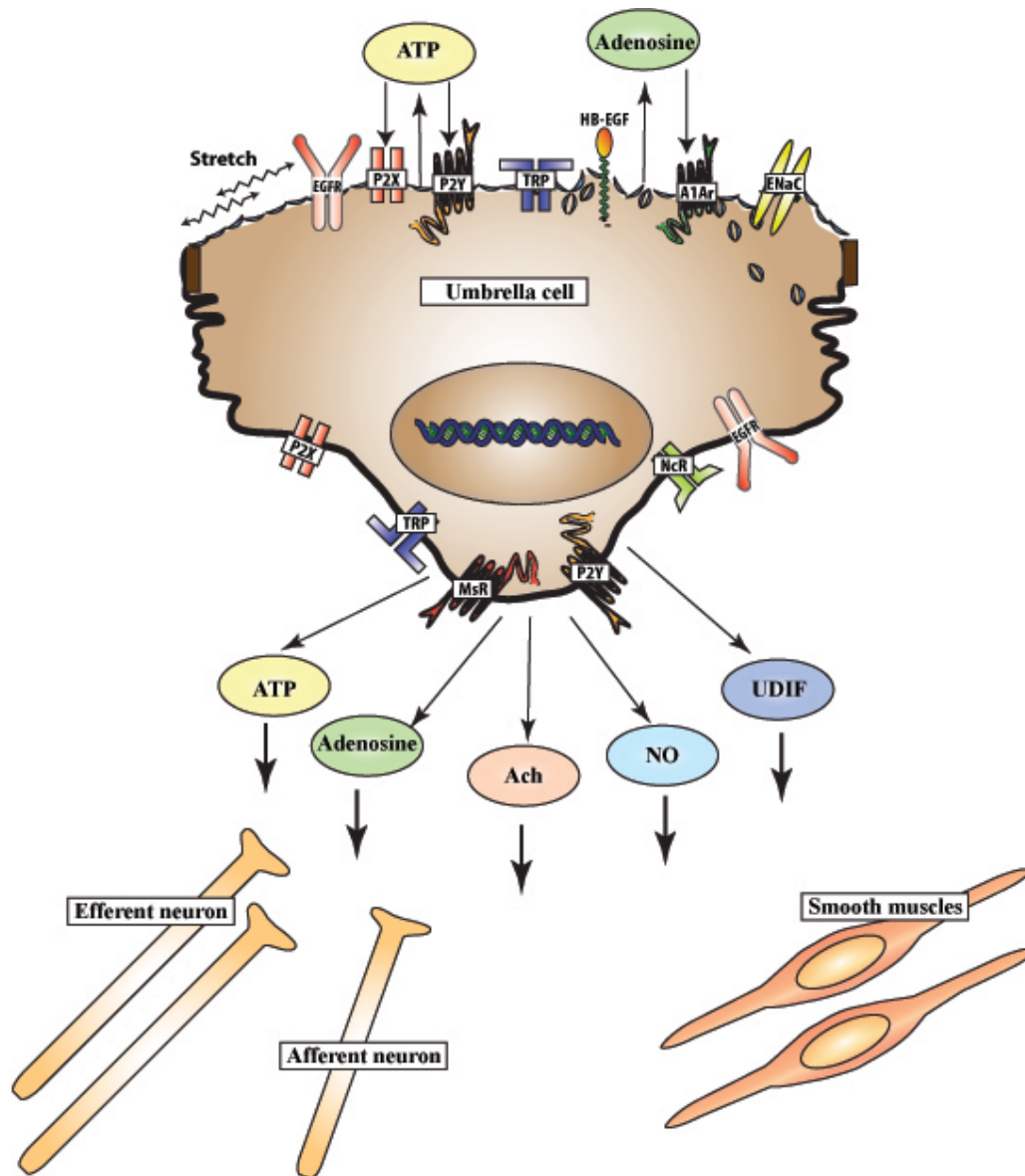
1.2.4 Release of hormones, neurotransmitters and signaling molecules from the uroepithelium:

There is considerable evidence to show that the release of the signaling compounds from the uroepithelium impacts bladder activity under both normal and pathologic conditions. For example, uroepithelium release numerous hormones, neurotransmitters, and signaling peptides including ATP, adenosine, Ach, prostaglandins, prostacyclin, nitric oxide (NO), and other cytokines (23,53,75,76). Incidentally, the afferent sympathetic and parasympathetic nerves which innervate the uroepithelium carry receptors for these molecules (61,68,77). Therefore, it is tempting to believe that these modulatory compounds can bind and excite the afferent nerve-processes, thereby modulating bladder function. There is some evidence in support of this hypothesis: For instance, intravesical instillation of oxyhemoglobin to oxidize luminal NO resulted in bladder hyperactivity (78). Further, in experiments where the uroepithelium was removed from the underlying musculature, the detrusor muscles showed increased contractile response, suggesting that regulatory factors released from the uroepithelium have an inhibitory effect on the detrusors (79). The compound that caused this effect is however not known, and termed uroepithelium derived inhibitory factor (UDIF), but is likely to be NO, adenosine or GABA, or mediated by calcium and potassium channels (79). Another possible mechanism of activating the afferent neurons is by triggering Ca^{2+} waves, which originate from the basolateral surface of the umbrella cells, and are amplified as they traverse through the intermediate cells and basal cells (71).

In summary, the “input”, which are biochemical compounds present in the urine and mechanical forces can activate receptors and ion channels on the umbrella cells. The umbrella cells in response to the ‘input’ can alter their apical surface by modulating membrane

trafficking events or release signaling factors, the “output”, which can be picked up and sensed by the detrusors and afferent nerve processes and thus results in regulation of bladder function.

Figure 6 The sensory web of the umbrella cell



The most prominent cell surface receptors that have been studied to understand the sensory function of the uroepithelium are presented.

1.2.5 Conclusion

Despite the wealth of information regarding ‘input’ and ‘output’ signals, the receptors and ion channels expressed on the umbrella cells and the innervation of the bladder, we still lack information regarding the precise signaling events in the umbrella cells downstream of the ‘input’ signal and how these signals alter the membrane trafficking events in the cell or modulate bladder function. One of the chief modulators that have a big impact on the regulation of other organs is adenosine. Adenosine is a well-known stress response hormone in other organ systems and is known to play a beneficial role especially in the heart and brain (80,81). Because the bladder lumen is a stressful environment, and because we have evidence that adenosine is released in the mucosal and serosal surfaces of the uroepithelium during stress, a promising candidate to study the sensory function of the uroepithelium is adenosine and its associated signaling.

1.3 ADENOSINE RECEPTORS

1.3.1 Introduction

The idea that adenosine, could function as an extracellular signaling molecule was put forth by Alan Drury and Albert Szent-Györgyi in 1929. They found that injecting cardiac extracts intravenously into the whole animal caused a transient slowing of the heart rate. On further purification of the extract, they determined that the factor that caused the slowing of the heart was an “adenine component”(82). The field of adenosine signaling has progressed exponentially

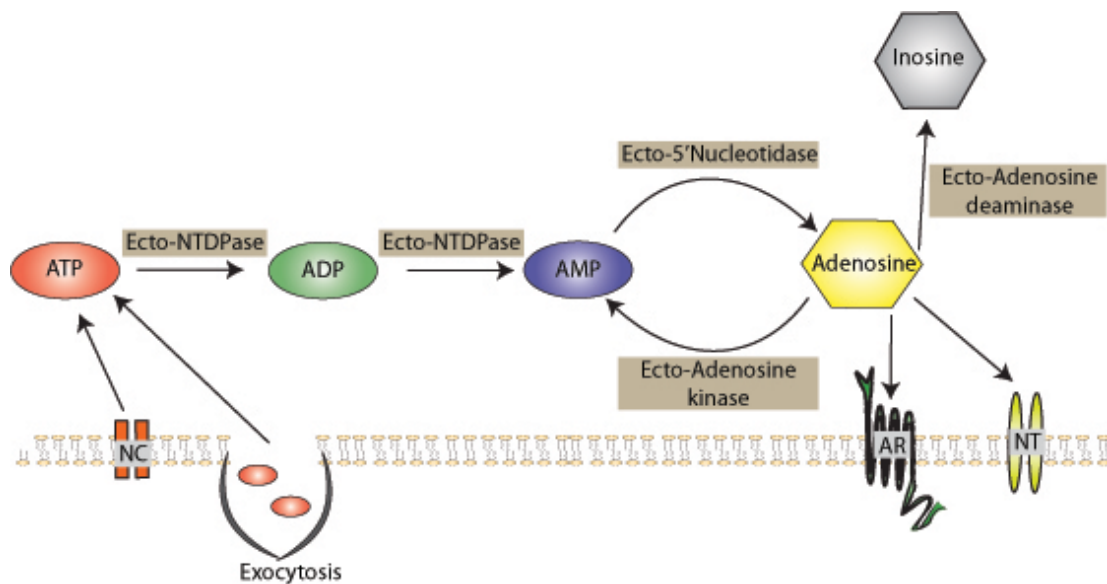
since this initial finding, and today intravenous injection of adenosine is the mainstay treatment for rapid relief from supraventricular tachycardia and cardiac arrhythmia (83,84).

1.3.2 Extracellular adenosine

Adenosine is released from most tissues in the body into the extracellular space, from where it acts as an autacoid on adenosine receptors. The extracellular adenosine levels in the heart has been estimated to be ~100 nM and in the brain ~30 nM under normal physiological states (85,86). However, in severe ischemic stress conditions, the levels can rapidly increase. In circulation, adenosine has an extremely short half-life of < 5 seconds. It is released from intracellular stores via concentrative or equilibrative bi-directional nucleoside transporters (CNTs and ENTs, respectively) or formed in the extracellular space by the metabolism of ATP or cAMP (Figure 7). CNTs are Na⁺ - dependent. CNT 1 is primarily localized on epithelial cells whereas CNT 2 and CNT 3 are widely expressed in other tissue types (87). ENTs transport adenosine across the plasma membrane and play an important role in the provision of nucleoside derived from diet and synthesis (88). ENT1 and 2 are widely expressed in organs including liver, heart, testis, spleen, kidneys, brain, placenta, thymus, prostate, and skeletal muscles. The cation dependent ENT 3 and 4 are more sparsely expressed. ENT3 is particularly abundant in the placenta and ENT4 is predominantly found in the heart and endothelial cells (89). Extracellular ATP is broken down by the ectonucleotidases, of which there are several different classes and have promiscuous nucleotidase function or show substrate and tissue specificity. Ecto-Nucleotide triphosphate diphosphohydrolase (E-NTDPases, CD39) hydrolyze extracellular tri-

and di-phosphates, converting $\text{ATP} \rightarrow \text{ADP} \rightarrow \text{AMP}$. Ectonucleotide pyrophosphate phosphodiesterases converts $\text{cAMP} \rightarrow \text{AMP}$. Ecto-5'nucleotidases (CD73) converts $\text{AMP} \rightarrow \text{adenosine}$ (90). Adenosine can be rephosphorylated back to AMP by ecto-adenosine kinase or acted upon by ecto-adenosine deaminase and broken down to inosine which is the final product of adenosine metabolism. Inosine is broken down to hypoxanthine by the removal of the ribose sugar by the action of purine nucleoside phosphorylases (PNP). Hypoxanthine is converted to xanthine and that in-turn is metabolized to uric acid by the action of xanthine oxidase. Uric acid is the final product of purine metabolism and is excreted in the urine.

Figure 7 Extracellular adenosine synthesis and turnover



ATP released from nucleotide channels (NC) and via exocytosis is converted to $\text{ADP} \rightarrow \text{AMP} \rightarrow \text{Adenosine}$. Adenosine can be converted back to AMP, bind adenosine receptors (AR), taken back into the cell by CNTs and ENTs (NT) or degraded to inosine.

1.3.3 A brief overview of G-protein coupled receptors (GPCRs)

As adenosine receptors are GPCRs, a brief overview of GPCR biology is warranted to better understand the cellular functions of the receptors.

Domain architecture and downstream signaling components of GPCRs

GPCRs are single polypeptides with seven transmembrane α helices. The N-terminus faces the extracellular region whereas the C-terminus is in the cytoplasm. The seven transmembrane α helical region gives rise to three extracellular and intracellular loops. The extracellular loops are regions of glycosylation and the intracellular loops have conserved amino acid sequences that are essential for the internalization and degradation of the receptor. The third intracellular loop and the C-terminal tail together form the binding site for G-proteins (hence the name for the receptors) (91).

G-proteins are called so because they are guanine-nucleotide regulatory protein complexes. Based on their activity, the G-proteins are divided into G_i (inhibits adenylyl cyclase activity), G_s and G_{olf} (stimulates adenylyl cyclase), $G_{q/11}$ (activates phospholipase C), G_o (stimulates K^+ ion channels) and G_{12} (activates Rho guanine exchange factors) (92). The G-proteins are normally in a tight heterotrimeric complex, consisting of α , β and γ subunits. Ligand binding causes conformational changes in the 6th loop of the receptor and leads to the formation of receptor-G-protein complex. Here G_α which is initially bound to GDP (guanosine diphosphate) switches to an active GTP-bound state by the action of the GEF (guanine exchange factor) domain. The GTP-bound active G_α uncouples from the $G_{\beta\gamma}$ subunits, which is free to interact with other downstream signaling proteins. The GTP-bound state is however short-lived,

and the G-proteins revert back to the GDP-bound state and re-associate with the $\beta\gamma$ subunits to form the “resting” heterotrimeric conformation (93,94).

1.3.4 Types of adenosine receptors

Extracellular adenosine is a potent cytoprotective agent under both normal physiological conditions and when organs undergo stress (95,96). The protective response can be in the form of increasing blood supply via vasodilation (97), ischemic preconditioning that protects against subsequent episodes of ischemia (98-100) or suppression of inflammation and its associated production of free radicals and cytokines, infiltration of inflammatory cells (101-103). Extracellular adenosine can perform these functions by binding to specific cell surface receptors and activating specific signal transduction pathways. As mentioned earlier, adenosine binds to four GPCRs termed A_1 , A_{2A} , A_{2B} and A_3 . The A_1 and A_3 receptors are coupled to the G_i protein whereas the A_2 receptors are coupled to the G_s or G_o proteins. Their affinities to adenosine are $A_1 > A_{2A} > A_3 > A_{2B}$, (K_i of 10-30nM for A_1 and A_{2A} , $\sim 1\mu M$ for A_3 and $> 1\mu M$ for A_{2B}) (104). In addition to G_s and G_o proteins, A_{2B} receptors, which have the lowest affinity to adenosine, also have the ability to activate G_q proteins (105). Physiological adenosine levels are thought to activate only few adenosine receptors, owing to the varying binding affinities of the receptors and the short half-life of the nucleoside. However, under stressful conditions such as ischemia, when the levels of extracellular adenosine increase rapidly, an all-out generalized activation of all the adenosine receptor subtypes can be observed (106,107). Recently it was reported that the human growth-hormone secretagogue receptor (GHS-R) also accepts adenosine as a partial

agonist in cell culture, in addition to its endogenous ligand ghrelin, and is likely to modulate the release of dopamine from hypothalamic neurons (108,109).

The G-proteins that are coupled to adenosine receptors are defined by the downstream activation states of adenylyl cyclase. However, they are not the only effectors of adenosine receptors. In fact, the far reaching physiological relevance of adenosine is because of the wide array of downstream signaling cascades triggered by the adenosine receptors. These actions of adenosine receptors may be initiated through the $G_{\beta\gamma}$ subunit of the G-proteins. They include activation of phospholipase C (PLC) (110,111), phosphoinositide 3-kinase (PI3K) (112), mitogen-activated protein kinase (MAPK) (113), extracellular receptor signal-induced kinase (ERK), arrestins and coupling to ion channels (113).

1.3.5 A_1 adenosine receptors (A_1AR)

A_1AR was the first identified adenosine receptor (hence the name) and incidentally this receptor was identified as a binding substrate for caffeine (114). They are coupled to G_i -proteins and are ubiquitously expressed. The role of A_1AR in the central nervous system (CNS) and heart have been especially well studied. A_1Ar is abundantly expressed in brain where it plays a major neuroprotective role by decreasing the release of excitatory neurotransmitters such as glutamate. A_1AR , acting via G_i -proteins decreases cAMP levels, opens K^+ channels and reduces calcium influx by blocking Ca^{2+} channels leading to inhibition of neurotransmitter release (115-118).

In the heart, the dramatic increase of adenosine during myocardial ischemia was first demonstrated in 1970 (119). Since then a growing body of evidence has shown that adenosine acts as a 'sensor' of imbalances in energy supply and demand and a local regulator of coronary flow (120,121). Studies on $A_1AR^{-/-}$ mice have shown that the receptor is involved in aortic and

coronary vasoconstriction and protects the heart against injury caused by myocardial infarction and ischemia by inhibiting the production of cAMP and activating ATP-dependent potassium channels (122,123). In addition, cardiac-specific A₁AR overexpression studies showed that the receptors were involved in reduction of diastolic dysfunction during ischemia/reperfusion and prolonged cardioprotection (124). Interestingly, it has been reported that the role of A₁AR in cardio-protection could depend on its ability to transactivate EGFR (discussed later).

In the kidney, adenosine modulates glomerular filtration rate (GFR), and prevents hypoxic injury in the renal medulla. The A₁AR induces vasoconstriction in the afferent arterioles and the A₂ receptors cause vasodilation in the post-glomerular arterioles, the concerted action of the adenosine receptors ensure smooth glomerular filtration and kidney function. A₁AR-mediated vasoconstriction occurs through G_{βγ}-mediated activation of PLC and its associated downstream signaling (125). Other functions of A₁AR activation at the different sections of the nephron include: increase in reabsorption of fluid, Na⁺, HCO₃⁻ and phosphates in the proximal tubule, inhibition of NaCl reabsorption in the medullary thick ascending limb, uptake of Mg²⁺ and Ca²⁺ in the cortical collecting duct and counteraction of vasopressin effects in the inner medullary collecting duct (126-128).

Despite the beneficial roles of A₁AR, the activity of this receptor under certain pathological conditions could lead to deleterious effects. Numerous reports have been made where activation of A₁AR during inflammation or pathological conditions has adverse effects. For instance: the expression of A₁AR is upregulated in asthma patients and activation of the receptors lead to bronchoconstriction, leukocyte activation and inflammation, bronchial hyper-responsiveness and mucous secretion (129,130). At least one anti-A₁AR therapeutic drug (EPI-2010) to treat asthma is currently in clinical trials (131). In diabetes and obesity, A₁AR is highly

expressed in the adipose tissues and inhibition of lipolysis is mediated by adenosine acting on A₁AR (132,133). Further, in the urinary bladder, antagonism of A₁AR reduced inflammation (134). Also, in my studies, I found further evidence in support of this, as activation of A₁AR triggered smooth muscle excitability and bladder over-activity in cyclophosphamide-induced cystitis studies (further discussed in Chapter 2). Finally, there is evidence that A₁AR antagonism resulted in reduced myocardial fibrosis and albuminuria in a model of uremic cardiomyopathy (135). These data indicate that, while A₁AR has a beneficial role under normal physiological conditions, during many pathological conditions and inflammation its activity further exacerbates the pathological state.

1.3.6 A₂ and A₃ adenosine receptors (A₂AR and A₃AR)

Though the focus of this dissertation is on A₁AR-mediated signaling, the uroepithelium express the other three adenosine receptors as well (53), thus a brief overview of the physiological role of A₂ and A₃ receptors will be beneficial in understanding the overall function of adenosine in the bladder.

A₂AR

As mentioned earlier, there are two A₂ARs: A_{2A} and A_{2B}. They are coupled to G_s and G_{q/11} proteins and hence perform an excitatory function. As with A₁AR, they are also ubiquitously expressed in the body including smooth muscles, vascular, intestinal, bronchial, chromaffin tissues, mast cells, heart, kidneys, lungs, and brain (136). They modulate cellular function by stimulating the production of inositol triphosphate (IP3)/diacylglycerol by the activation of PLC. They play a major role in manifestation of many diseases including asthma,

inflammation, wound healing, cancer, reperfusion injury of the heart and neurodegeneration (137).

Physiologically, the role of A₂ receptors in modulating organ function depends on their ability to limit inflammation and tissue injury. A_{2A} receptors are highly enriched on inflammatory cells including neutrophils, mast cells, macrophages, eosinophils, platelets, and T-cells (138,139). The anti-inflammatory properties of the receptors include inhibiting T-cell activation and limiting the production of inflammatory mediators such as IL-12, TNF- α and INF- γ (140,141).

In support of their role in immune suppression, studies have shown that in human neutrophils, activation of A_{2A} reduces neutrophil adherence to the endothelium, inhibits formyl-Met-Leu-Phe (fMLP)-induced oxidative burst and inhibits superoxide anion generation (142). Further, A_{2A}^{-/-} mice have increased oxidative stress in the lungs and airway smooth muscles due to activation of inducible nitric oxide synthase (iNOS) and nicotinamide adenine dinucleotide phosphate (NADPH), two events which are normally kept under control by action of A_{2A} (143).

In contrast, A_{2B} activation aids in the progression of inflammatory diseases such as asthma. A_{2B} can activate G_q proteins, and downstream cytokines including IL-4, IL-8 and IL-13, which can in-turn induce immunoglobulin E (IgE), the immunoglobulin involved in progression of allergic response and asthma (144,145). Hence antagonist therapy against A_{2B} to treat asthma has been proposed. However, the full role of A_{2B} in asthma progression is yet to be understood (131).

In the brain, unlike A₁AR which has a direct impact on neurotransmitter release at neuronal synapses, the functions of the A₂ receptors in the brain rely predominantly on their ability to generate an immune response in the induction of long-term brain response to trauma

and ischemia (117). A_{2A} occurs predominantly on the neurons in the striatum, cholinergic interneurons, hippocampus, cerebral cortex, nucleus accumbens and olfactory tubercles (117,146,147). A_{2B} are distributed at low levels in the brain with moderate expression in the human cerebellum and hippocampus (95,148). There has been special interest in A_{2A}/D₂ dopamine receptor interactions, because of its implications in the manifestation of Parkinson's disease and basal ganglia dysfunction (149).

In summary, A₂ receptors are beneficial in instances where inflammation is a detrimental component, but adversely effects treatment of cancer or neurological diseases where an immune response is required. For instance, upregulation of A₂ receptors protects cancer cells from attack by T-cells, and in fact A_{2A}^{-/-} mice showed a remarkable decrease in tumor size and increased survival rate (150).

A₃AR

A₃AR were the last members of the adenosine receptor family to be cloned. It is expressed in the testes, lungs, kidney, heart and brain. Though, the distribution of the receptor in the brain differs by species (151). A₃ receptors are also highly expressed in the inflammatory cells including human eosinophils, neutrophils, monocytes, macrophages, lymphocytes and dendritic cells. It is coupled to G_i proteins and hence has an inhibitory role on adenylyl cyclase, similar to A₁AR (152).

A₃ receptor activation on immune cells has both pro- and anti-inflammatory responses and hence their role in progression of inflammatory diseases is controversial. Initially A₃ agonist therapy was suggested for treating asthma, because of their role in mast cell degranulation (153). However, the impact of A₃ receptors on mast cells has been challenged by many groups which claim that the response is actually mediated by A₂AR (145,154,155). In addition, selective A₃

antagonism prevented airway eosinophilia and mucous production in adenosine deaminase knockout ($ADA^{-/-}$) mice. Similar results were found in $ADA^{-/-}/A_3^{-/-}$ double knockout mice suggesting that A_3 activation plays a detrimental role in chronic lung diseases (156).

The contradicting roles of A_3 are evident in other organ systems also. For instance, the beneficial role of A_3AR was demonstrated in murine septic peritonitis, where activation of the receptor decreased mortality and renal and hepatic injury. The effect was the result of blocking the release of $TNF\alpha$, IL-12 and $IFN\gamma$ (157,158). Similarly, A_3 activation plays a protective role in lung injury and protection of skeletal muscles from ischemia and reperfusion injuries (159,160). On the other hand, its detrimental role was shown in studies where activation of the receptor exacerbates renal dysfunction and the expression of the receptors is increased in ocular ischemic diseases and in conditions with oxidative stress (161,162).

1.3.7 Positive and negative impact of adenosine signaling

Extracellular adenosine has an impact on most of the tissues and organ systems in the body by acting on its four receptors. It is apparent from the preceding section that all four adenosine receptors have both beneficial and detrimental effects. A_1AR predominantly has a positive role in most organisms. Adenosine, binding and activating A_1AR imparts neuro, cardio, skeletal- and smooth muscle-protection. Similar beneficial functions stem from A_2AR receptor activation. The anti-inflammatory function of A_2AR receptors are currently being aggressively studied for therapy against numerous auto-immune and other inflammatory diseases (163,164). However, it is also clear that activation of A_1 and A_2AR under pathological conditions such as inflammation of the gut, bladder overactivity and inflammatory disease such as asthma further exacerbates the pathological state. Therefore, adenosine receptors mediated therapeutics have to be approached

with caution, and a fuller understanding of the receptor biology under physiological and pathological states is necessary.

Furthermore, it is interesting to note the gradient of adenosine having a beneficial function when activating A₁AR and A₂AR and beneficial and detrimental effects when activating A_{2b}AR and A₃AR. Intriguingly, this pattern reflects the affinity of adenosine to the receptors. As mentioned earlier, adenosine binding affinity is A₁>A_{2a}>A₃>A_{2b}. Excessive extracellular adenosine would activate A_{2b} and A₃ receptors whereas normal physiological levels of adenosine would primary activate A₁ and in some cases A_{2a} receptors. Hence, the level of adenosine in systemic circulation, i.e. extracellular adenosine may also be a deciding factor on whether it has a beneficial role or a detrimental role.

1.3.8 Role of adenosine in membrane trafficking and EGFR transactivation

Despite our deep understanding of the role of adenosine signaling in normal and physiological states in many organs we lack information on the role of adenosine in regulating the urinary bladder. Furthermore, though we understand AR's role in activating or inhibiting cAMP, we do not have much knowledge of the other signaling pathways downstream of AR activation. Interestingly, William-Pritchard et al. recently reported that the cardioprotective role of A₁AR occurs via EGFR transactivation. In mice heart perfusion experiments, they found that inhibitors of metalloproteinases, HB-EGF and EGFR blocked adenosine agonist-mediated reduction of post-ischemic diastolic pressure (290). In addition, studies performed on rat ventricular myocytes indicated that, A₁AR stimulation lead to membrane localization of PKC δ (165). Further, in Cos-7 cells, the G $\beta\gamma$ -subunit of A₁AR stimulated PLC activation (111). PLC activation and PKC-membrane localization are classic upstream signals for activation of membrane bound

metalloproteinases (described later) that lead to cleavage and release of EGFR ligands leading to EGFR transactivation. Because adenosine is released during bladder stress and because stress-mediated late phase exocytosis requires EGFR transactivation, in the second part of my dissertation, I tested the hypothesis that *A₁AR transactivates EGFR in umbrella cells leading to apical exocytosis.*

1.4 GPCR-MEDIATED EGFR TRANSACTIVATION

1.4.1 Introduction

Signal transduction pathways inside the cell are seldom linear events leading to a single endpoint. In most cases, signaling cascades are interconnected and proper cellular function requires the coordinated cross-communication between myriad signals. One of these intriguing ‘cross-talk’ between cellular pathways is the phenomenon where GPCRs transactivate EGFR. Numerous GPCR ligands including Ach, bradykinin, adenosine and LPA, on binding to their respective receptors trigger a signal transduction pathway that leads to activation of certain membrane-bound metalloproteinases. These metalloproteinases, in-turn cleave membrane-bound EGFR ligands and release them into the extracellular space. The released EGFR ligands bind and activate EGFR and leads to ERK/p38 MAPK pathways (166-176). EGFR transactivation is responsible for numerous stimuli-dependent cellular modulation, including protein synthesis, exocytosis, endocytosis, proliferation, and differentiation (175-181).

1.4.2 EGFR

EGFR signaling is one of the most extensively studied areas of signal transduction. The ligands that bind and activate EGFR are EGF, heparin-binding EGF (HB-EGF), amphiregulin, transforming growth factor alpha (TGF α), epiregulin, neuregulin and betacellulin (182,183). EGFR belongs to the ErbB family of receptor tyrosine kinases, which also includes ErbB2, ErbB3 and ErbB4 (184). Umbrella cells express EGFR, ErbB2, and ErbB 3 (43). The receptors are expressed as single-pass membrane proteins. On ligand-binding they form hetero or homodimer and catalyze the phosphorylation of tyrosine residues in the cytoplasmic tail of the receptors (185-187).

The phosphorylated tyrosine residues serve as docking sites for phosphotyrosine binding scaffolding proteins including SH2 or PTB (phosphotyrosine binding) domain containing proteins (188). The adaptor proteins that contain the SH2 domains, such as Grb2 and docking proteins such as Gab1, LAT and Dos assemble a signal transduction complex which triggers ERK and p38 MAPK, phosphatidylinositol3-phosphate-Akt pathway and the p70S6k/p85S6K pathway (186,189,190). Which pathway is triggered and the potency of the pathway depends on the ligand that binds and activates the EGFR, and the EGFR heterodimer pair. The signal transduction pathways that are initiated trigger distinct transcription programs in the nucleus. This is achieved by activating *fos*, *jun*, *myc* proto-oncogenes, zinc-finger containing transcription factors including Sp-1 and Egr-1 and GA-binding proteins (173,191,192). The output of this complex signaling network is cell proliferation, differentiation, adhesion, migration, apoptosis, in embryonic development and cellular remodeling (193,194).

1.4.3 Transactivation

The first report on GPCR transactivating EGFR was discovered in 1996 by Axel Ullrich. They found that activation of GPCR in Rat-1 fibroblasts with lysophosphatidic acid (LPA) and endothelin-1 lead to the tyrosine phosphorylation of a 170kD glycoprotein. Further analysis revealed that this glycoprotein was EGFR (191). This was a landmark finding in cellular signaling and initiated a salvo of studies across the world to determine the molecular events that lead to EGFR transactivation and the identification of the proteins players involved in this intriguing pathway.

Soon after the initial discovery, the transactivation pathway was discovered in a variety of cell types including PC 12 cells, astrocytes and vascular smooth muscle cells and was established as a widely relevant pathway towards activation of MAPK (171,195). GPCRs coupled to G_i and G_q proteins are known to be involved in this pathway. Studies performed on PC12 cells, vascular smooth muscle cells, intestinal epithelial cells and ovarian cancer cells showed that activation of GPCRs with ligands including Angiotensin II (AngII), bradykinin, endothelin-1 or carbachol resulted in a G_q -dependent spike in intracellular Ca^{2+} concentration that resulted in EGFR transactivation (178,195-197). Whereas in other cell types such as gonadotropin α T3-1 cells and rat liver epithelial cells, activating GPCRs with gonadotropin releasing hormone, AngII or bradykinin triggered a $G_i \rightarrow PKC$ pathway that resulted in EGFR transactivation (198,199). Furthermore, in COS-7 and HEK293 cells, activation of G_i via β_2 adrenergic receptor resulted in transactivation of EGFR via a Src-dependent pathway (200).

The transactivation pathway (figure 8)

In addition to GPCRs, ROS, UV irradiation, mechanical and sheer stress also trigger EGFR transactivation (177). While there are still numerous gaps in our understanding of the

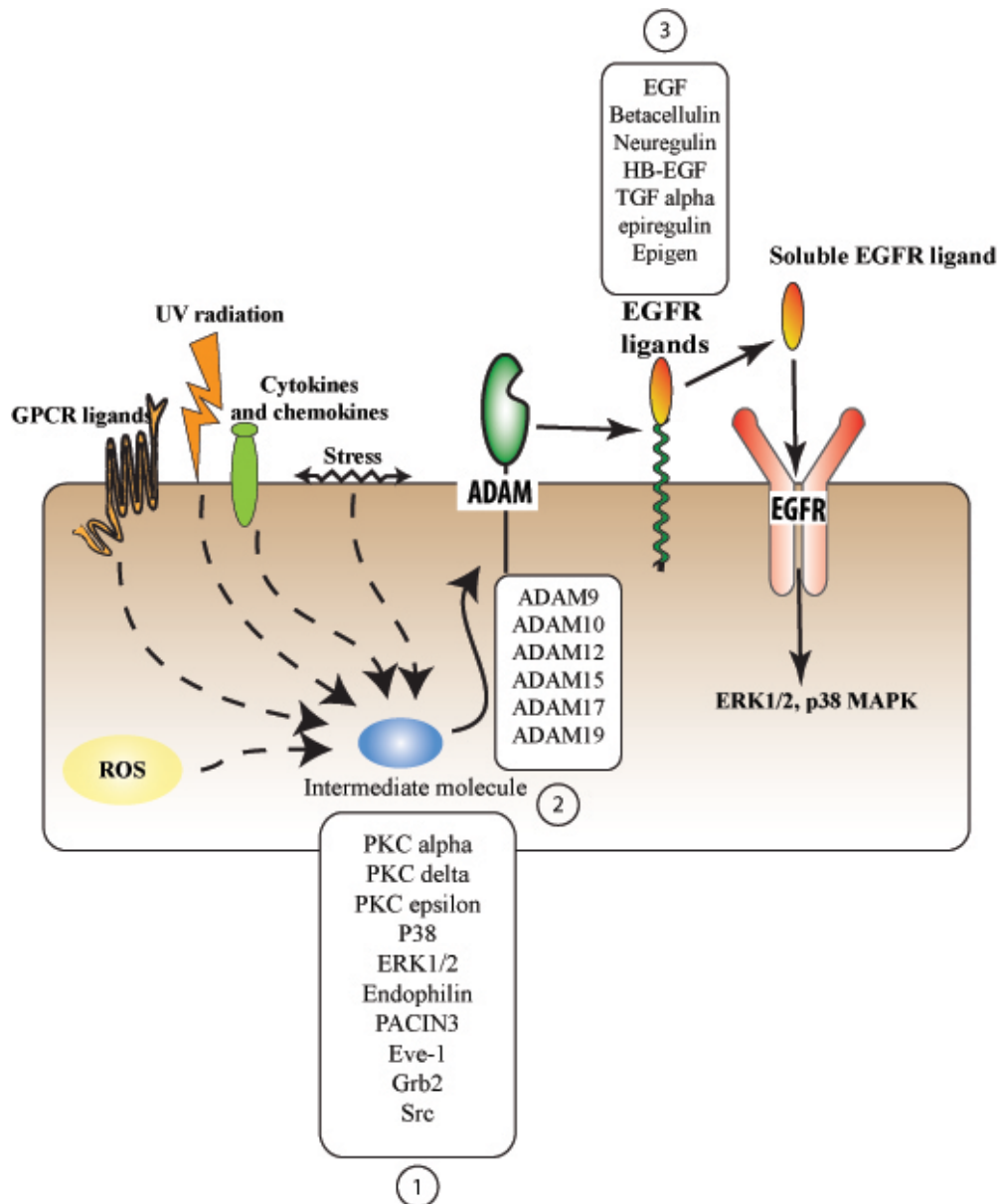
precise signaling pathway leading to transactivation, there seem to be few signaling molecules that play a major role in the pathway. I will focus on GPCR-mediated EGFR transactivation as that is relevant to this dissertation. EGFR transactivation by GPCRs is triggered by the $G_{\beta\gamma}$ subunits and requires second messengers such as elevation of intracellular Ca^{2+} , activation of PKC, Src or reactive oxygen species (169).

While many second messengers are known to be involved in activation of ADAMs, most pathways seem to converge on PKC-mediated activation. The diacylglycerol analog PMA has been used in numerous studies to activate ADAMs. PKC activates membrane bound metalloproteinases called ADAMs (described in the next section). The precise mechanism of activation is not clear and has been the focus of numerous research studies around the world. Data so far indicate that PKC could directly phosphorylate ADAMs or activate indirectly via other secondary messengers such as p38 MAPK and ERK1/2 (201,202). ADAMs, on activation, cleave membrane-bound EGFR ligands. Following cleavage and release, the soluble EGFR ligands are free to bind EGFR and trigger receptor dimerization and phosphorylation in an autocrine or paracrine fashion. Subsequently ERK1/2 and/or p38 MAPK pathways are initiated leading to activation of transcription factors, which initiate numerous signaling pathways characteristic of EGFR signaling such as cell differentiation or proliferation, secretion of chemokines and hormones, autophagy, apoptosis, and cell migration (179).

As mentioned earlier, in the uroepithelium stress induced by mechanical stretching trigger EGFR transactivation leading to apical exocytosis. However, the metalloproteinase involved, or the upstream signals that triggered it are not known. In my studies, I found that adenosine is released from the uroepithelium in response to mechanical stretching and activation of apical A_1AR triggered apical exocytosis that mirrored late phase stretch-mediated apical

exocytosis. Further, I report that the exocytosis was dependent of EGFR transactivation, and ADAM17 is the metalloproteinase that mediated this pathway. In the following section, I will introduce ADAMs and ADAM17 in particular.

Figure 8 EGFR transactivation



The numerous extracellular stimuli that trigger EGFR transactivation, the known intermediate molecules, the list of ADAMs that cleave the EGFR ligands and the list of EGFR ligands that are involved in the transactivation pathway are shown.

1.5 A DISINTEGRIN AND A METALLOPROTEINASE (ADAM)

1.5.1 Introduction

ADAMs (a disintegrin and a metalloproteinase) belong to the family of metalloproteinases called metzincins. They contain a zinc cation at their active site which imparts the catalytic property of these enzymes (203). Structurally, they closely resemble class III snake venom metalloenzymes or reprotins. To date 21 functional ADAM proteins have been identified in the human genome, out of which only 13 have the HEXXHXXGXXHD motif, a characteristic of the reprotin-type catalytic site, and hence are presumed to be catalytically active (204).

Of the catalytically active ADAMs, 20, 21 and 30 are expressed in the testis and play roles in the capacitation of the sperm and fusion of sperm and egg. ADAMs 9, 10, 12, 15, 17, 19 and 33 are widely expressed in somatic cells and are involved in the ectodomain processing of numerous transmembrane proteins (204,205). Though not widely studied, ADAMs 9, 12, 11, 15 and 28 display splice variants (206-209). At least one report has shown that ADAM17 displays a splice variant called SPRACT consisting of mostly the cytoplasmic tail (210). The physiological relevance of the splice variants and their role in ectodomain shedding are not well understood.

1.5.2 Subcellular localization, domain architecture and functional regulation of ADAMs

ADAMs are single pass transmembrane proteins that contain an N-terminal signal sequence, followed by a pro-domain, a metalloproteinase domain, a cysteine-rich domain, an EGF-like domain, transmembrane domain and a cytoplasmic tail. Studies indicate that the functional site of the protein is at the cell surface (201,211,212). However, other reports have suggested that the

metalloproteinase activity of ADAMs 10, 17 and 19 can also be detected in intracellular compartments (213,214).

The catalytic domain has the conserved HEXXH motif (215,216). The active site contains a zinc ion and water atoms that are required for the hydrolytic processing of the substrates. The processing is aided by three histidines and a methionine which faces the conserved motif [refer to (217) for the structure of the catalytic site].

The disintegrin domain gets its name because of high sequence similarity to snake-venom disintegrins (218). Disintegrins found in viper venom functions as an inhibitor of platelet aggregation and integrin-dependent cell adhesion. They contain the RGD peptide sequence, that binds with great affinity to the integrin IIa and IIb receptors on the surface of blood platelets and prevent aggregation by blocking fibrinogen binding. However, with the exception of ADAM15, none of the ADAMs contain the RGD motif which is a functionally important amino acid sequence present in the snake-disintegrins. Nevertheless, the disintegrin domain and cysteine rich domain have been suggested to play a role in the substrate specificity of the ADAMs (219,220).

The cytoplasmic tails of ADAMs contain numerous motifs that may play important roles in the post-translational modification of the protein.

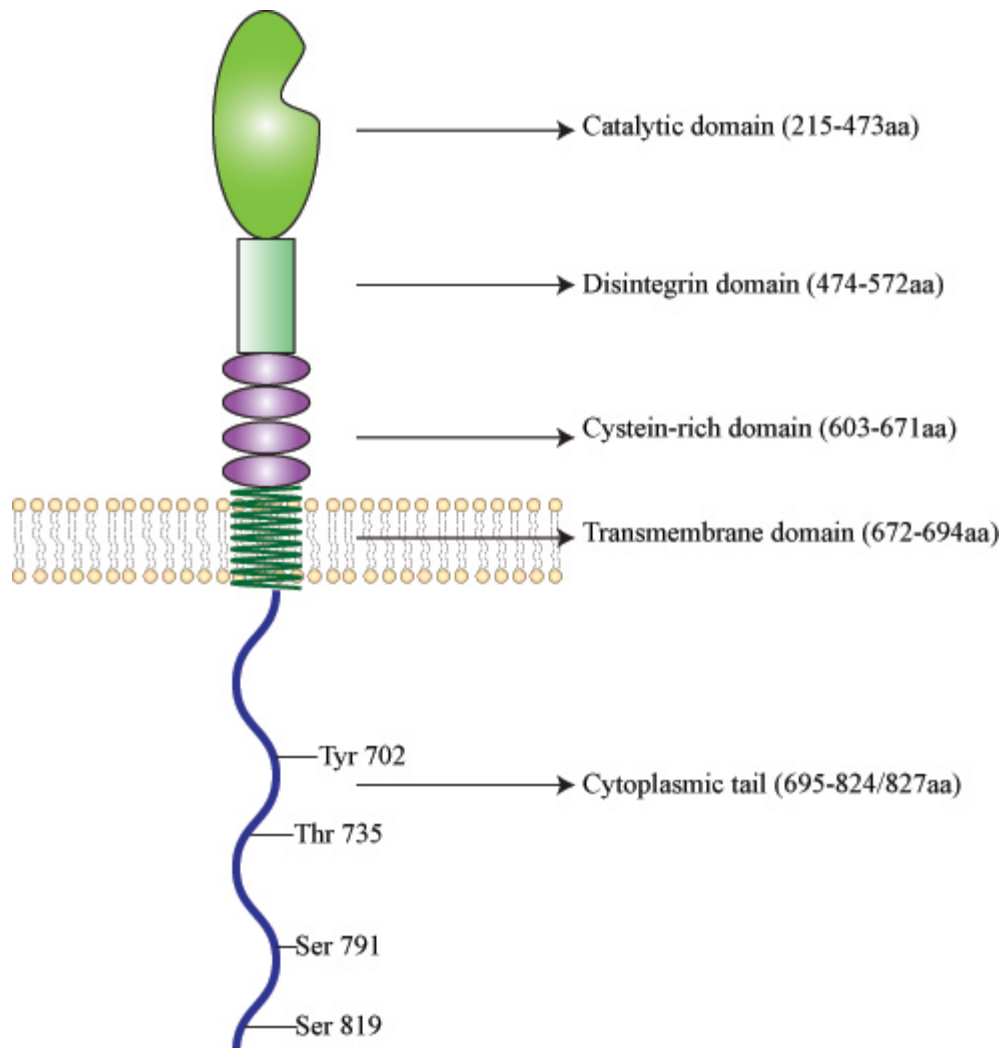
1.5.3 ADAM17

ADAM17, discovered in 1997 by two separate groups, is the metalloproteinase responsible for the cleavage and release of membrane-bound tumor necrosis factor- α (TNF- α). Therefore, it is also called TNF- α cleaving enzyme (TACE) (215,216). Because of the crucial role played by TNF- α in inflammation, the identification of the metalloproteinase that processes the cytokine

was a significant discovery. It is a transmembrane protein spanning 824 amino acids in humans and 827 amino acids in rats and mice. It is widely expressed in most tissues including heart, lungs, brain, kidney, skeletal muscles and the bladder (205). In addition, ADAM17-mediated ectodomain cleavage plays an important role during embryonic development (221).

Because of the wide array of substrates that ADAM17 handles, it has a major impact in the manifestation of many diseases. Elevated ADAM17 levels were found in patients suffering from inflammatory diseases such as osteoarthritis, rheumatoid arthritis and early systemic sclerosis. Further, ADAM17 plays an indirect role in inflammatory disease manifestation by cleaving a host of molecules such as L-selectins, JAM-1 and V-CAM which play critical roles in leukocyte activation and diapedesis (205,222). The role of ADAM17 in pulmonary inflammation, psoriasis, inflammatory bowel disease, septic shock, Alzheimer's disease, multiple sclerosis, cardio-vascular diseases, diabetes, kidney disorders and a wide range of malignancies have also been discovered (205). These reports further highlight the significant role played by ADAM17 in normal physiology. Therefore, it is clinically relevant to understand how ADAM17 is regulated at the transcriptional, translational and post-translational level.

Figure 9 ADAM17 domain architecture



ADAM17 domain architecture: The different domains of ADAM17 once it reaches the cell surface are shown. The known phosphorylation sites in the cytoplasmic tail are also shown.

1.5.4 Molecular structure and regulation of ADAM17 activity

ADAM17 protein consists of the following domains: a signal sequence (1-17aa), a prodomain (18-214aa), a catalytic domain which contains the HEXXHXXGXXHD domain (215-473aa), a disintegrin domain (474-572aa), a cysteine-rich domain (603-671aa), a transmembrane domain (672-694aa), and a cytoplasmic tail (695-824aa in humans and 827aa in rats and mice) (Figure 9). The protein has numerous N-glycosylation sites, which may play a role in the regulation of its function. Similar to other ADAMs the prodomain maintains the catalytic site in an inactive state. In a protein chimera study where ADAM9 and ADAM10 prodomains were used to inhibit ADAM17 catalytic function, the key inhibitory amino acid was identified as Phe72 and the Asp-Asp-Val-Ile (residues 134-137) motif (223). Others have identified a 19-amino acid leucin-rich region from amino acids 30-48 to play role in partial ADAM17 autoinhibition (224). The prodomain is however cleaved by furin at the last four amino acids (Arg-Val-Lys-Arg) preceding the catalytic site as the protein traverses through the trans-Golgi network (225,226). Interestingly, reports have indicated that the prodomain remains non-covalently bound to the mature ADAM17 even after furin-mediated cleavage, and plays a role in the proper trafficking of the enzyme (227,228).

The catalytic domain cleaves ectodomains of numerous substrates, but the substrate specificity and the identity of the amino acid sequences identified in the substrates by ADAM17 is not clearly understood. While in TNF α , the sequence was identified to be Ala76/Val77 (-Arg-Ser-Ser-Ser) (229), in growth hormone receptor proteolysis, the cleavage site was identified as the eighth residue from the cell membrane (226). It is believed that the sequence of the substrate is less important when compared to the position of the sequence. ADAM17 seems to prefer

cleaving ectodomains at the ‘stalk region’ between the transmembrane region and the first globular part of the extracellular domain of the substrates.

The catalytically active form of ADAM17 is released from the *trans*-Golgi network and reaches the cell surface. However, the enzyme does not indiscriminately cleave substrates, it requires a secondary signal, such as activation of GPCRs, ROS, UV irradiation or mechanical sheer stress to initiate a signaling pathway that ‘triggers’ ADAM17 to cleave its substrates. A prominent question in the field of ADAM17 research is: *how do external stimuli trigger ADAM17 activity?*

1.5.5 Regulation of ADAM17 activity

Inside-out signaling

Understandably, the cytoplasmic-tail of ADAM17 has been intensively studied to identify protein binding partners that activate an inside-out signal response. These studies are driven by the fact that the 130aa length cytoplasmic tail of ADAM17 has a rich array of conserved motifs and protein binding sites. It contains a potential tyrosine phosphorylation site DKKLDKQYESL proximal to the transmembrane domain and an SH-3 binding site (731-738) PAPQTPGR. Thr735 in the cytoplasmic tail has been shown to be phosphorylated by ERK and p38 in response to phorbol-ester (PMA) and EGF treatments in transfected HEK293 cells (202,230). Other studies have shown that Ser819 is phosphorylated by ERK in response to PMA, though the phosphorylation did not seem to affect the activity of the protein. Interestingly, it was shown that Ser791 undergoes dephosphorylation in response to growth factor stimulation (210).

Though numerous studies have used PMA as an activator of ADAM17, few studies have focused on physiological activation of the enzyme. Zhang *et.al* showed that phosphoinositide

kinase-1 (PKD1) directly phosphorylates serine and threonine residue in the cytoplasmic tail in response to activation by the GPCR-ligand gastric releasing peptide (231). In another study, mechanical stretching triggered src-mediated phosphorylation ADAM17 at Tyr702 in C2C12 cells (232).

Apart from phosphorylation studies, numerous proteins have been found to be bound to the cytoplasmic tail of the enzyme. Yeast two hybrid (Y2H) studies revealed that Mitotic arrest deficient (MAD2) protein bound between residues 706-740 in the cytoplasmic tail of ADAM17 (233). Though the functional significance of this interaction is not clear, the data indicates that ADAM17 plays a role in cell cycle progression. Furthermore Y2H studies identified SAP9, which promoted ADAM17 activity by binding to the cytoplasmic domains of ADAM17 and TGF α (234). A possible mechanism of ADAM17 regulation could be via binding partners such as SAP9 that bind both the cytoplasmic tails of the substrate and the enzyme and thus brings them into closer proximity. Y2H studies also identified Eve-1, which also promoted catalytic function of the enzyme (235). Another protein, four-and-half LIM domain 2 protein (FHL2) interacts with ADAM17 between amino acids 721-739 and also the cytoskeleton and hence could potentially regulate the localization and activity of the enzyme (236). A study showed that that cytoplasmic tail of ADAM17 and ADAM10 interact with ACE-s (angiotensin converting enzyme-2) and facilitate entry of severe acute respiratory syndrome (SARS) causing coronavirus into the host cells (237).

While these data underscore the importance of the cytoplasmic tail of ADAM17 and suggests an inside-out mechanism of regulation, where phosphorylation or binding of other protein partners could modulate the catalytic activity of enzyme, another set of studies indicate that the cytoplasmic tail of the enzyme is dispensable for the catalytic activity of the protein.

Cytoplasmic-tail-independent ADAM17 regulation

Blobel *et. al* has shown that the ADAM17 constructs which lacked the cytoplasmic tail were still functional and trafficked to the cell surface which is the site of activity of the enzyme (238,239). In support of this, others have found that PKC-mediated phosphorylation of the substrate but not the enzyme or conformational changes in the substrate are critical for the substrate specificity and function of the enzyme (166,240). Further, the redox state of two highly conserved cysteine-X-X-cysteine group in the disintegrin domain of the enzyme is also known to play an important role in regulating ADAM17 activity, as discovered by its role in L-selectin secretion (241).

In conclusion, we still require a deeper understanding of the mode or function of ADAM17 and how it is regulated by a complex network of cellular signals that integrate extracellular stimuli with intracellular events such as protein trafficking, exocytosis, endocytosis and cellular morphological changes.

Tissue inhibitors of metalloproteinases

Tissue inhibitors of metalloproteinases (TIMPs) are endogenously expressed proteins that bind and inactivate metalloproteinases. TIMP3 is released into the extracellular space, where it binds directly to the catalytic domain to ADAM17 in a 1:1 ratio. It is thought to be highly specific for ADAM17 (242). TIMP3 binds to the catalytic site of ADAM17 and keeps it in a dormant state. The enzyme regains activity when TIMP3 binding is removed (243). Therefore, many studies have focused on the activity of TIMP3 in regulating ADAM17. In a fascinating model that was recently reported, TIMP (possible dimers) binds ADAM17 dimers at the cell surface and keeps the enzyme in the inactive state. On activation of the enzyme by phosphorylation of the cytoplasmic tail, the dimerization is disrupted, thus removing TIMP3

inhibition. How exactly phosphorylation leads to monomerization of ADAM17 is yet to be understood, but a possible mechanism could be: phosphorylation could lead to binding of yet unknown proteins to the cytoplasmic tail of ADAM17 that causes monomerization of the enzyme (244). This data however, has been refuted by a study which found that TIMP3 binding does not affect ADAM17 activation (238).

1.5.6 Role of ADAM17 in EGFR transactivation

The role of ADAM17 in activating EGFR is of particular importance to this dissertation and hence warrants a brief overview of what is known so far in this regard. The ectodomain shedding function of ADAMs is one of the most well studied features of these metalloproteinases. The consequence of ectodomain shedding is to allow a membrane-tethered growth factor or cytokine to participate in paracrine signaling or enter the blood stream and carry the signal to distant regions. Although other somatically expressed ADAMs including ADAM 9, 12 and 15 have been shown to process EGFR ligands, knockout studies revealed that these ADAMS are not essential for EGFR activation (245). However, ADAM17 and ADAM10 together act as molecular switches that regulate the proteolytic processing of all seven known EGFR ligands. Specifically, ADAM17 was found to be the physiological metalloproteinase involved in the processing of EGFR ligands including TGF α , HB-EGF, epiregulin, epigen and amphiregulin (245,246).

An important landmark in the study of ADAM17 came in 1998 when *in vivo* studies in Adam17 ^{Δ Zn/ Δ Zn} mice (which contain a mutation in the ADAM17 active site) revealed that these animals had abnormalities that resemble TGF α ^{-/-} such as defective maturation and

morphogenesis of epithelial structures including eyelid fusion and defective release of pro-TGF α (247-249). Exon deletion studies and genetically modified mice expressing ADAM17 versions lacking several key residues displayed the classic *woe* (waved with open eyes) phenotype which is a hallmark of defective EGFR signaling (250). In addition, *Adam17 Δ Zn/ Δ Zn* mice die between embryonic day 17.5 and their first day of birth with numerous defects including those that affect their eyes, their coat, and several of their organs. Furthermore, the phenotypes observed in *Adam17 Δ Zn/ Δ Zn* mice are phenocopied in TNF α ^{-/-}, TGF α ^{-/-}, HB-EGF^{-/-} knockout mice, or mice expressing an uncleavable form of HB-EGF (221,247,249,251,252), findings that are consistent with a critical role for ADAM17 in EGFR transactivation. Finally, those phenotypes associated with defective EGFR activity (e.g. open eyes at birth and defects in heart-valve morphogenesis) are observed in ADAM17^{-/-} mice, or in quadruple ADAM9^{-/-}, ADAM12^{-/-}, ADAM15^{-/-}, and ADAM17^{-/-} mice, but not in triple ADAM9^{-/-}, ADAM12^{-/-}, and ADAM15^{-/-} mice (245). These results provide further evidence that of these four ADAM members, ADAM17 is likely to be the “physiologically” relevant metalloproteinase for EGFR transactivation. Based on these studies, it is now universally accepted that ADAM17 along with ADAM10 are important for EGFR transactivation under normal physiological conditions.

1.6 EGFR TRANSACTIVATION IN MEMBRANE TRAFFICKING

1.6.1 Overview of the physiological importance of EGFR transactivation

Cross-communication between diverse signaling pathways is essential for the translation of complex environmental stimuli into appropriate cellular reactions and adaptations. The transactivation phenomenon has placed EGFR at the convergence point of diverse extracellular stimuli. Cellular signaling components including GPCR ligands, cytokine and chemokines, cell adhesion elements, and environmental factors including UV and gamma radiation, osmotic shock, membrane depolarization, heavy metal ions, reactive oxygen species and sheer stress all trigger signaling pathways which result in activation of ADAMs (especially ADAM17), leading to the release of one or more of the seven EGFR ligands, which in-turn bind and activate EGFR (177). Thus EGFR signaling is critical for most functions of the cell and aberrant signaling can results in numerous developmental defects, metabolic disorders and cancer.

1.6.2 EGFR transactivation in secretion and membrane trafficking

One feature of polarized epithelial cells that is of special interest is membrane trafficking and exocytosis. Little is known about the role of EGFR transactivation in membrane trafficking. Previous work from Dr. Apodaca's lab have shown that mechanical stretching of the uroepithelium results in a late phase, slow apical exocytosis of umbrella cells, that is dependent on EGFR transactivation. However, the upstream signaling events or the metalloproteinase that is involved in the transactivation was unknown (43). Kanno *et.al* reported that in goblet cells that line the upper and lower epithelial lining of the eyelids, activation of M1 and M2 muscarinic

GPCR triggered EGFR transactivation and exocytosis resulting in secretion of mucin. The pathway involved the activation of Pyk2 and Src, which in-turn lead to EGFR phosphorylation. However, the ADAM involved in the transactivation pathway was not determined (176). In prostate cancers, parathyroid hormone-related protein (PTHrP), which plays an important role in bone formation and development, is released in higher amounts by the malignant organ. Yano, *et.al* reported that the secretion of PTHrP was a result of activated calcium sensing receptors transactivating EGFR. The phosphorylation was sensitive to inhibitors of MMPs and HB-EGF. However, the identity of the MMP or ADAM was once again not determined (253). Similarly EGFR-transactivation-mediated secretion of interleukin-8, urokinase-type plasminogen, collagenase-1 and numerous other secretory components have been reported (254-256). More recently, Mostov, *et.al* reported that transcytosis of activated polymeric immunoglobulin G receptors in polarized epithelial cells is dependent on Rab11a-mediated EGFR transactivation (257).

These studies underscore the role played by EGFR transactivation in membrane trafficking and exocytosis. However, a fuller understanding of the transactivation pathway, the upstream signals that trigger the pathway, the identity of the metalloproteinase (ADAMs) , how the ADAMs are activated, and how they cleave they selectively cleave EGFR ligands are not clear. One of the goals of this dissertation was to understand the signaling mechanism that links A₁AR-mediated signaling to EGFR transactivation and how it impacts membrane trafficking events of umbrella cells.

1.7 GOALS OF THIS DISSERTATION

1.7.1 Broad focus of this dissertation

I undertook this study to understand the role played by adenosine receptors in regulating bladder function. It is the offspring of two seemingly disparate sets of evidence that were previously reported. Yu *et.al* reported that A₁AR is expressed at the apical surface of the umbrella cells and mechanical stretching of the uroepithelium resulted in release of adenosine from the apical and basolateral surfaces of the umbrella cells (53). Further, activation of the apically localized A₁ receptors results in slow apical exocytosis, the kinetics of which was similar to stretch-mediated late phase exocytosis (53). In the second study, Balestreire *et.al* reported that mechanical stretching of the uroepithelium results in EGFR-dependent late phase apical exocytosis (43). This dissertation is a bridge between the two studies. The goal of this dissertation is to understand a global picture of the cellular events of the umbrella cells where diverse signals and extracellular stimuli converge onto a common pathway and results in membrane trafficking.

1.7.2 Goal 1: To study the mechanism behind adenosine release and turnover in the bladder and understand the physiological relevance of the same

In the first study I focus on adenosine release and turnover at the apical and basolateral surfaces of the umbrella cells. As mentioned earlier, the umbrella cells express all four adenosine receptors and release adenosine from the apical and basolateral surfaces on mechanical stretching. The goal was to study the impact of this adenosine released upon stretching on the

overall regulation of bladder activity. I found that the level of adenosine on the mucosal surface of the uroepithelium is kept in check by adenosine deaminase and ENTs whereas the serosal adenosine levels were regulated by adenosine kinase. Further, specific activation of A₁AR at the apical surface of the umbrella cells lowered the threshold pressure of bladder voiding. Intriguingly, in cyclophosphamide-induced bladder hyperactivity, I found that activation of the A₁AR exacerbated the condition and did not ameliorate it as expected. Similar results were later reported by Aronsson *et.al* (134).

1.7.3 Goal 2: To understand how activation of apically localized A₁AR triggered apical exocytosis in umbrella cells

In the second section of this dissertation, I focused on the signaling events downstream of A₁AR activation that lead to apical exocytosis. Intriguingly, activation of apically localized A₁AR triggered an exocytic response at the apical surface of umbrella cells that was very similar to the late phase stretch-mediated apical exocytosis. In addition, the exocytosis required protein synthesis and was sensitive to treatment with Brefeldin A. Because, these results were similar to EGFR transactivation-mediated late phase exocytosis, I tested the hypothesis that A₁AR triggered apical exocytosis by transactivating apical EGFR. This hypothesis indeed turned out to be true and ADAM17 was identified as the critical player that linked A₁AR signaling to EGFR transactivation. ADAM17 is expressed at the apical surface of the umbrella cells and activation of A₁AR by a receptor specific agonist triggered an A₁AR→G_i→G_{βγ}→PLC→PKC signaling cascade that resulted in ADAM17 activation. ADAM17 in-turn cleaved HB-EGF which activated EGFR and initiated downstream ERK1/2 signaling leading to protein synthesis and exocytosis. Further, ADAM17 was also found to be important in stretch-mediated EGFR

transactivation and exocytosis through the signaling pathway that links mechanical stretching to ADAM17 activation is yet to be identified.

1.7.4 Summary

In summary, this dissertation furthers our understanding of the role of adenosine in regulating bladder function and A₁AR-mediated membrane trafficking in umbrella cells. This work also underlines the importance of EGFR signaling in regulating membrane trafficking umbrella cells. Interestingly, ADAM17 has emerged from this study as a critical membrane protein that is at the epicenter of various signaling networks. It acts as a converging point for stretch- and A₁AR-mediated membrane trafficking pathways and hence a better understanding of the function and regulation of ADAM17 is warranted.

2.0 MODULATION OF BLADDER FUNCTION BY LUMINAL ADENOSINE TURNOVER AND A₁ RECEPTOR ACTIVATION

2.1 ABSTRACT

The bladder uroepithelium transmits information to the underlying nervous and musculature systems, is under constant cyclical strain, expresses all four adenosine receptors (A₁, A_{2A}, A_{2B} and A₃), and is a site of adenosine production. Although adenosine has a well-described protective effect in several organs, there is a lack of information about adenosine turnover in the uroepithelium or whether altering luminal adenosine concentrations impacts bladder function or overactivity. We observed that the concentration of extracellular adenosine at the mucosal surface of the uroepithelium was regulated by ecto-adenosine deaminase and by equilibrative nucleoside transporters, whereas adenosine kinase and equilibrative nucleoside transporters modulated serosal levels. We further observed that enriching endogenous adenosine by blocking its routes of metabolism or direct activation of mucosal A₁ receptors with 2-chloro-N6-cyclopentyladenosine (CCPA), a selective agonist, stimulated bladder activity by lowering the threshold pressure for voiding. Finally, CCPA did not quell bladder hyperactivity in animals with acute cyclophosphamide-induced cystitis but instead exacerbated their irritated bladder phenotype. In conclusion, we find that adenosine levels at both surfaces of the uroepithelium are modulated by turnover, that blocking these pathways or stimulating A₁ receptors directly at the

luminal surface promotes bladder contractions, and that adenosine further stimulates voiding in animals with cyclophosphamide-induced cystitis.

2.2 INTRODUCTION

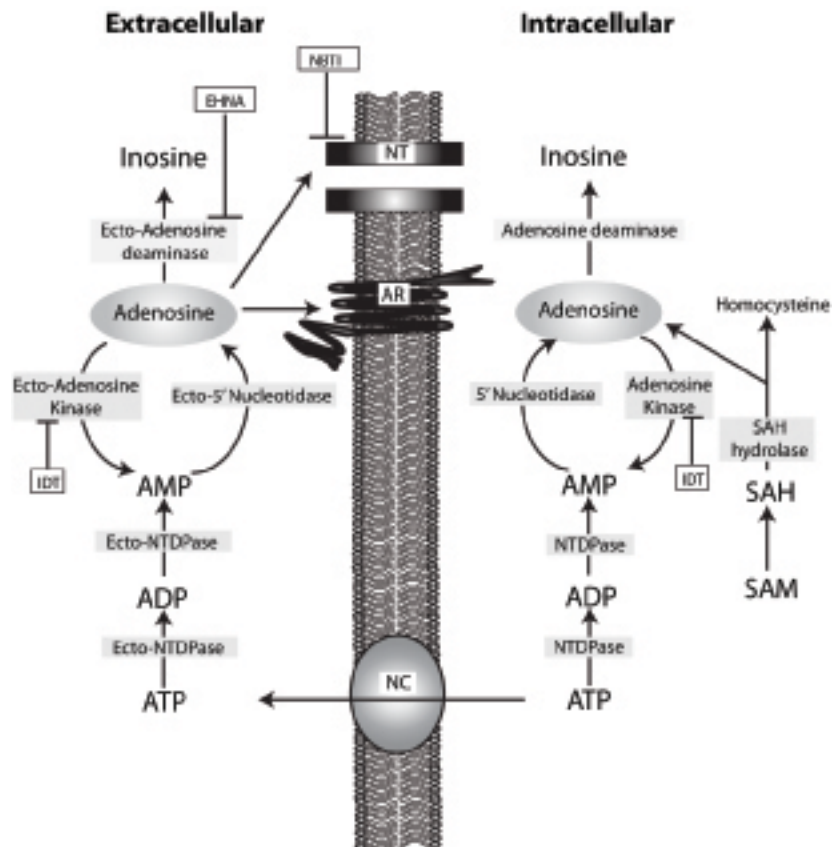
Adenosine is a ubiquitously occurring nucleoside that is important for the homeostasis of diverse organ systems including the kidneys, heart, lungs, and brain (96,258,259). It is found both intracellularly and in the extracellular space, and its concentration in these compartments is dependent on its biogenesis and turnover (260,261). The intracellular pool of adenosine is synthesized *de novo* by the hydrolysis of S-adenosylmethionine or is generated from the nucleotidase-dependent breakdown of ATP to ADP to AMP to adenosine. The extracellular pool of adenosine is also formed from the hydrolysis of ATP by ecto-nucleotidases or alkaline phosphatases or by metabolism of cAMPs to AMPs to adenosine. In addition, sodium-coupled concentrative or equilibrative nucleoside transporters shuttle adenosine in a concentration-dependent manner between the intracellular and extracellular compartments (262). The turnover of extracellular and intracellular adenosine is mediated by two enzymes: adenosine deaminase and adenosine kinase, which decrease adenosine by converting it to inosine or AMP, respectively (263-266). When present, adenosine elicits its effects on tissues by binding to and activating one or more members of a family of four heptahelical G-protein coupled receptors, which have distinct affinities for adenosine where $A_1 > A_{2A} > A_{2B} > A_3$ (95,99,267,268). The receptors are further differentiated based on their coupling to downstream heterotrimeric G proteins: A_1 and A_3 receptors couple to G_i , whereas the A_2 receptors couple to G_s .

Adenosine can counteract the effects of excitatory mediators such as ATP and also has a well-known protective effect in several organs (267). An example of the former is observed in the brain, where activation of the A₁ receptor has a sedative, anticonvulsant, and locomotor depressing effect, as opposed to the excitatory effects of P2X receptor activation by ATP (269). A prominent example of the protective effect of adenosine is seen in the heart, where during periods of metabolic stress and inflammation the concentration of extracellular adenosine increases by several orders of magnitude (99,270). Furthermore, when this organ is experimentally stimulated to produce large amounts of adenosine by exposure to short bouts of ischemia and reperfusion, there is a cardio-protective effect that limits tissue damage when the heart is exposed to a subsequent, larger occlusion (124,271). This effect is mediated downstream of adenosine receptors, which stimulate protein kinase C (PKC) and may act to alleviate stress by stimulating NO production through induction of iNOS (95,270). Likewise, treatment with an A₁ receptor agonist such as 2-chloro-N⁶-cyclopentyladenosine (CCPA) is also cardio-protective and similar roles for adenosine and its receptors have been identified in kidney and airway epithelial cells exposed to acute ischemic injuries (126,272-274). In contrast, adenosine can also potentiate events including the stimulation and activation of immune cells. For instance, activation of A_{2B} receptors in T84 cells stimulates secretion of IL-6, resulting in a Ca²⁺-mediated pro-inflammatory signaling loop (275,276).

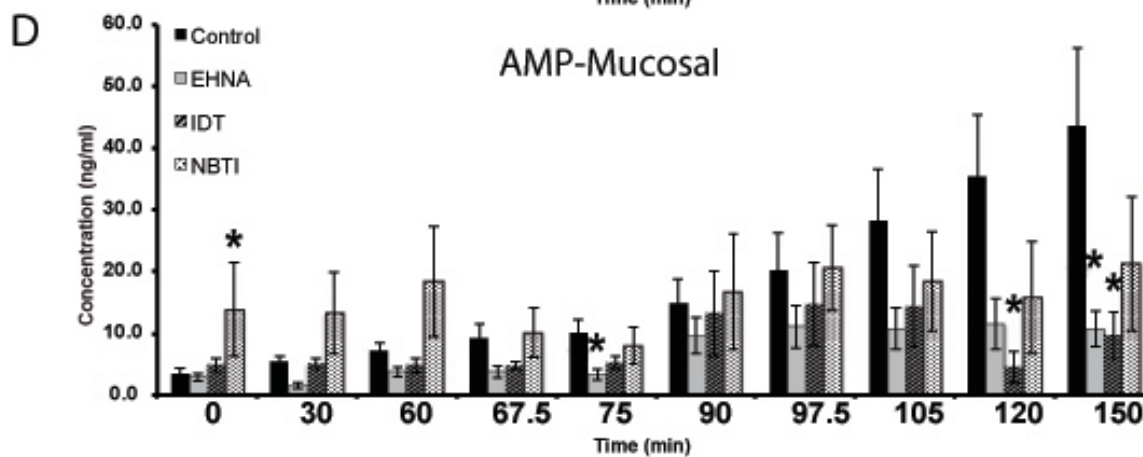
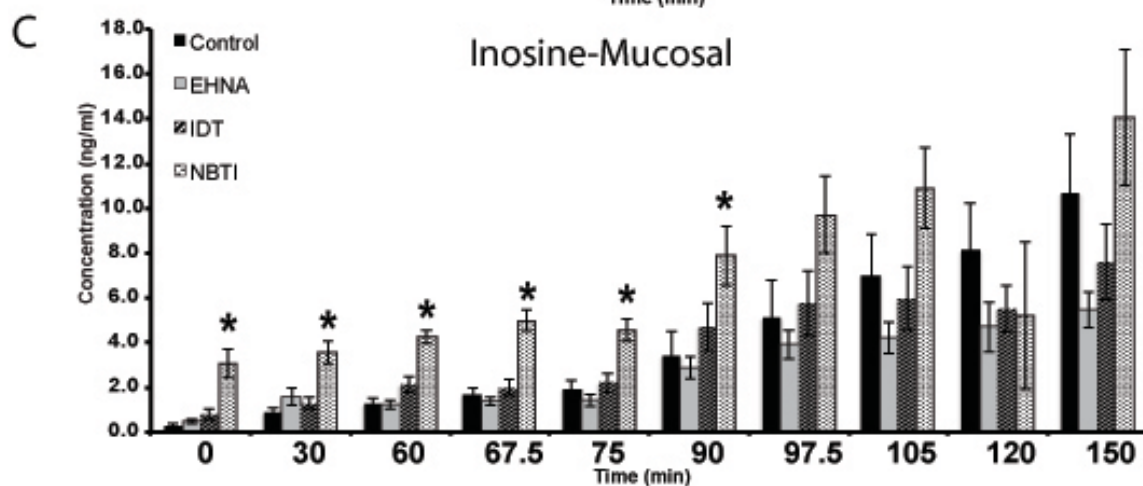
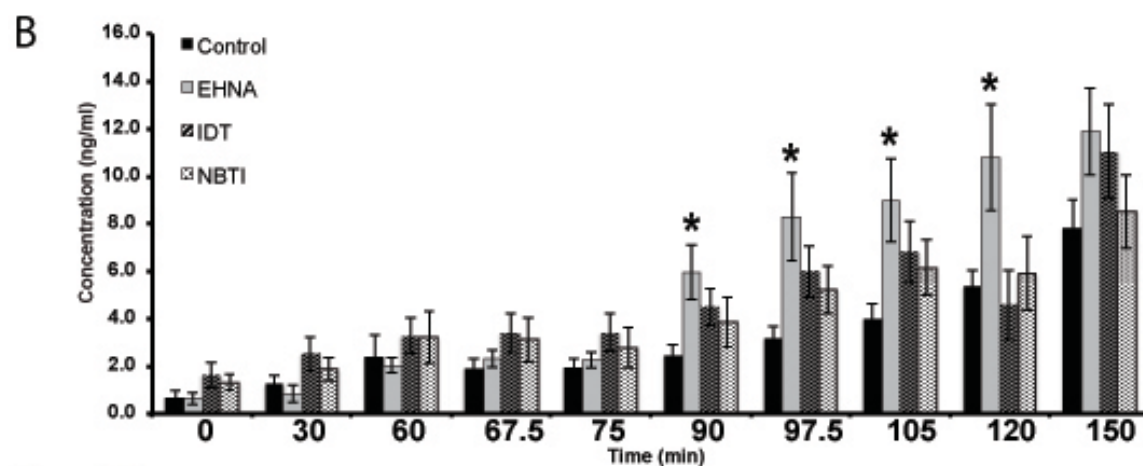
The role of adenosine in other organs and tissues, such as the bladder uroepithelium, is less well understood even though this tissue is exposed to high concentrations of waste products and is in a physiologically taxing environment that is in constant flux as the bladder fills and empties. Furthermore, the uroepithelium is not just a high resistance barrier but can act as a sensory transducer, responding to chemical and mechanical stimuli at its luminal surface by releasing

mediators such as ATP, acetylcholine, adenosine, or NO from its basal side (1,71). In turn, these mediators transmit information to the underlying nervous and muscular systems, altering bladder function. Interestingly, all four adenosine receptors are expressed in the uroepithelium and this tissue is also a site of adenosine production (53), but the mechanism(s) of adenosine turnover at the mucosal or serosal surface of the uroepithelium is unknown. Furthermore, the A₁ receptor is prominently expressed at the apical surface of the outermost umbrella cell layer and activation of this receptor by the mucosal addition of adenosine causes the umbrella cells to add apical membrane (53). However, it is not known if stimulating this lumen-facing receptor has any impact on overall bladder function, nor is there information about whether increasing adenosine concentrations can be used to quell or modulate bladder hyperactivity.

Using isolated rabbit uroepithelial tissues mounted in Ussing stretch chambers, we find that adenosine production is increased during periods of extended stress. The mechanism for modulating adenosine turnover at the mucosal surface of this tissue is adenosine deaminase or equilibrative nucleotide transporters, while adenosine kinase and nucleoside transporters keep adenosine levels in check on the basal surface. We also observe that the A₁ receptor agonist CCPA or drugs that impair adenosine turnover significantly lower the threshold pressure needed to trigger voiding in the bladders of rats undergoing cystometry. Furthermore, A₁ receptor activation causes an increase in detrusor activity in animals acutely treated with cyclophosphamide, decreasing the cycle time between voids. Our results indicate that the uroepithelium, particularly in response to stress, is an active site of adenosine production and turnover. Furthermore, increasing luminal adenosine by blocking its turnover or stimulating A₁ receptors with CCPA lowers the threshold pressure for voiding in normal bladders and increases



Adenosine-Mucosal



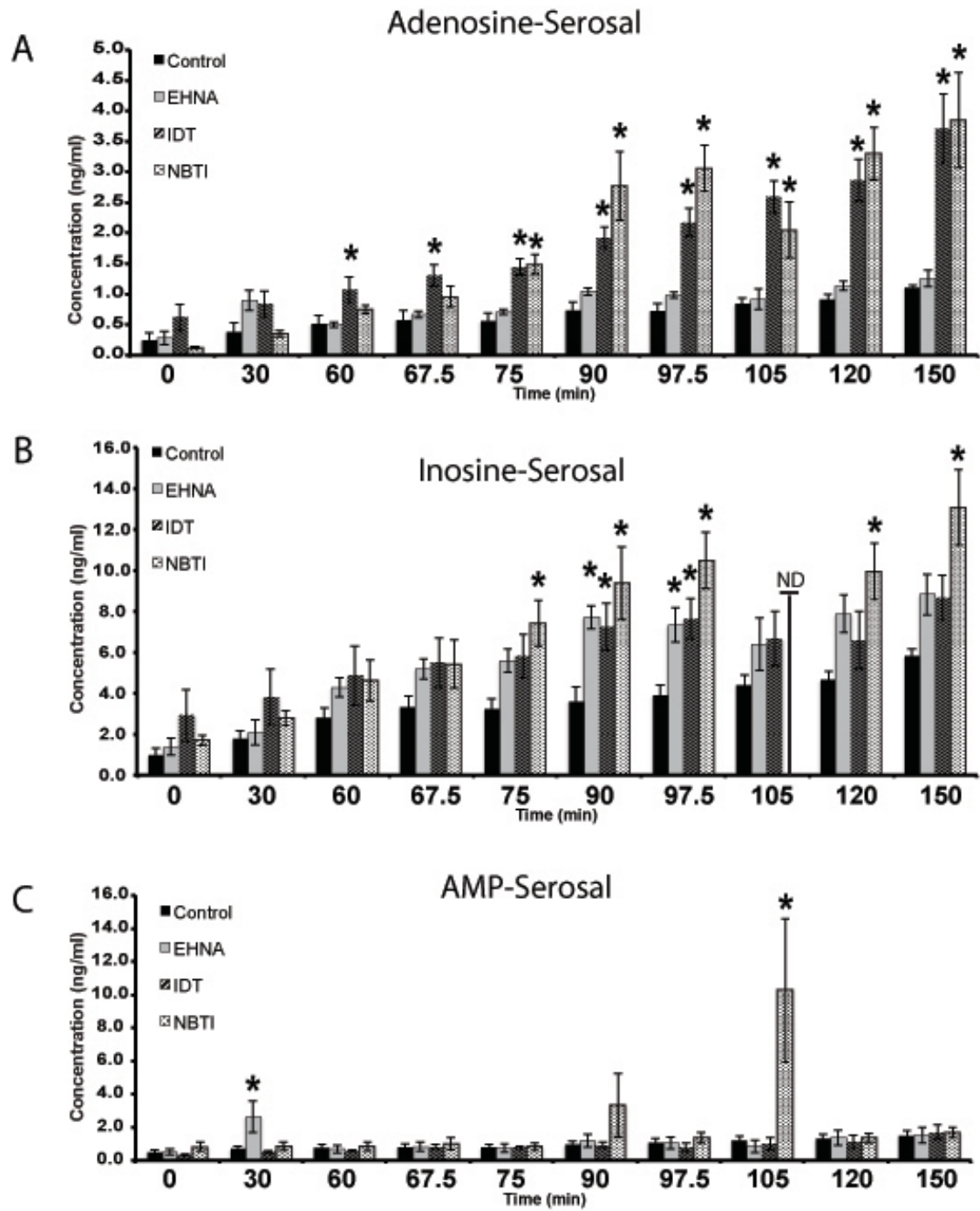
(A) Schematic of adenosine biosynthesis and turnover in the intracellular and extracellular spaces. Intracellular adenosine is formed either by the conversion of S-adenosylmethionine (SAM) to S-adenosylhomocystine (SAH) to adenosine, or by the hydrolysis of ATP. The latter is expelled from the cells via nucleotide channels (NC). The extracellular ATP is converted to adenosine by the ecto-nucleotide triphosphate diphosphohydrolases (NTDPases) ecto-NTDPase (CD39) and ecto-5' nucleotidases (CD73). Extracellular adenosine can have multiple fates: 1) transport back into the cell by nucleoside transporters (NT); 2) binding to and activation of adenosine receptors (AR); 3) metabolism to inosine by adenosine deaminase; or, 4) conversion to AMP by ecto-adenosine kinase. (B-D) Rabbit uroepithelium was mounted in Ussing stretch chambers, and pretreated with the indicated drug for 60 min prior to start of experiment. The tissue was left in its quiescent state for 60 min and then stretched by increasing the fluid in the mucosal chamber for 30 min. The tissue was then left in this stretched state for an additional 60 min. Samples were drawn at the indicated times and then analyzed by mass spectrometry to determine the concentration of adenosine, inosine and AMP. The experiment was performed on three separate occasions and the data are expressed as mean \pm SEM (control n=7, EHNA n=7, IDT n=7, NBTI n=4). Statistically significant differences ($p<0.05$) between control samples and treated ones are indicated with an asterisk.

2.3 RESULTS

2.3.1 Distinct pathways for adenosine biogenesis are found at the mucosal and serosal surfaces of the rabbit uroepithelium

Isolated rabbit uroepithelium is ideal for studying adenosine biosynthesis and turnover because the tissue can be manipulated in a physiologically relevant manner and samples can be taken from both the mucosal and serosal surfaces of the tissue. We previously showed that the adenosine concentrations increased in the fluid bathing isolated rabbit uroepithelium mounted between two halves of an Ussing stretch chamber (53). Furthermore, in response to an abrupt change in stretch, there was a large increase in the amount of adenosine found in both hemichambers of the device (53). To gain a better understanding of the relationship between adenosine production and bladder filling, we again used these isolated rabbit preparations, but employed the following stretch protocol. First, following washing, we incubated the tissue for 60 min in the absence of stretch to measure baseline production of the nucleoside. Then, to mimic the filling phase of the bladder micturition cycle, the mucosal hemichamber was slowly filled for ~ 30 min during which time the tissue was in a dynamic state as it slowly bowed outwards. At the 90 min mark, when the tissue had completely bowed outwards, filling was stopped and the tissue was incubated for an additional 60 min under this potentially more stressful “filled” state. At the indicated time points, we took samples and then measured, using ultra performance liquid chromatography-tandem mass spectrometry (LC-MS/MS), the concentration of adenosine, inosine, or AMP in the mucosal (Figure. 10) or serosal (Figure. 11) hemichambers of the stretch device.

Figure 11 Adenosine turnover at the serosal surface of the uroepithelium



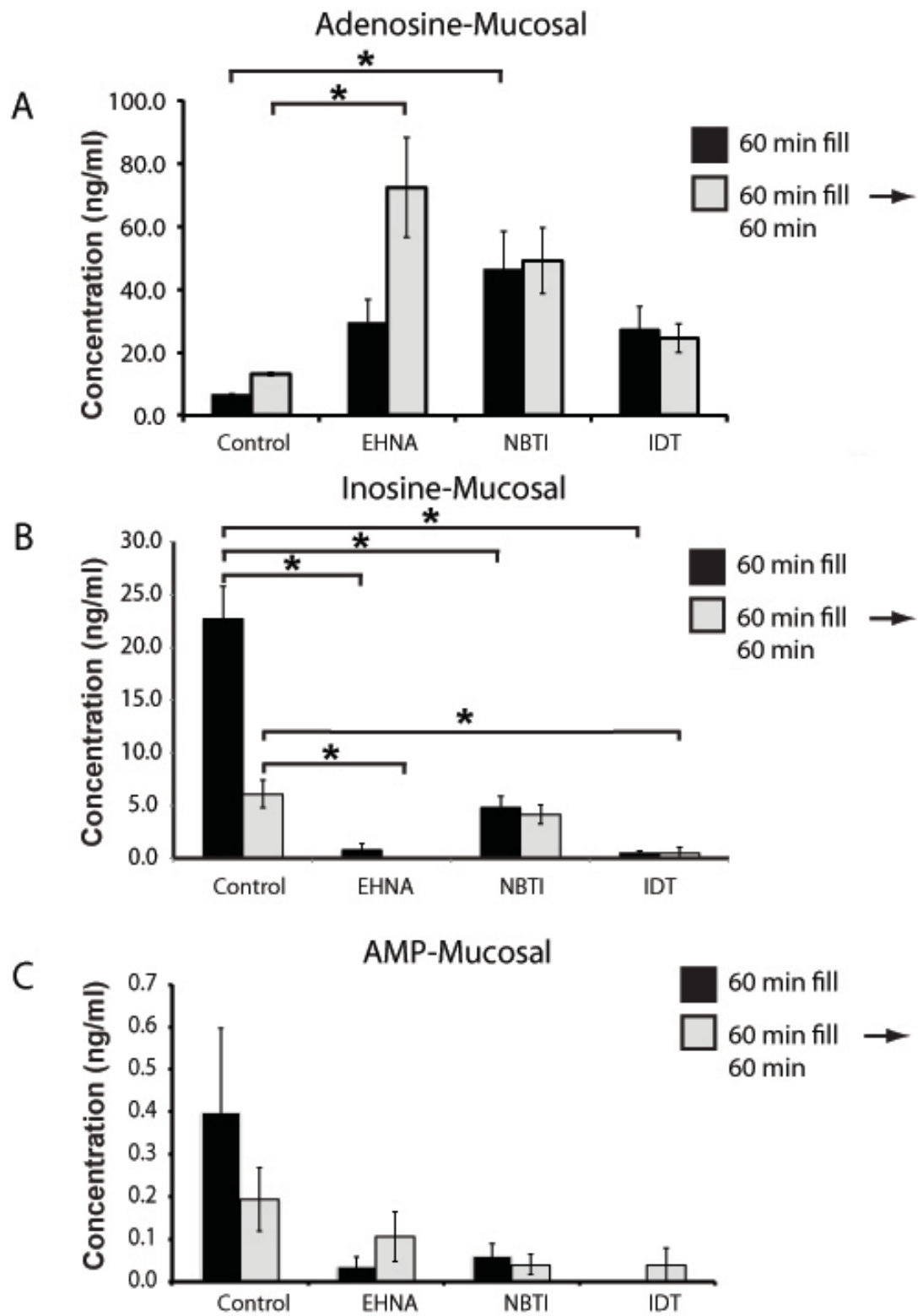
(A-C) Tissue was treated as in Figure 1, but samples were taken and analyzed from the serosal surfaces of the tissue. The data are expressed as means \pm SEM (control n=7, EHNA n=7, IDT n=7, NBTI n=4). Statistically significant differences ($p<0.05$) between control samples and treated ones are indicated with an asterisk.

We found that the concentrations of adenosine, AMP, and inosine slowly increased in the mucosal hemichamber during the first 60 min when the tissue was left un-stretched (Figure. 10 B-D). While the levels of adenosine remained somewhat stable during the period of experimental filling (i.e. 60-90 min; Figure. 10 B), the concentrations of inosine and AMP increased by ~100% or ~50%, respectively (Figure. 10 C-D). By 90 min, and during the subsequent 60 min incubation in the presence of continual stretch, there was a pronounced increase in the concentration of the three nucleosides (Figure. 10 B-D).

Next, we used inhibitors of enzymes known to be critical for adenosine turnover and assessed their impact on the levels of adenosine, AMP, and inosine. Inhibitors employed included: the adenosine deaminase inhibitor EHNA (262), the adenosine kinase inhibitor IDT (277), or the general blocker of the widely expressed equilibrative nucleoside transporter-1 NBTI (278) (Figure. 10 A). None of these drugs affected the production of adenosine in unstretched tissue or during experimental filling. However, by 90 min the concentration of adenosine in the EHNA-treated tissues was significantly increased by ~140% above that observed in the untreated samples (Figure. 10 B). The other drugs appeared to have some effect on the amounts of mucosal adenosine, but these effects did not reach statistical significance. A precursor-product relationship between mucosal adenosine and the other two nucleosides we examined was not clear-cut (Figure. 10 C-D). For example, the inosine concentrations trended downwards in tissue treated with the adenosine deaminase inhibitor EHNA but the effect was not significant. Furthermore, treatment with the nucleoside transporter inhibitor NBTI did not alter adenosine concentrations, but did significantly impact inosine concentrations in the absence of stretch or during filling (compare Figure. 10 B to 10 C).

Similar measurements were made at the serosal surface of the tissue (Figure. 11). We found that the levels of adenosine, AMP, and inosine gradually increased over the length of the experiment; however, in these control samples there was no obvious change in rates of nucleoside production during the varying tissue manipulations (Figure. 11 A-C). In contrast, treatment with the adenosine kinase inhibitor IDT caused a significant increase in serosal adenosine toward the end of experimental filling, raising its concentration by ~160%, and was also stimulatory after the 90-min time point (Figure. 11 A). Furthermore, the nucleoside transporter inhibitor NBTI also caused a large increase in the concentration of serosal adenosine, an effect that was especially enhanced at time points ≥ 90 min (Figure. 11 A). In contrast, we found no evidence that adenosine deaminase plays a significant role in modulating adenosine concentration at the serosal surface of the uroepithelium. In general, there was no obvious correlation between effects of the drug treatments on adenosine versus its metabolites AMP or inosine (Figure. 11 A-C). However, treatment with the nucleoside transport inhibitor NBTI increased inosine concentrations by ~130% during the end of the experimental filling phase, continuing into the period of extended stretch (Figure. 11 B). The AMP levels were generally unaffected by any of the drugs, except for two time points which showed large variations in values (Figure. 11 C).

Figure 12 Effect of EHNA, NBTI, or IDT on adenosine release in the rat bladder



(A-C) Rat bladders were filled with PBS containing DMSO (control), EHNA, NBTI, or IDT at a rate of 6 μ l/ min, and the intravesicle fluid collected for analysis. Subsequently, the bladder was slowly filled for 60 min, and then maintained in its filled state for an additional 60 min prior to collecting samples. The concentration of adenosine (A), inosine (B), or AMP (C) are indicated. Data are mean \pm SEM ($n \geq 4$). Significant differences ($p < 0.05$) are indicated by an asterisk

2.3.2 Adenosine release from the mucosal surface of filled rat bladders is sensitive to inhibitors of adenosine deaminase and concentrative nucleoside transporters

To further confirm that adenosine was released from the uroepithelium *in situ*, we examined the release of adenosine and its metabolites from the luminal surface of filled rat bladders. Unlike *ex vivo* tissue, we did not have access to the serosal surface of the uroepithelium in this setting. We observed that adenosine was released into the lumen after slowing filling the bladder for 60 min, and the release was further potentiated by an additional 60 min in the filled state (Figure. 12 A). Inosine and AMP were also released during bladder filling, but their levels appeared to decrease as the bladders were left in their filled state (Figure 12 B-C). The adenosine deaminase inhibitor EHNA caused adenosine concentrations to trend upwards during bladder filling (an effect that did not reach statistical significance), but did result in a significant increase in adenosine levels when the bladder was left filled for 60 min (Figure. 12 A). This was coupled with a significant decrease in inosine levels (Figure. 12 B). The nucleoside transporter inhibitor NBTI also caused a significant increase in adenosine concentrations during bladder filling and these trended higher upon extended time in the filled state, but did not reach significance (Figure. 12 A). NBTI also caused a large decrease in inosine concentrations (Figure.12 B). The adenosine kinase inhibitor IDT significantly decreased inosine concentrations, but had no effect on adenosine levels, even though these values trended higher than control ones. Finally, none of the treatments affected the concentration of AMP in the experimental groups, although the amount of AMP trended downwards in all of the treatment groups (Figure. 12 C). In sum, our data indicate that adenosine is released at the luminal surface of the bladder *in situ*, and that like isolated rabbit tissue adenosine release was sensitive to inhibition by adenosine deaminase. However, we also observed that nucleoside transporters played a more active role in rat bladder

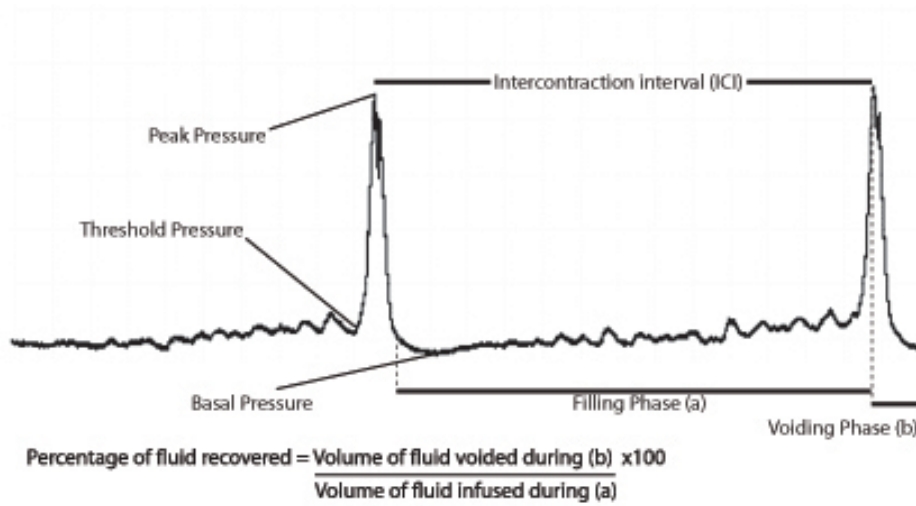
uroepithelium versus that of rabbit bladders, possibly indicating a difference between species or a difference in our methods (i.e, *ex vivo* preparations versus analysis *in situ*).

2.3.3 Stimulation of luminal A₁ receptors decreases the threshold pressure of bladders during cystometry

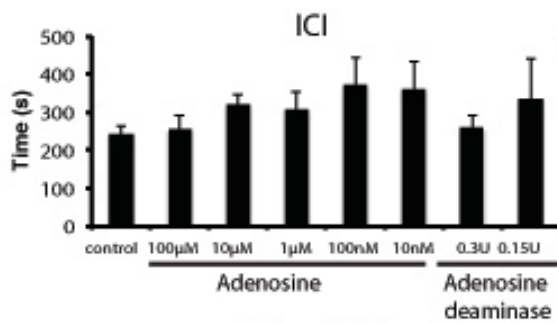
Considering its established role in modulating stress and countering the effects of stimulatory modulators such as ATP (279,280), we next sought to determine whether the luminal addition of adenosine had any impact on bladder function. To test such a role we used continuous cystometry, a technique in which a solution is introduced into the bladder lumen (via a catheter inserted in to the bladder dome) and the pressure monitored as the bladder fills and then actively empties (281). A representative cystometrogram (CMG) is shown in Figure. 13 A. We measured five parameters: 1) the basal pressure, which is the lowest pressure measured following a void; 2) the threshold pressure, which is that measured just before the detrusor contracts and voiding is initiated; 3) the peak pressure, which is the maximum pressure during detrusor contraction and coincides with voiding; 4) the inter-contraction interval (ICI), which is the distance between two peaks, and correlates with the time between two consecutive voids; 5) the percent fluid recovery, which is a ratio of the volume of fluid released versus that infused into the bladder. This latter parameter is useful to evaluate if the bladder voids efficiently or if there is fluid retention that results from, for example, a spastic urethra that does not allow complete voiding. Average values for these parameters are shown in Figure. 13.

Figure 13 Adenosine does not alter bladder function

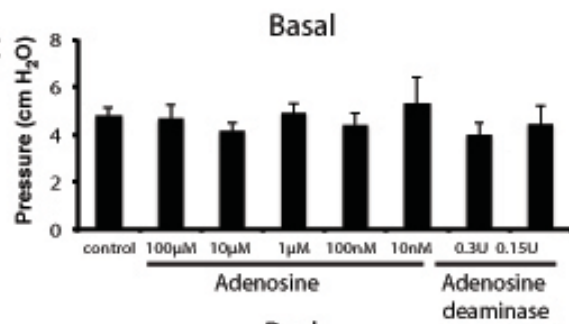
A



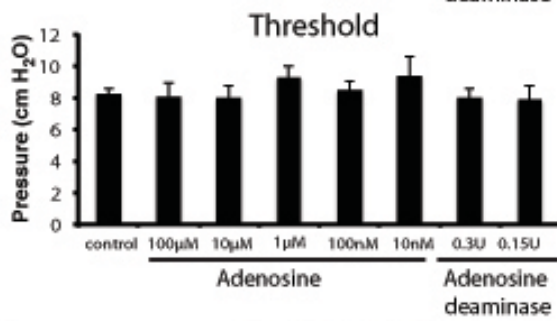
B



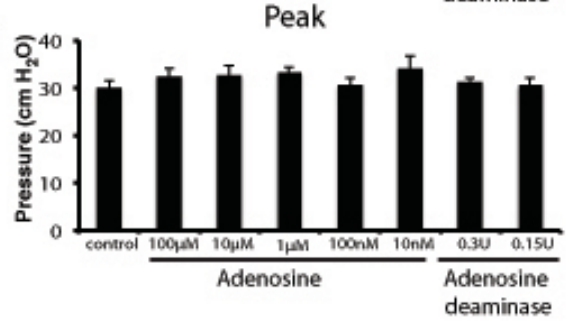
C



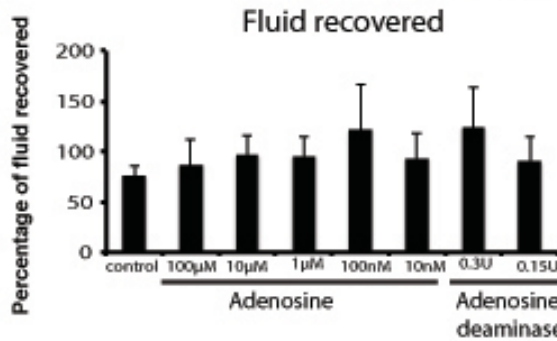
D



E



F



Continuous cystometry was performed using the indicated concentration of adenosine or adenosine deaminase dissolved in BUS. The parameters measured included ICI (B), basal pressure (C), threshold pressure (D), peak pressure (E), and fluid recovered (F). Data are expressed as mean \pm SEM (Control n=7, 100 μ M adenosine n= 8, 10 μ M adenosine n= 8, 1 μ M adenosine n= 8, 100 nM adenosine n= 9, 10 nM adenosine n= 6, 0.3 U adenosine deaminase n= 8, 0.15 U adenosine deaminase n=6). No parameters were significantly different from those of controls.

Cystometry is typically performed using unbuffered normal saline or low tonicity phosphate-buffered saline (PBS) that has a pH of 7.4. However, normal urine is decidedly more complex and contains electrolytes not found in saline or PBS. In addition, the average pH of rats housed at the University of Pittsburgh animal facility and fed rat chow was 6.5. Thus, we also tested BUS in addition to normal saline or PBS. We found that BUS had no adverse effects on the bladder and all the five parameters that we studied did not vary significantly between the three solutions (data not shown). Because BUS better reflects the physiological composition of urine, we employed it in our subsequent studies.

We first determined what happened if adenosine was introduced into the bladder lumen during cystometry. A broad range of concentrations was used (10 nM – 100 μ M), and although there was an upward trend in the ICI as the concentration of adenosine dropped, the difference failed to reach statistical significance (Figure. 13 B). Furthermore, there was no significant change in the basal pressure, threshold pressure, peak pressure, or fluid recovery (Figure. 13 C-F). We also explored what happened to the CMG parameters when adenosine levels were decreased by continuously infusing the bladder with exogenous adenosine deaminase, which converts adenosine to inosine. Again, we did not identify any significant difference between the control group parameters and those in which adenosine was depleted (Figure. 13 B-F).

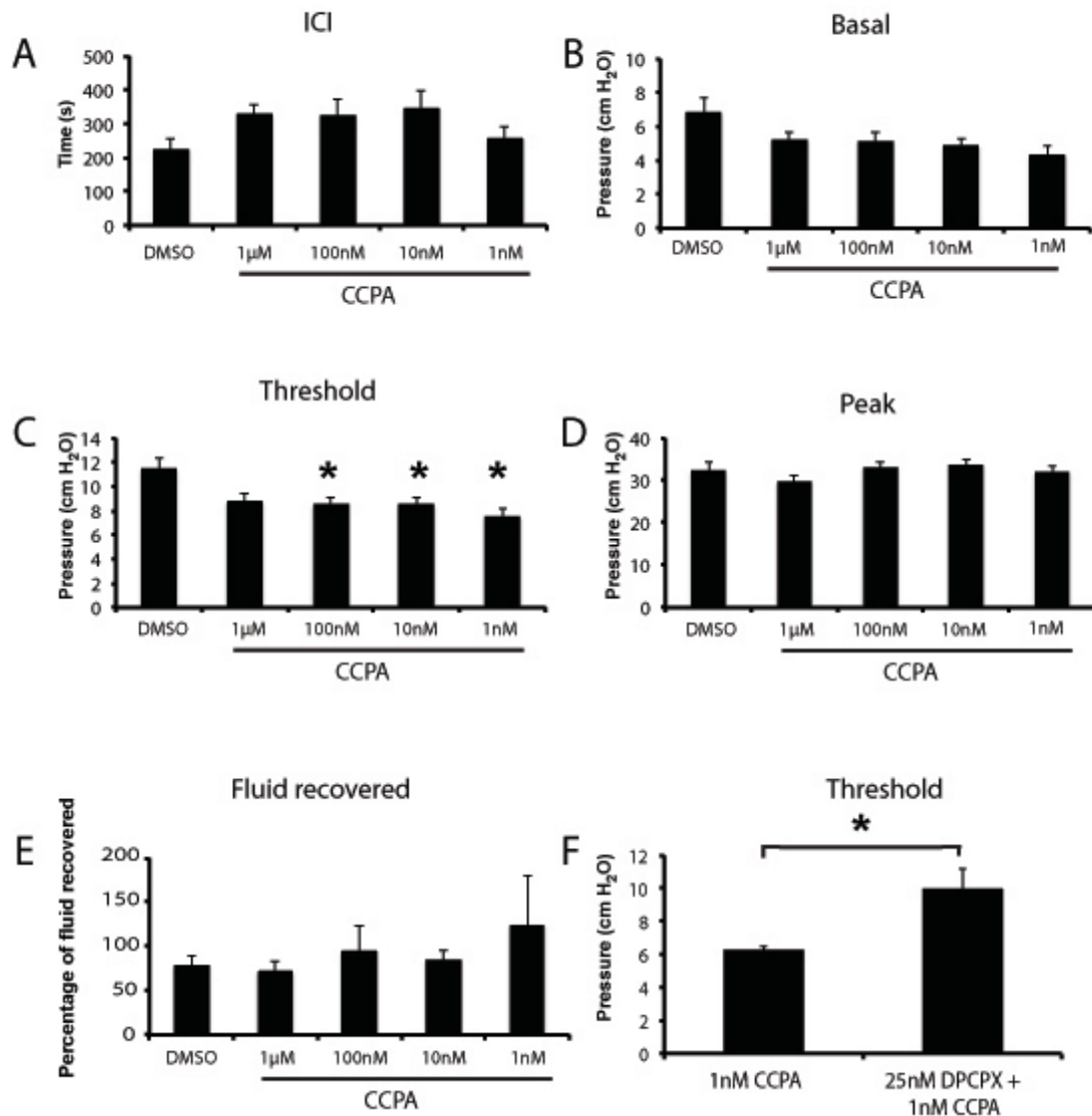
We previously reported that the apical surface of umbrella cells expresses the A₁ receptor. Hence, we infused bladders with BUS containing CCPA, which when used at low nM concentrations is an A₁-selective agonist (282). In addition to its high affinity, CCPA has other beneficial characteristics including its lack of conversion to AMP or inosine and its failure to be shuttled from the lumen to the cell interior by nucleoside transporters (283). Remarkably, when CCPA was infused at a concentration as low as 1 nM it decreased the threshold pressure by

~55% (Figure. 14 C). There was no statistically significant effect at 1 μ M, possibly because non- A_1 receptor targets were activated and counteracted the effects of CCPA-mediated A_1 receptor activation at these high concentrations. There was no significant effect on the other parameters measured (Figure. 14 A-B, D-E). To confirm that these effects were a result of A_1 receptor activation, we treated bladders with the A_1 receptor antagonist DPCPX in addition to CCPA. This blocked the effect of CCPA, and raised threshold levels back to those of controls (Figure. 14 C&F). DPCPX alone had no significant effect on the CMG parameters (data not shown). In summary, activation of luminal A_1 receptors appeared to lower the pressure needed to stimulate bladder contractions, but without changes in ICI, basal pressure, peak pressure, or fluid recovery.

2.3.4 Blocking pathways for adenosine turnover reveals an adenosine and A_1 receptor-like response

The ability of CCPA to elicit responses, but not adenosine, led us to examine whether adenosine turnover could account for the differences. We infused EHNA, IDT, or NBTI, individually or in combination, and measured the effects on bladder function. Consistent with our *in situ* rat bladder experiments, we observed that the adenosine deaminase inhibitor EHNA and the nucleoside transporter inhibitor NBTI decreased the threshold pressure for voiding (Figure. 15 C), presumably because they increased luminal adenosine concentrations. These drugs did not alter the other parameters (Figure 15 A-B and D-E). The adenosine kinase inhibitor IDT was without affect (Figure 15). As expected, treatment with all three inhibitors also decreased threshold pressure (Figure. 15 C). We also assessed whether the inhibitors of adenosine turnover would unmask a further sensitivity to exogenously added adenosine. However we found no such effect (data not shown).

Figure 14 Activation of apical A1 receptors with CCPA lowers the threshold pressure for voiding



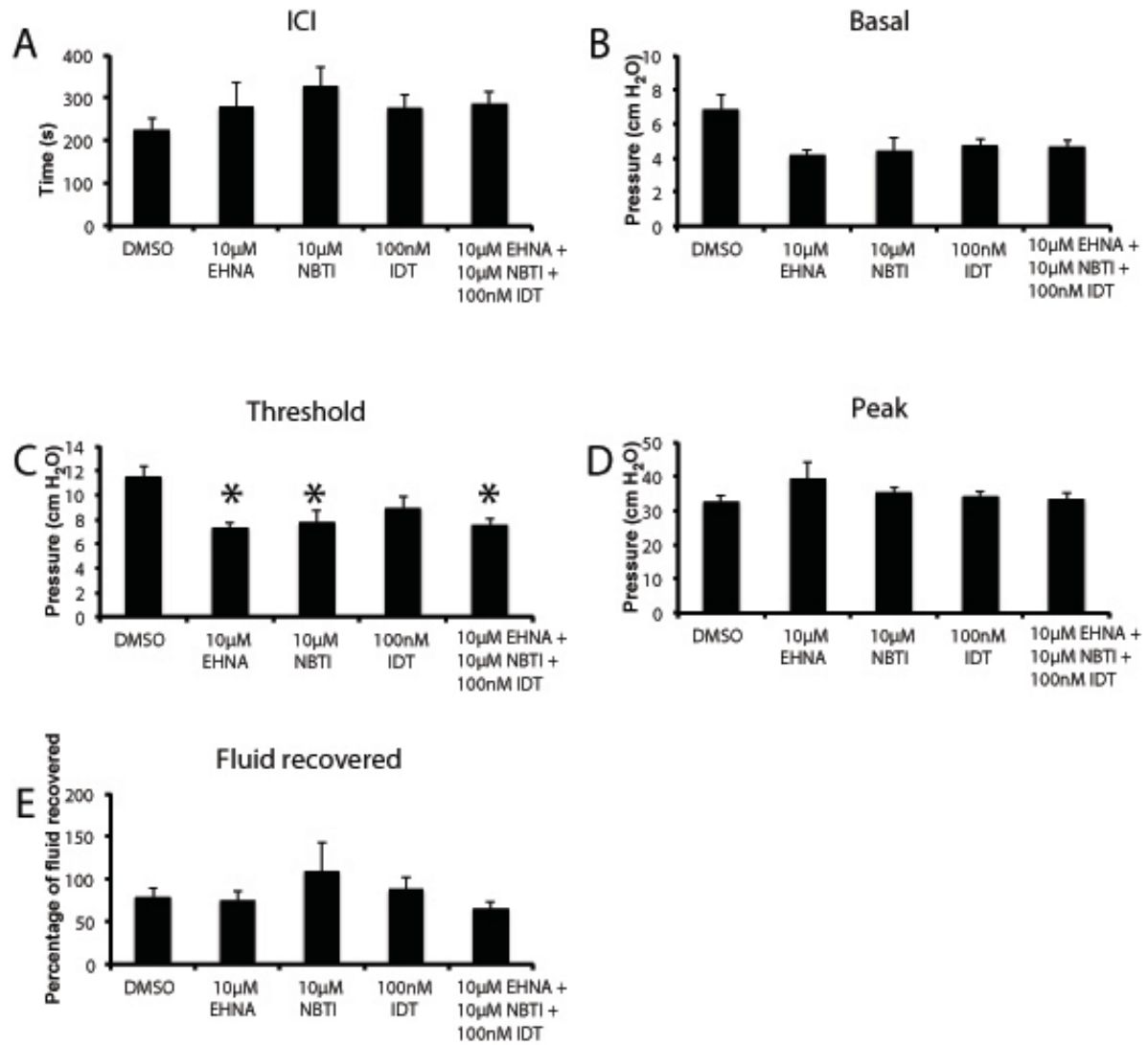
Continuous cystometry was performed using the indicated concentration of drug dissolved in BUS. (A-E) Cystometry parameters were measured as described in Fig. 4. Data are expressed as mean \pm SEM (DMSO control n=10, 1 mM CCPA n= 7, 100 nM CCPA n= 13, 10 nM CCPA n=12, 1 nM CCPA n=9). Statistically significant differences ($p<0.05$) between DMSO-treated bladders and CCPA-treated ones are indicated with an asterisk. (F) The specificity of the effect of CCPA was tested by including DPCPX in the cystometry buffer. Data are expressed a mean \pm SEM (CCPA n = 7; DPCPX + CCPA n= 8). DPCPX significantly antagonized the affects of CCPA alone.

2.3.5 A₁ receptor activation stimulates bladder activity in bladders with cyclophosphamide-induced cystitis

Finally, we determined whether adenosine modulated the hyperactivity found in bladders with acute cyclophosphamide-induced cystitis. Cyclophosphamide is a chemotherapeutic agent that is converted to acrolein and can cause a hemorrhagic cystitis within a short period of time (284). After a 4-h treatment with cyclophosphamide, we observed that this drug caused a marked decrease in ICI and an increase in the basal pressure (Figure. 16 A-B, D). The threshold pressure, peak pressure, and fluid recovery were not significantly altered (Figure. 16 C,E-F). We then treated the inflamed bladders with 10 μ M adenosine, but did not find any significant difference between control and test samples (Figure. 17 A-E). In contrast, 1 nM CCPA exacerbated the effect of cystitis by further reducing the ICI compared to animals treated with cyclophosphamide and DMSO diluent (Figure. 17 A). However, no other parameters were altered in this setting (Figure. 17 B-E).

One possible explanation for the altered effects of CCPA on cyclophosphamide-treated versus control animals is that cyclophosphamide changed the expression or distribution of A₁ receptors in the uroepithelium. However, we found that A₁ receptor expression was largely limited to the apical surfaces and subapical region of the umbrella cells in both control and cyclophosphamide-treated tissues (Figure 17 F-G). Furthermore, there was no obvious effect on the amount of A₁ receptor expressed in the uroepithelium (Figure 8H). However, we did note that the submucosal region of the cyclophosphamide-treated tissue was edematous in some regions, which appeared as large dilated regions (compare submucosa in Figure. 17 F to Figure. 17 I).

Figure 15 Inhibitors of adenosine turnover lower the threshold pressure for voiding



Continuous cystometry was performed using the indicated concentration of drug dissolved in BUS. (A-E) Comparison of CMG parameters for bladders treated with EHNA, NBTI, IDT or a cocktail containing all three inhibitors. The DMSO values in Fig. 14 are reproduced in panels A-E to aid in making comparisons (DMSO control n=10, 10 μ M EHNA n= 7, 10 μ M NBTI n= 8, 100nM IDT n= 8, drug cocktail n= 7). Statistically significant differences ($p<0.05$) between DMSO-treated bladders and those treated with drugs are indicated with an asterisk.

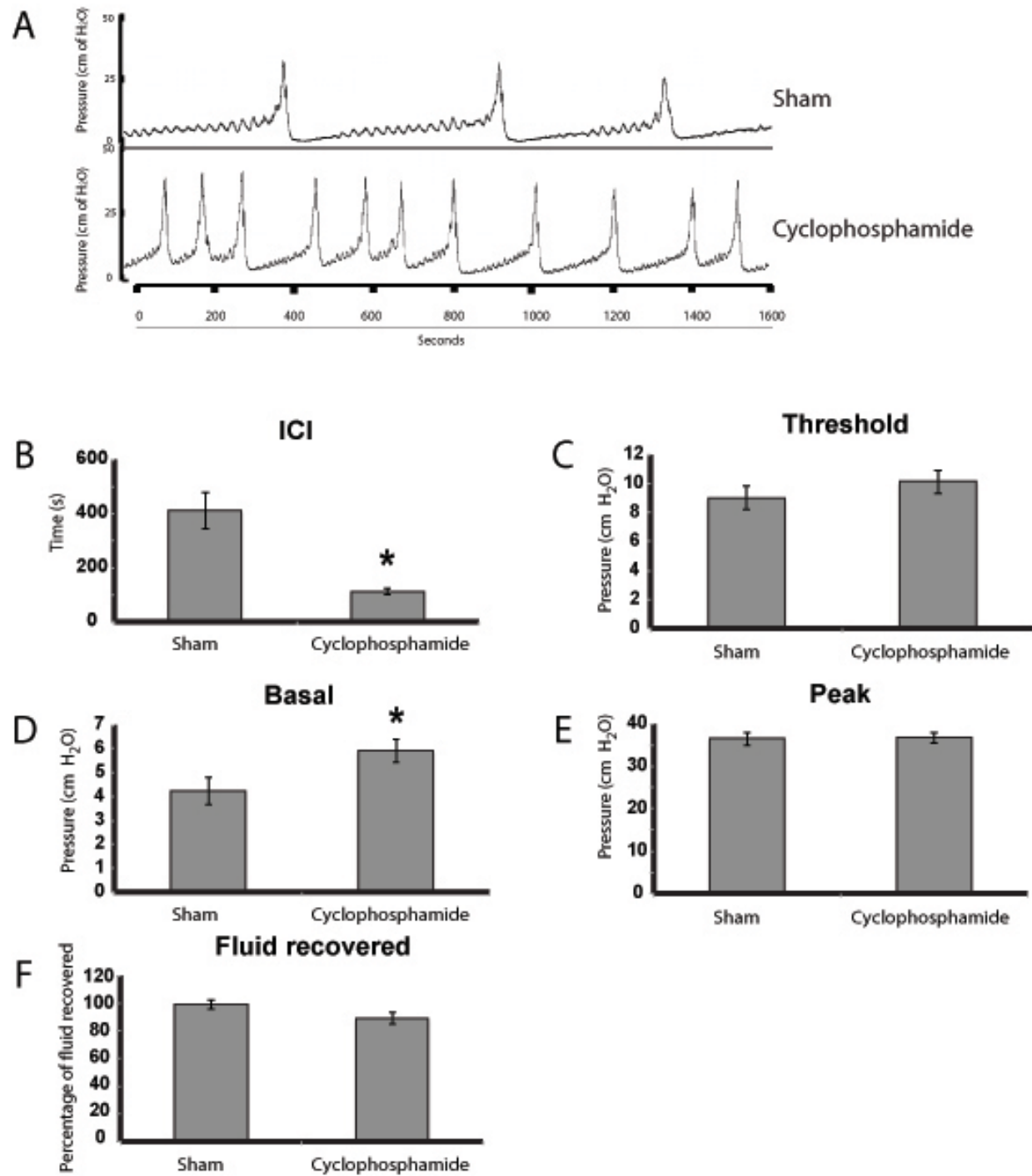
2.4 DISCUSSION

We undertook this study to determine the mechanism(s) of adenosine turnover associated with the uroepithelium and to understand whether adenosine would exert a quieting effect when its concentration was increased in the normal or inflamed bladder. Our analysis revealed that there were distinct mechanisms of adenosine turnover operating at each surface of the uroepithelium, which limited the amount of available adenosine. Furthermore, and contrary to our expectations, we observed that adenosine, likely acting through A₁ receptors, decreased the threshold pressure needed to stimulate bladder contractions and increased bladder hyperactivity in a model of cyclophosphamide-induced cystitis.

2.4.1 Distinct mechanisms of adenosine turnover at either surface of the uroepithelium

Stresses such as hypoxia promote the breakdown of extracellular ATP, leading to a sharp increase in tissue adenosine levels (267). Whereas free adenosine binds to its receptors and imparts an organ-protective function (99), chronic elevation of extracellular adenosine is harmful to the tissue (285). Hence, the half-life of extracellular adenosine is kept short (seconds to minutes, depending on species) through the action of enzymes and transporters. This may be particularly important at the luminal surface of the bladder, which is not only a site of adenosine biosynthesis, but is also impacted by adenosine produced by the kidney and present in the urine (286).

Figure 16 Cyclophosphamide treatment induces urinary bladder cystitis



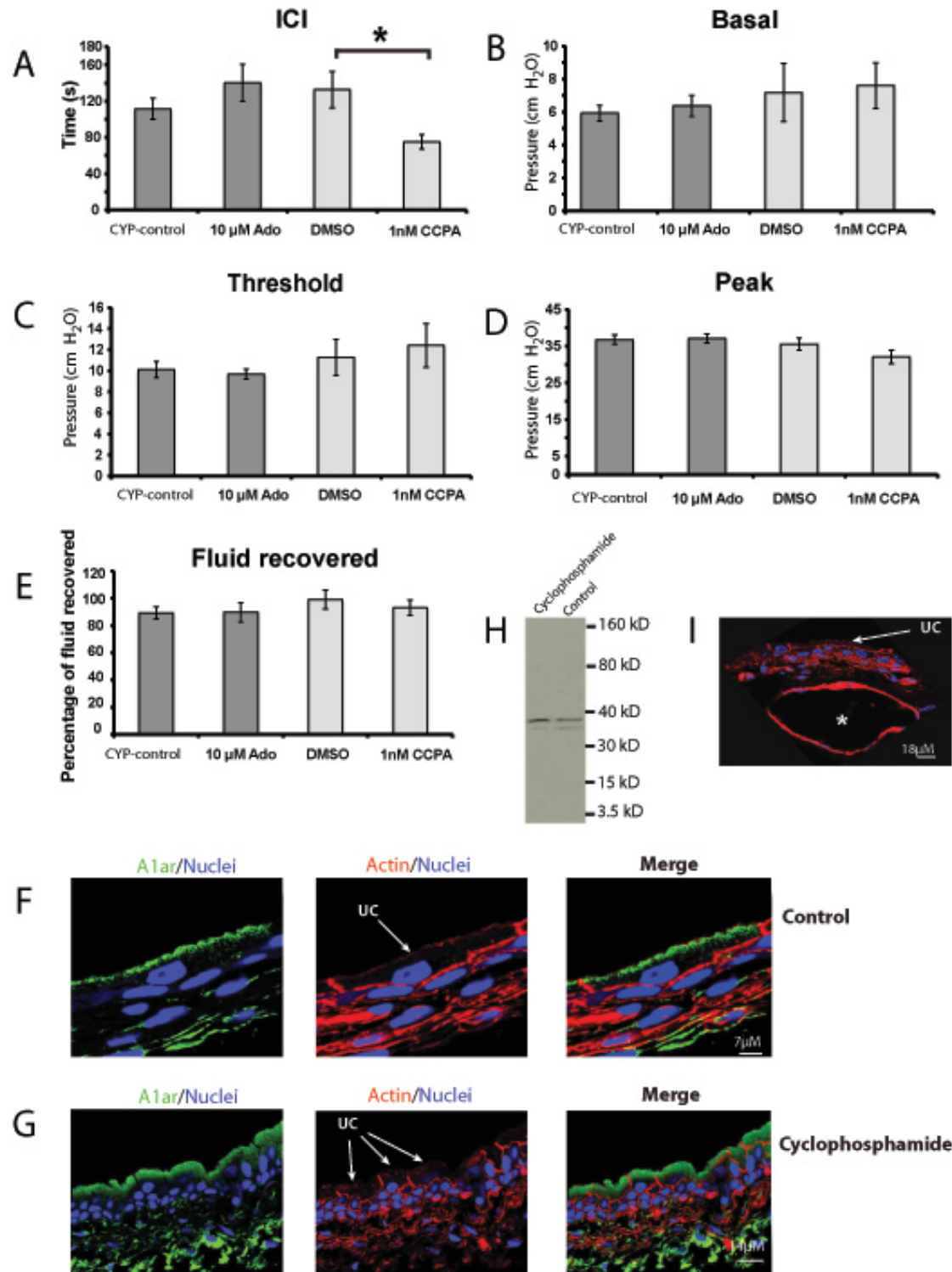
Rats were either injected with saline (sham-treatment) or with 150 mg/kg cyclophosphamide. Four hours later the rats were prepared for cystometry and BUS was intravesically infused at a constant rate of 50 μ l/min for a period of 90 min. (A) Representative images of CMGs obtained from sham- or cyclophosphamide-treated bladders. (B-F) CMG parameters for sham- or cyclophosphamide-treated bladders. Data are expressed as mean \pm SE (Sham n=8, cyclophosphamide n=9). Statistically significant differences ($p<0.05$) are indicated with an asterisk.

We found that adenosine was released from mucosal surface of rat bladders in response to filling or from the luminal surface of isolated rabbit uroepithelium, particularly when the epithelial tissue was subjected to a prolonged stress. Blocking adenosine deaminase with EHNA further potentiated adenosine levels, indicating that adenosine concentrations are likely kept in check by ecto-adenosine deaminase, which converts the released adenosine to inosine. The importance of the adenosine deaminase pathway for turnover was further supported by our observation that EHNA reduced the threshold pressure for contractions in rat bladders undergoing cystometry. In rat bladders the EHNA-induced increase in adenosine release was coupled to a decrease in inosine levels. However, in isolated rabbit tissue the mucosal inosine levels trended downwards, but the effect was not significant. Thus, a simple precursor-product relationship was not immediately apparent. However, inosine can be phosphorylated to generate IMP and extracellular inosine levels are governed, in part, by nucleotide transporters (287). As a result, we may have been unable to detect correlative changes between adenosine and inosine levels in rabbit tissues. We further observed that when rat bladder equilibrative nucleoside transporters were blocked with NBTI, there was an increase in adenosine. This rise likely explains why NBTI mimicked the effects of CCPA and lowered the threshold pressure for contractions. In contrast, NBTI caused inosine levels to increase in rabbit tissue, but there was no effect on adenosine. This may indicate species differences, or differences in the models employed, but it is also possible that extracellular adenosine was increasing in the NBTI-treated rabbit tissue, but was rapidly converted to inosine by ecto-adenosine deaminase.

While adenosine deaminase was important at the mucosal surface, adenosine kinase and nucleoside transporters played a more significant role at the serosal side of uroepithelial tissue. These results are in agreement with previous studies showing that the basolateral surface of

polarized epithelial cells show robust equilibrative nucleoside activity (288). Like the mucosal surface, we observed no simple precursor-product relationship between adenosine and its metabolites. For example, treatment with the adenosine kinase inhibitor IDT led to an increase in adenosine levels, but did not cause a corresponding decrease in AMP. The conversion of ATP, which is released from the serosal surface of the uroepithelium (23), to AMP could explain this anomaly. Equilibrative nucleoside transporters were of particular significance at the basal surface of the uroepithelium; their inhibition led to a significant increase in adenosine and inosine levels. We also observed that the levels of inosine increased in the presence of the adenosine deaminase inhibitor as the uroepithelial tissue reached its fully stretched state. Because there was no corresponding loss of adenosine, the source of this inosine is unknown but could be via the pathways described above. As a final note, while the uroepithelium is likely the predominant source of serosally released adenosine in our studies, the preparations we used contain scattered rests of endothelial cells, fibroblasts, interstitial cells, and smooth muscle cells, and that may also contribute to adenosine production and turnover at the serosal surface of this tissue.

Figure 17 CCPA exacerbates the hyperactive bladder phenotype



(A-E) Rats were treated with cyclophosphamide for 4 h to induce an acute cystitis and then cystometry was performed. Data are expressed as mean \pm SEM (Cyp-control n=9, 10 μ M adenosine n=8, DMSO control n= 7, 1 nM CCPA n= 7). Statistically significant differences ($p<0.05$) are indicated with an asterisk. (F-G, I) Cross sections of frozen uroepithelial tissues obtained from sham-treated animals or cyclophosphamide-treated ones. Images were captured with a confocal microscope and the Z-series projected. The A1 receptor is shown in green, actin staining is shown in red, and nuclei are shown in blue. The location of umbrella cells (UCs) is indicated. The asterisk in panel I shows a region of cyclophosphamide-treated bladders where the submucosal tissue is expanded, most likely a result of edema. (H) Western blot showing A1 receptor expression in sham (control) or cyclophosphamide-treated animals. Epithelial lysates from at least two rats were pooled for this analysis.

2.4.2 Luminal adenosine, acting through A₁ receptors, modulates threshold pressure

The uroepithelium was long thought of as a passive barrier, but is now realized to play a more active role in regulating bladder function (1,73). Receptors and channels, sensitive to a broad array of chemicals, mediators, and noxious stimuli are found on the apical surface of the outermost umbrella cell layer, making it possible to detect small changes in the luminal milieu of the bladder (71). In the case of adenosine, A₁ receptors are prominently expressed at this surface of the rat bladder (53), and we showed that luminally added CCPA, used at low nM concentrations (K_D for CCPA is in the 1-5 nM range), was sufficient to trigger a change in threshold pressure. This effect was blocked when tissue was simultaneously treated with the highly selective A₁ receptor antagonist DCPCX. While we cannot rule out a function for other adenosine receptors, our results indicate that A₁ receptors play a critical role in this response. Intriguingly, adenosine cannot pass the high resistance barrier imparted by the apical plasma membrane and tight junctions of the umbrella cell (2). Thus, activation of the A₁ receptor most likely initiates a signaling cascade that results in the release of mediators from the uroepithelium. Although known mediators include acetylcholine, adenosine, ATP, NO, and prostaglandins (73), we do not know which of these, if any, is responsible for transduction of the adenosine signal.

On the receiving end are interstitial cells, which are subjacent to the uroepithelium and may interface with nerves and smooth muscle cells (289). In addition, there are neuronal processes in close proximity to the uroepithelium that transmit information from the lower urinary tract to the lumbosacral spinal cord (290,291). The afferent processes of these nerves are predominantly myelinated A δ fibers and unmyelinated C-fibers, and subclasses of these processes intercalate deep into the uroepithelium where they can abut the basolateral surfaces of the umbrella cells (55). Interestingly, the effect of adenosine was highly specific and this nucleoside had no effect

on basal or peak pressure, the ICI, or fluid retention, but did decrease the threshold pressure. The latter was likely the result of sensitizing the sensory afferent nerve processes so that they responded to lower pressure stimuli. The nature of this sensitization is unknown but could be due to altered release of acetylcholine (292). However, we cannot rule out that adenosine also affected urethral function, possibly by stimulating nitric oxide synthesis and release resulting in urethral muscular relaxation (293).

2.4.3 Adenosine as a stimulatory factor in bladder function

In other organs, such as the heart, kidney, lungs and brain, adenosine has a well-established protective and anti-inflammatory effect, especially during stress and pathological insult. Thus A_1 -receptor dependent stimulation of micturition by lowering the threshold pressure could be viewed as a protective mechanism to accelerate the elimination of substances that may be injurious to the uroepithelium. However, we also observed that A_1 receptor activation exacerbated the bladder hyperactivity seen in rats with cyclophosphamide-induced cystitis. Interestingly, only the ICI was affected in the cystitis model, and not the threshold pressure. This difference did not appear to be the result of altered A_1 receptor expression or distribution. However, it is possible that cyclophosphamide-induced inflammation could alter signaling downstream of the A_1 receptor, which could change the amount of, or types of, mediators released in response to adenosine. Furthermore, some classes of C-fibers, which are normally quiescent, become activated during cystitis (294), and it is possible that the effects of adenosine were a result of activating these nerve fibers. Thus, adenosine (or other mediators) released from

a damaged or inflamed uroepithelium could contribute to bladder hyperactivity by affecting the activity of other cell types and tissues in the bladder proper.

In addition to its protective function, adenosine can also have a stimulatory effect and a strong pro-inflammatory role, which is cell type, adenosine concentration, and receptor dependent (99). For example, low concentrations of adenosine act through A₁ receptors to promote neutrophil adherence to endothelial cells as well as their chemotaxis and tissue infiltration (295). In contrast, high concentrations of adenosine (e.g. at sites of inflammation) activate A_{2B} receptors (EC₅₀ = 25 μM), which are thought to suppress these responses (296). Furthermore, adenosine pre-exposure can affect the function of T-cells and dendritic cells (297). In the case of the umbrella cell, adenosine, acting through A₁ receptors, stimulates bladder function by lowering the threshold for micturition. Such a response may be important as the bladder fills, which our data indicates would stimulate adenosine release and may aid micturition by modulating the threshold pressure. Adenosine-stimulated responses could also play a role in pathological conditions such as bacterial infections and other forms of cystitis, which are often accompanied by increased micturition and pain. Interestingly, gut strains of *Escherichia coli* may release adenosine in response to enterocyte-released beta-defensins (276). If adenosine were produced by uropathogenic *E. coli*, even at low levels, it could be sensed by the umbrella cell A₁ receptors, which could promote the clearance of the bacterial infection by lowering the threshold for micturition.

In conclusion, we have identified likely mechanisms of adenosine turnover on the mucosal and serosal surfaces of the uroepithelium, which we show can govern the amount of free adenosine found within the bladder lumen. Furthermore, we have established that adenosine has a selective modulatory effect and can promote bladder function by lowering the threshold for

micturition. The latter role may be important during bladder filling and may also play a role during pathological conditions such as cystitis.

3.0 ADENOSINE PROMOTES UMBRELLA CELL EXOCYTOSIS VIA A PROTEIN- KINASE C-STIMULATED, ADAM17-MEDIATED, EGF RECEPTOR TRANSACTIVATION PATHWAY

3.1 ABSTRACT

A disintegrin and a metalloproteinase 17 (ADAM17) is responsible for the shedding of transmembrane protein ectodomains, including those of a subset of ligands for the epidermal growth factor receptor (EGFR). Despite the importance of this cleavage to normal biology and disease, the effector pathways that promote ADAM17-dependent shedding and the mechanisms that control its activity remain unresolved. One reported mechanism of regulation is phosphorylation of residues in the cytoplasmic domain of ADAM17; however, other studies show that the cytoplasmic domain is dispensable for stimulus-evoked shedding. To further address the requirements for ADAM17-dependent shedding, we exploited the bladder umbrella cell, which in response to stress undergoes a form of apical exocytosis that depends on cleavage of heparin-binding EGF by an unknown proteinase and subsequent transactivation of the EGFR, resulting in MAPK activation, protein synthesis, and exocytosis. Using isolated uroepithelial tissues combined with biochemistry, electrophysiology, pharmacology, and *in situ* adenoviral-mediated knockdown of protein, we report that the stress-relieving hormone adenosine binds apically localized A₁ adenosine receptors and triggers a G_i-G_{βγ}-phospholipase C-protein kinase C

cascade that promotes ADAM17 phosphorylation and subsequent EGFR transactivation, leading to apical exocytosis. We further show that the cytoplasmic tail of ADAM17 contains a Ser residue at position 811, which resides in a canonical PKC phosphorylation site and when mutated to an Ala residue blocks A₁AR-mediated secretion. We conclude that adenosine plays a protective role during bladder stress by stimulating exocytosis downstream of ADAM17-dependent EGFR transactivation, and that this process may be regulated by phosphorylation of Ser811 in the cytoplasmic domain of ADAM17.

3.2 INTRODUCTION

Protein ectodomain shedding, a process regulated by proteolysis, is a fundamental mechanism for the release of cytokines, growth factors, and cell adhesion molecules (298), and is altered in cancer, autoimmune and inflammatory diseases, cardiovascular disease, and neurodegeneration (217). The best understood sheddases include the a disintegrin and a metalloproteinase (ADAM) family members ADAM10 and ADAM17 (also known as TACE), both of which shed a variety of substrates including the transmembrane ligands for the epidermal growth factor receptor (EGFR). Whereas ADAM10 targets betacellulin, EGF, and neuregulin, ADAM17 is the principal sheddase for transforming growth factor (TGF) □, amphiregulin, epiregulin, epigen, and heparin-binding epidermal growth factor (HB-EGF) (245,246,299). Indeed, the physiological relevance of ADAM17 in shedding is supported by research showing that knockout mice lacking this proteinase have a similar phenotype to mice deficient in expression of TGF □, amphiregulin, epiregulin, epigen, and heparin-binding epidermal growth factor (HB-EGF) (221,250,251,300,301). While the

physiological cues that trigger shedding are not completely defined, ADAM17-elicited shedding occurs in response to many stimuli including ligands for G-protein-coupled-receptors (GPCRs) and treatment with ionomycin or phorbol-12-myristate-13-acetate (PMA), a diacylglycerol mimic and activator of classical protein kinase C (PKC) isoforms, whereas ADAM10-dependent shedding responds to Ca^{2+} ionophores (e.g. ionomycin), but not PMA (when used for less than 2 h)(167,239,302). Our understanding of the signaling and associated effector pathways that act downstream of these stimuli remains incomplete, although the extracellular signal-regulated kinase (ERK), as well as the p38 mitogen-activated kinase

regulated protein phosphatase inhibitor 14D have been linked to ADAM17-dependent shedding, and PKC

An additional unresolved question is how these effectors promote ADAM-dependent shedding of EGFR ligands, although evidence to date indicates they work by multiple mechanisms and perhaps in a cell and stimulus dependent manner (168,202,210). Potential regulatory steps include membrane trafficking of the ADAM or its ligands (201), effects on the ADAM17 dimer-monomer equilibrium and association with tissue inhibitor of metalloproteinases (TIMP) 3 (244), or changes in the redox potential of extracellular protein disulfide isomerase, which is hypothesized to alter ADAM17 activity by rearrangements of its disulfide bonds (305). An additional regulatory mechanism is phosphorylation of ADAM17. Indeed, ADAM17 phosphorylation of cytoplasmic residues Ser791, Ser819, Tyr702 and Thr735 is reported (210,232,303). However, Ser791 is phosphorylated prior to stimulation, and mutations of Ser819 do not appear to impact shedding (210). Tyr702 was phosphorylated by src kinase in response to mechanical stretching of rat myoblasts (232). In the case of Thr735, very high doses of PMA (1 μM) are reported to promote extracellular signal-regulated kinase (ERK)-

dependent phosphorylation of this residue (201). However others report that phosphorylation of this residue is mediated by the p38 mitogen-activated kinase and this posttranslational modification is required for ADAM17-dependent shedding in response to various forms of stress, but not PMA (202). A significant argument against this hypothesis are several reports that show shedding of ADAM17-dependent ligands (in response to a variety of stimuli) occurs in cells expressing truncated versions of this metalloproteinase lacking its C-terminus (220,238,239). Finally, a recent study shows that substrate cleavage is regulated independently of a major change in ADAM proteinase activity, and that in the case of neuregulin it is PKC δ -mediated phosphorylation of cytoplasmic residue Ser286 that regulates cleavage of this ligand by ADAM10 (166).

A useful and physiologically relevant model system to study the signals, effector pathways, and mode of ADAM activation is the uroepithelium, a tissue that can be studied both *ex vivo* and *in vivo* (22,24,42). Bladder filling triggers the exocytosis of an abundant subapical pool of discoidal- and/or fusiform-shaped vesicle (DFV) in the outer umbrella cell layer (28,29). Stretch-induced exocytosis progresses in two phases. “Early-phase” exocytosis occurs during bladder filling, as the epithelium is bowing outward, and is triggered by apical Ca²⁺ entry, likely conducted by a non-selective cation channel (41). In contrast, “late-phase” exocytosis is initiated once the tissue is maximally bowed outward (i.e. in response to a full bladder), and requires metalloproteinase-dependent cleavage of HB-EGF leading to “transactivation” of apical EGFRs and initiation of a downstream ERK pathway that culminates in protein synthesis and exocytosis (43). We now report that adenosine, which is released from the epithelium in response to stress (306), spurs a late phase-like response in umbrella cells, that a G_i-, G _{$\beta\gamma$} -, PLC-, and PKC-dependent effector cascade is initiated downstream of the adenosine A₁ receptor (A₁AR), and

that a previously unreported canonical PKC site centered at Ser811 in the cytoplasmic domain of ADAM17 is critical for adenosine-induced exocytosis.

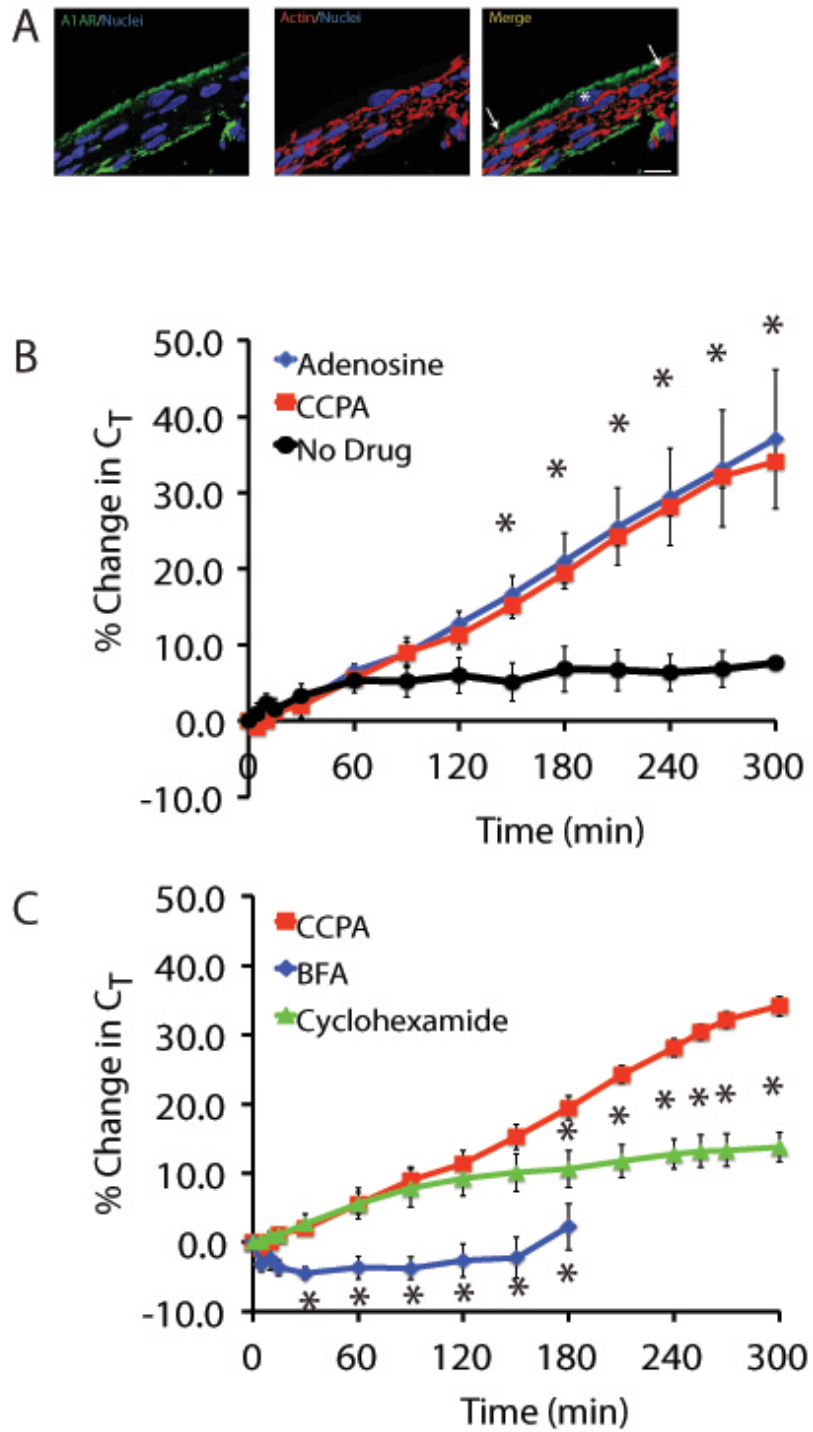
3.3 RESULTS

3.3.1 A₁AR-stimulated apical exocytosis occurs through transactivation of the EGFR

Late-phase exocytosis is triggered when uroepithelial tissue is maximally stretched (43), but if other stimuli promote a similar response is unknown. Because adenosine is dramatically increased as the bladder reaches its capacity (306), and because it can also trigger exocytosis (53), we tested the hypothesis that adenosine stimulates exocytosis by way of EGFR transactivation. Consistent with our previous report (306,307), the A₁AR was distributed at the apical pole of umbrella cells (as well as in the underlying lamina propria; Figure. 18 A) and when adenosine was added to the mucosal surface of the tissue it stimulated increased tissue capacitance (C_T ; where $1 \mu\text{F} \approx 1\text{cm}^2$) (Figure. 18 B), which in this tissue correlates well with other measures of apical exocytosis (27,28). Similar results were observed for the highly selective and high affinity A₁AR agonist CCPA. Unlike adenosine, CCPA it is not rapidly converted to inosine (306,308), and was thus used in our subsequent studies. We next determined whether A₁AR-stimulated exocytosis was dependent on protein synthesis and whether it was

sensitive to BFA. Indeed, treatment with BFA or cycloheximide significantly blocked CCPA-mediated exocytosis (Figure 18 C), although the effect of BFA was particularly pronounced.

Figure 18 Activation of A1AR triggers apical exocytosis in umbrella cells

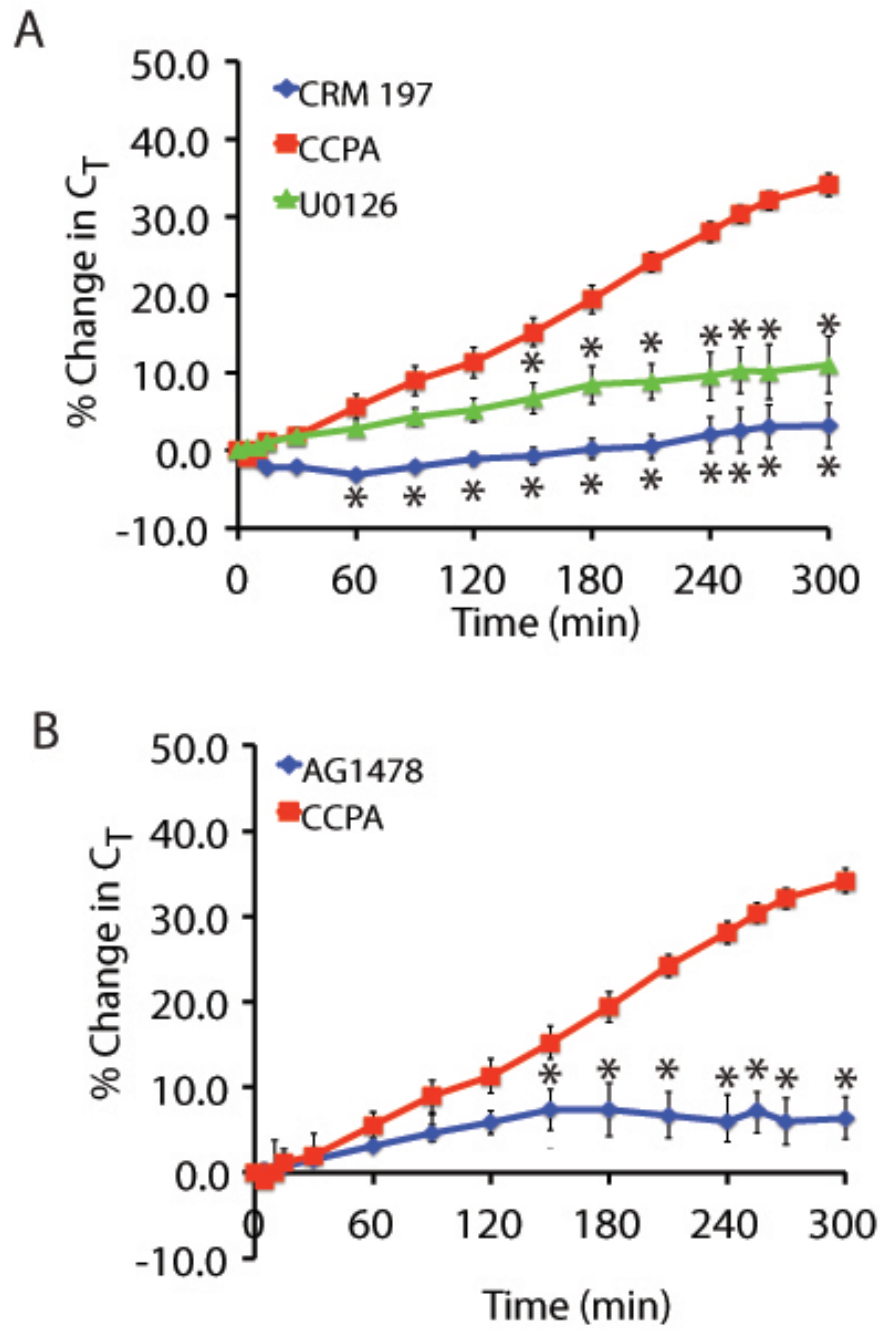


A. 4 μ m rat bladder cryosections were labeled with antibody to A₁AR (green), rhodamine phalloidin to label the actin cytoskeleton and TOPRO-3 to label the nucleus. The merged panel is shown on the right. The white arrows mark the apical borders of the cell. B. Rabbit uroepithelium was mounted on using chambers and after equilibration, were either left untreated (Black), or treated with 1 μ M adenosine (Blue) or 500nM CCPA (Red) on the mucosal side. The C_T measurements were recorded for a period of 300 min and plotted against time. C. Rabbit uroepithelial tissues were mounted on Ussing chambers and equilibrated as above. The tissues were then treated with either 5 μ g/ml Brefeldin A (BFA) for 30 min (Blue) or 100ng/ml Cyclohexamide for 60 min (Green). Then 500nM CCPA was added to the mucosal chamber and the C_T was recorded for 300 min post addition and plotted against time. The CCPA alone data (Red) was reproduced from Figure 1B. In panels B and C, the mean changes in C_T \pm SEM (N \geq 4) are shown. Statistically significant difference of ($p < 0.05$) relative to no drug in A and CCPA in B are marked by *. In panel A, the umbrella cell is marked with the *. Scale bar is 12 μ M and the cell junctions are marked by white arrows.

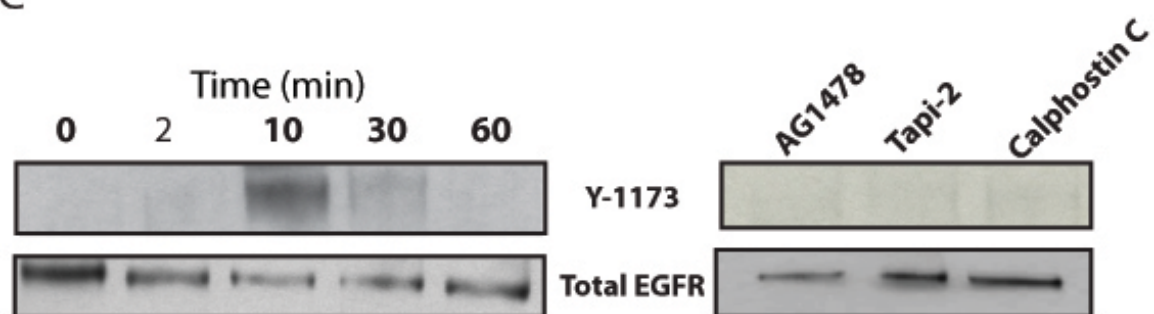
We next determined whether CCPA triggered apical exocytosis by transactivating the EGFR. We first tested the effect of treating the mucosal surface of the tissue with CRM197, a mutant version of Diphtheria toxin that binds with high affinity to membrane bound HB-EGF and prevents its cleavage (309). Indeed, we observed that CRM197 almost completely blocked CCPA-mediated apical exocytosis (Figure 19 A). Next, we pretreated tissue with AG1478, a small molecule inhibitor of EGFR, which also significantly blocked CCPA-mediated apical exocytosis (Figure 19 B). As further evidence that the EGFR was transactivated, we generated lysates from CCPA-treated epithelium, and then probed western blots with an antibody that detects phosphorylation of the EGFR at tyrosine 1173 (Y₁₁₇₃). This residue promotes assembly of a MAPK signaling cascade downstream of other G-protein-coupled receptors that stimulate EGFR transactivation (43). Phosphorylation of Y₁₁₇₃ was maximally stimulated 10 min after continuous treatment with CCPA, decreased at 30 min post treatment, and returned to control levels after 60 min (Figure 19 C). Y₁₁₇₃ phosphorylation was prevented when the tissue was pretreated with the EGFR inhibitor AG1478 prior to CCPA treatment (Figure 19 C-D), confirming that phosphorylation of Y₁₁₇₃ likely results from autophosphorylation. Finally, we observed that U0126, an inhibitor of ERK1/2 activity, also caused a significant decrease in CCPA-stimulated changes in C_T.

Taken together, these data indicated that, like the previously described late-phase response (43), A₁AR activation stimulates apical exocytosis by promoting transactivation of the EGFR downstream of HB-EGF cleavage, leading to MAPK activation and protein synthesis.

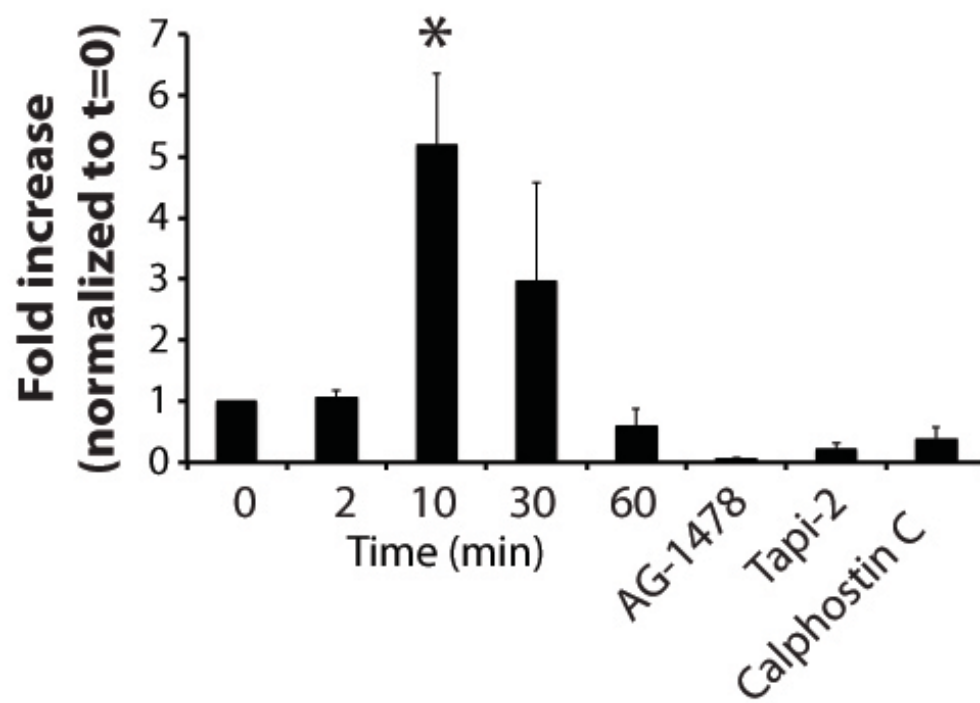
Figure 19 A1ar-mediated apical exocytosis occurs through transactivation of EGFR



C Rabbit tissue treated with CCPA



D EGFR Y-1173 activation



A. rabbit uroepithelium was mounted on Ussing chambers and equilibrated as explained earlier. The tissue was pretreated with 1 μ M AG1478 for 30min and then CCPA was added to the mucosal chamber to a final concentration of 500nM. The C_T was measured for a period of 300min and plotted against time (Blue). Control CCPA data was reproduced from Fig 1B (Red).

B. The tissue was mounted and equilibrated as above. The mucosal surface was pretreated with 5 μ /ml CRM-197 for 25min (Blue) or the tissue was treated with 10 μ M U0126 (Green) for 60 min. CCPA was then added to the mucosal chamber to a final concentration of 500nM and the C_T was measured for 300 min. The CCPA control data was reproduced from Fig 1B. The mean changes in $C_T \pm$ SEM ($n \geq 3$) are shown. Statistically significant difference ($P < 0.05$) relative to the CCPA data (Red in both the panels) are marked by *.

C. Rabbit uroepitheliums were mounted on Ussing chambers and equilibrated as above. CCPA was added to the mucosal chamber to a final concentration of 500nM. At different time points (0', 2', 10', 30' and 60') the tissue was unmounted from the chambers, spread on rubber dissection mats and the uroepithelial lysates were prepared in the presence of 0.5% SDS lysis buffer (with protease and phosphatase inhibitors). In the case of inhibitor studies, the rabbit tissues were pretreated with either 1 μ M AG1478 for 25min, 15 μ M Tapi-2 for 90 min or 500nM Calphostin C for 60 min and then CCPA was added to the mucosal chamber to a final concentration of 500nM. 10min post CCPA treatment, the tissue was unmounted from the chambers and the lysate was prepared as expaliend. Equal amounts of the protein were resolved on 4-15% SDS PAGE and immunoblotted with either rabbit-anti EGFR-phosphoY1173 antibody or rabbit-anti total EGFR antibody.

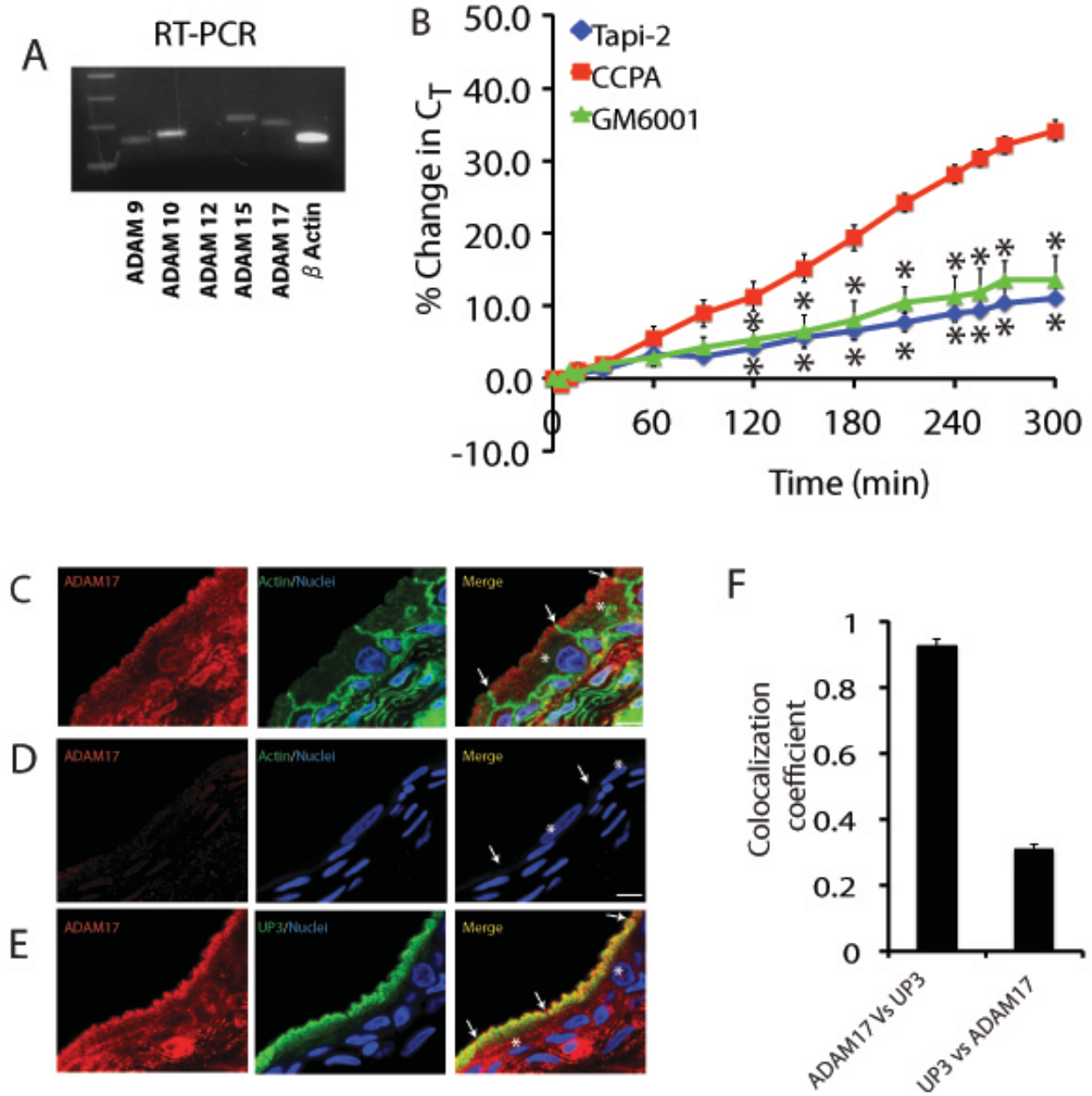
D) Quantification of Y1173 in response to CCPA treatment, relative to untreated ($t=0'$) tissue samples. The mean band density \pm sem ($n > 3$) are shown. Statistically significant values ($p < 0.05$) are marked by *.

3.3.2 ADAM17 is localized to the apical surface of umbrella cells where it stimulates CCPA-induced EGFR transactivation and exocytosis

To determine the mechanism by which HB-EGF is cleaved, we performed qualitative reverse-transcriptase mediated (RT)-PCR and detected message for several ADAM family proteinases previously implicated in EGFR transactivation including ADAM-9, -10, -15 and -17, but not ADAM12 (Figure 20 A) (169). In our subsequent studies we focused our attention on ADAM17 because previous *in vivo* studies implicate it as the physiologically relevant ADAM in HB-EGF-mediated transactivation (245,300,310).

Consistent with our hypothesis that ADAM17 is required for EGFR transactivation in umbrella cells, we observed that ADAM17 was localized to small vesicular elements under the apical surface of the umbrella cells (Figure 20 B), the site of HB-EGF cleavage and EGFR transactivation during the late-phase response (43). Rat tissues were employed in these experiments because our antibody was produced in rabbits. The signal for ADAM17 was diminished when the anti-ADAM17 antibody was preincubated with immunizing peptide, confirming the specificity of the antibody (Fig. 3C). ADAM17 showed a high degree of colocalization with uroplakin 3a, which is associated with DFVs and the apical surface of umbrella cells (Figure 20 D-E) (1). ADAM17 was also detected in the intermediate and basal cell layers of the uroepithelium, as well as cells in the underlying lamina propria (Fig. 3B and D). We also observed that the broad-spectrum metalloproteinase inhibitor GM6001 and the ADAM17 selective inhibitor Tapi-2 (43,311) both significantly inhibited the CCPA-mediated increases in C_T (Figure 20 F). Moreover, Tapi-2 blocked CCPA-mediated phosphorylation of EGFR Y₁₁₇₃ (Figure 19 C-D).

Figure 20 ADAM17 is localized to the apical surface of Umbrella cells



A. Total RNA was isolated from rat uroepithelium and RT-PCR used to assess the expression of ADAMs 9, 10, 12, 15 and 17 and the positive control β -Actin. B. Rabbit uroepithelium was mounted on Ussing chambers and equilibrated as explained earlier. The tissue was pretreated with 15 μ M Tapi-2 (Blue) or 15 μ M GM6001 (Green) for 90 min and then CCPA was added to the mucosal chamber to a final concentration of 500nM. The C_T was measured for a period of 300min and plotted against time. Control CCPA data was reproduced from Fig 1B (Red). Mean \pm SEM is presented for all data points, and the statistically significant values ($n \geq 3$; $P < 0.05$) on comparison to CCPA alone data are marked with an *. C. 4 μ m sections of rat bladder cryoblocks were treated with rabbit-anti ADAM17 alone (Red), Rabbit-anti-ADAM17 + inhibitory peptide (Red) or Rabbit-anti ADAM17 (Red) + mouse UP3 antibodies (Green). The proteins were visualized with Goat-anti Rabbit Cy3 in the upper two panels and with Goat-anti Rabbit Cy3 and Goat-anti mouse Alexa 488 in the bottom panel. TOPRO-3 was used to visualize the nucleus (Blue) in all the cases. The merge panel is presented in the far right column. The umbrella cells are marked with the * D. Colocalization of ADAM17 with UP3 was measured using the Mander's co-localization index with a threshold of 40. >90% of UP3 positive vesicles colocalized with ADAM17 positive vesicles. Scale bar is 10 μ M and the cell junctions are marked by white arrows.

To provide further evidence that ADAM17 is required for EGFR transactivation, we exploited our previously described *in situ* viral transduction approach to express ADAM17-specific shRNAs or scrambled shRNAs in the rat bladder uroepithelium. We used rat bladders in these studies because the volume capacity of the bladder, and therefore number of virus particles needed, was relatively small (~ 500 μ l) when compared to the volumes required to fill the rabbit bladder (~ 60-100 ml). This technique targets the umbrella cell layer and achieves transduction efficiencies of 70-95% (22,42). Indeed, we were able to achieve a > 90% knockdown of ADAM17 expression (Figure 21 A-B). By examining the expression and distribution of ADAM17 in cross sections of uroepithelium, we confirmed that knockdown was confined to the umbrella cells and that expression of ADAM17 in the intermediate and basal cells was not disturbed (Figure 21C).

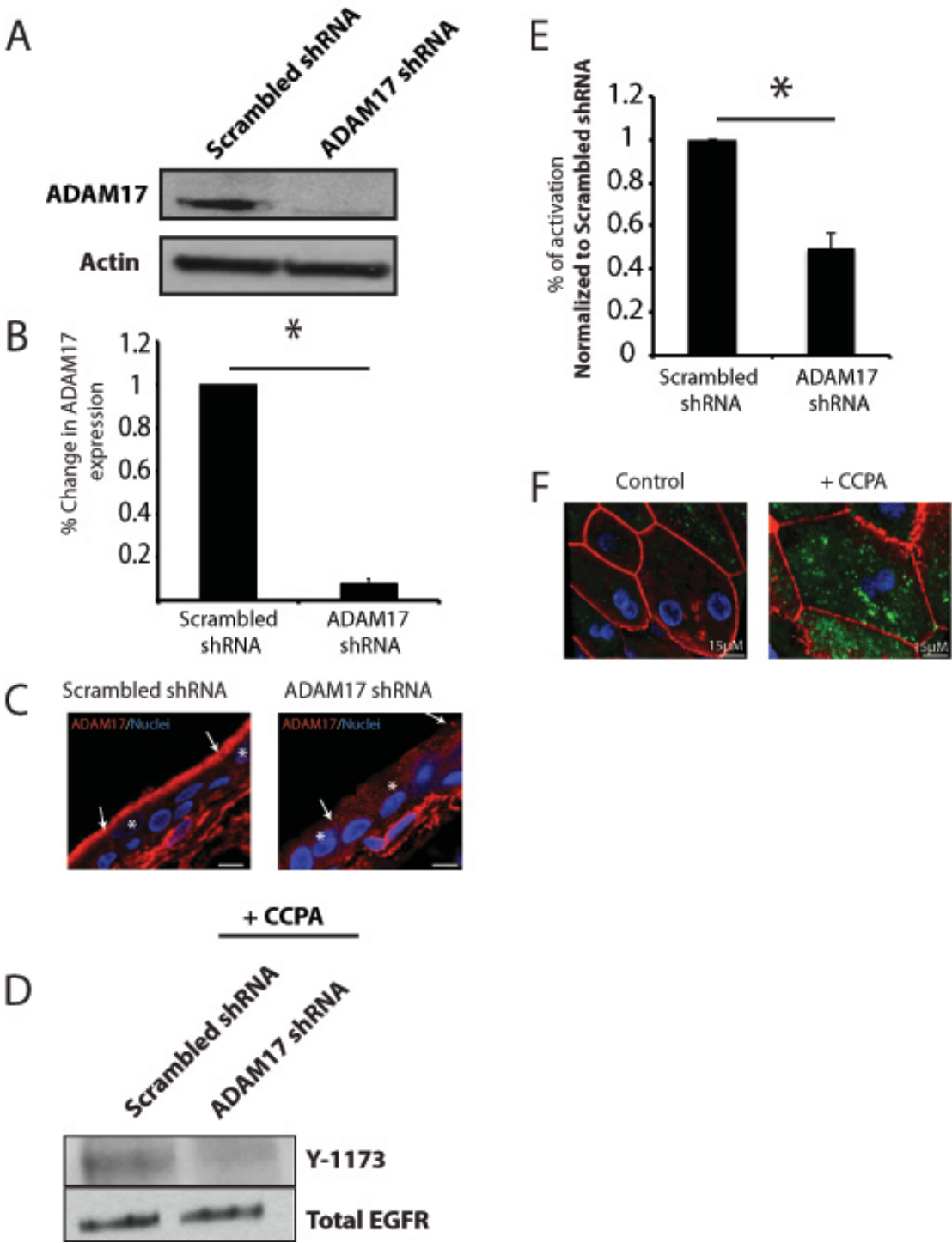
Next, we used ADAM17-specific shRNAs to test whether ADAM17 was required for CCPA-stimulated EGFR transactivation and exocytosis. Treatment with ADAM17-shRNA, but not scrambled shRNA, decreased EGFR phosphorylation (Figure 21 D-E). We also attempted to measure changes in C_T in the rat bladders treated with apical CCPA; however, we did not observe a response. Because C_T is dependent on the rates of membrane addition and removal, we reasoned that one possible explanation was that CCPA stimulated both exocytosis and endocytosis, thus obviating any change in apparent C_T . Indeed, we observed that WGA-FITC, added to the apical hemichamber of mounted rat bladders, was endocytosed in CCPA-treated tissue, but much less so in control, untreated tissue (Figure 21F). To circumvent the effects of endocytosis, we measured release of exogenously expressed human growth hormone (hGH), which is packaged into DFVs and released from the luminal surface of the bladder into the urinary space (21,22). Compared to control bladders, CCPA stimulated a 2.7-fold increase in the

mucosal release of hGH from the tissue (Figure 21 G-H), whereas expression of ADAM-17 specific-shRNA, but not scrambled shRNA, caused a large inhibition (> 95%) in mucosal hGH release (Figure 21 G-H). Taken together our results provide strong evidence that ADAM17 is critical for CCPA-induced transactivation and exocytosis.

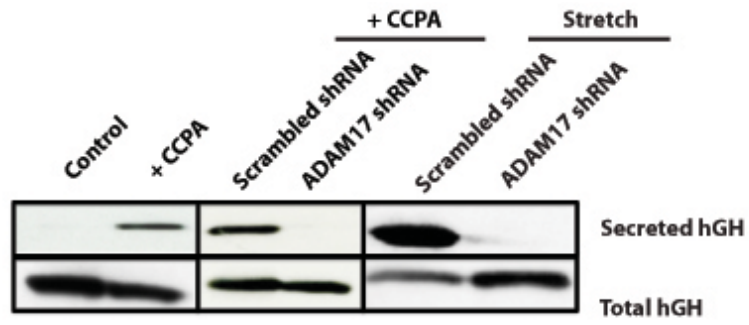
3.3.3 ADAM17 is also critical for stretch-mediated apical exocytosis in rat, but not rabbit uroepithelium

Because stretch-mediated, late-phase exocytosis is dependent on EGFR transactivation and sensitive to metalloproteinase inhibitors (43), we hypothesized that ADAM17 may also play a role in stretch-mediated EGFR transactivation. Surprisingly, and despite the sensitivity of CCPA-induced exocytosis in rabbit tissue to Tapi-2, this inhibitor had no effect on the stretch-induced, late-phase exocytic response in this tissue (data not shown). In contrast, in rat bladders shRNA-mediated ADAM17 knockdown significantly reduced the stretch-induced apical release of hGH by > 60% compared to tissues transduced with scrambled shRNA (Figure 21G-H). In sum, these data indicate that ADAM17 is required to promote EGFR transactivation downstream of the A₁AR and stretch in rat tissues; however in rabbits a different metalloproteinase may be required for stretch-induced, late-phase exocytosis.

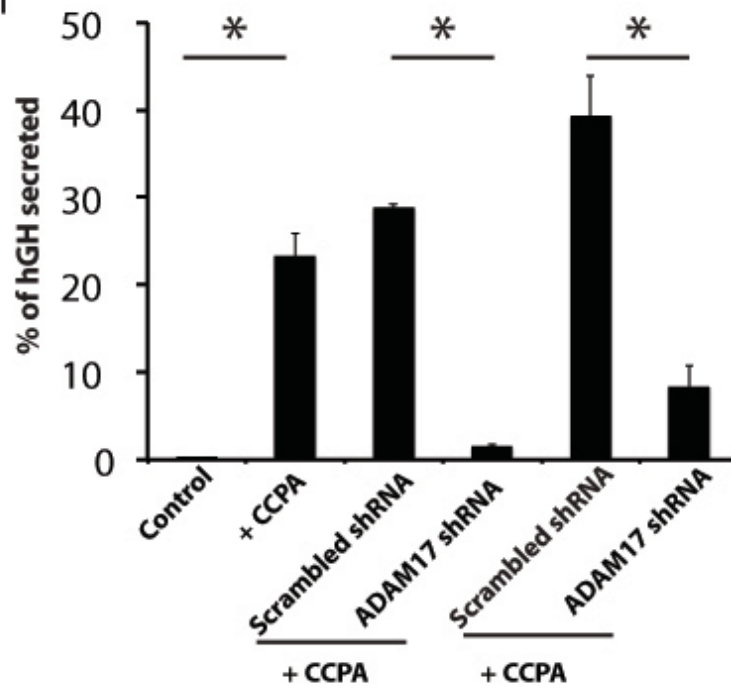
Figure 21 In situ knockdown of ADAM17 impairs A1ar- and stretch-mediated apical exocytosis:



G



H



A. Equal volumes of rat uroepithelial lysates from scrambled shRNA and ADAM17 shRNA infected bladders were resolved in 4-15% SDS PAGE and the westernblots were probed with rabbit-anti ADAM17 antibody (top panel) or Mouse-anti actin (bottom panel). B. Quantification of intensity of ADAM17 bands in ADAM17 knockdown rat uroepithelial lysates. Data is presented as mean change in the band intensity \pm SEM on comparison to ADAM17 band intensity in the scrambled shRNA group. Statistically significant values are marked by $*(n \geq 4, p < 0.05)$ C. 4 μ m cross sections of scrambled shRNA expressing rat bladder (left) and ADAM17shRNA expressing rat bladder cryosections were stained for ADAM17 (red) and nuclei with TOPRO-3 (blue). D. Equal quantities of rat bladder lysate from the treatments were resolved in a 4-15% SDS PAGE and the western blots were probed with either rabbit anti-EGFR-phospho-Y1173 or rabbit anti-EGFR antibody, E. Quantification of D. The quantification of the data is represented as band intensity \pm sem on comparison to the control band. F. Rat bladders treated with WGA-FITC (green) , Actin with rhodamine phalloidin (red) and nuclei with TOPRO-3 (blue). G. hGH assay: In the top panel equal volumes of buffer concentrate from the various treatments were resolved in 4-15% SDS PAGE and the western blots were probed with rabbit-anti human growth hormone antibody. In the bottom panel, equal quantity of proteins from the uroepithelial lysates corresponding to the treatment groups of the top panel were resolved in 4-15% SDS PAGE and the western blots were probed with rabbit-anti human growth hormone antibody. H. Quantification of G. Data is presented as mean band density \pm SEM on comparison to the control bands. In panel C the umbrella cell is marked by *. The scale bar in C is 13 μ M. The cell junctions are marked by white arrows. Statistically significant values are marked by * over a horizontal bar depicting the treatment groups used for the statistical analysis ($n \geq 3, p < 0.05$).

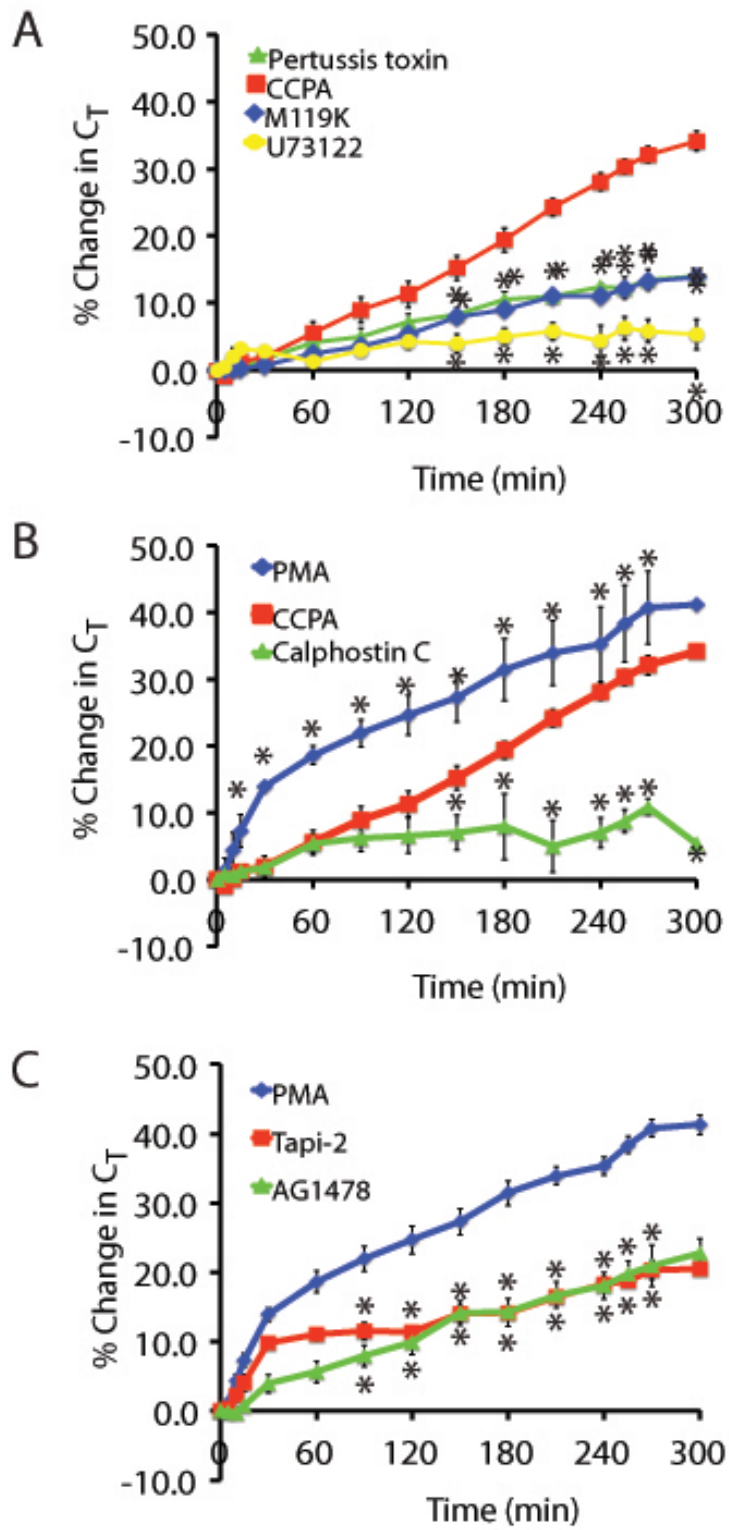
3.3.4 G_i , phospholipase C, and PKC act upstream of ADAM17 to promote A_1AR -mediated EGFR transactivation

How ADAM17 activity is coupled to A_1AR activation was addressed next. Previous studies showed that A_1AR signals through $G_{i\alpha}$ to inhibit the activity of adenylyl cyclase, while the $\beta\gamma$ subunits of G_i increase the activity of phospholipase C- β (PLC β), which hydrolyzes phosphatidylcholine to generate IP3 and diacylglycerol (312-314). The latter stimulates the activity of PKC, a well-known regulatory kinase that was previously implicated in ADAM17 activation (167,311,315). We found that pertussis toxin-mediated inhibition of G_i , or inhibition of $G_{\beta\gamma}$ subunit activity by the inhibitor M119K (316), significantly impaired CCPA-mediated apical exocytosis in rabbit bladder umbrella cells (Figure 22 A). Furthermore, the PLC-selective antagonist U73122 caused a marked inhibition of CCPA-induced changes in C_T (Fig. 22A). Thus, ADAM17 activation downstream of A_1AR likely occurred by way of a classical G_i -stimulated signaling cascade involving $G_{\beta\gamma}$ and PLC.

Next, we examined whether PKC was important for A_1AR -dependent EGFR transactivation and exocytosis. Strikingly, the PKC inhibitor calphostin-C caused a marked decrease in CCPA-stimulated changes in C_T and EGFR transactivation (Figure 19C-D and 22 B). In contrast, treatment with PMA, an activator of classical PKCs (317), caused a robust stimulation of exocytosis in the absence of CCPA (Figure 22 B). Interestingly, the kinetics of PMA-mediated exocytosis was faster than those mediated by CCPA, particularly during the first 30 min, and then appeared to increase at a similar rate to CCPA thereafter. This may indicate that PKC not only stimulates late-phase-like responses, but perhaps early-phase ones as well. To confirm that PMA acted by way of ADAM17, we treated the tissue with Tapi-2, which

significantly inhibited PMA-mediated apical exocytosis (Figure 22C). Furthermore, we observed that AG1478 also blocked PMA-mediated exocytosis (Figure 22C).

Figure 22 PKC mediates A1ar-induced ADAM17 activation

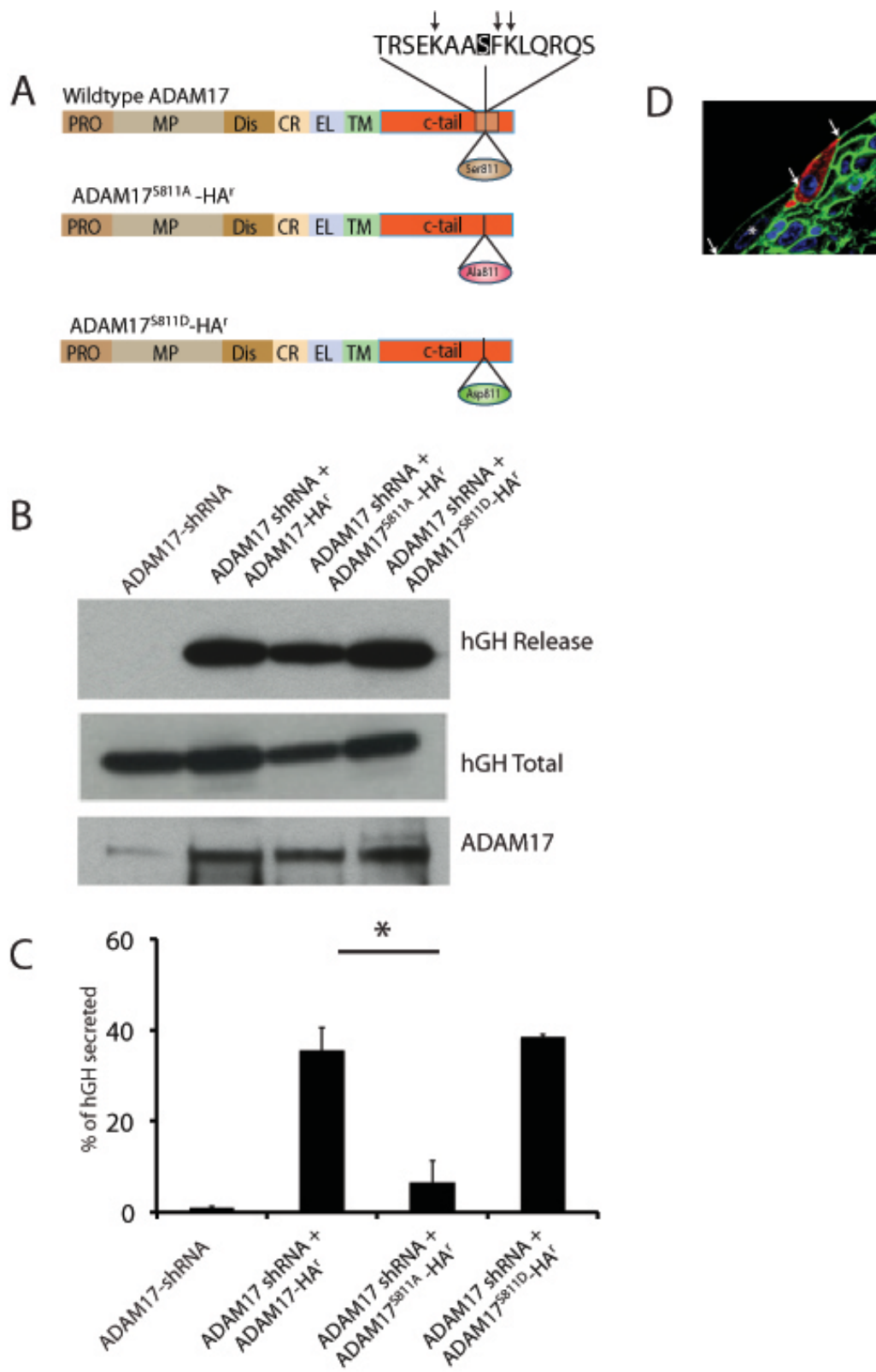


In A, B and C Rabbit uroepithelium was mounted on Ussing chambers and equilibrated as explained earlier. In A and B The CCPA alone data (red) was reproduced from figure 1B. A) The tissue was pretreated with 100ng/ml pertussis toxin (Green) for 90 min or 10 μ M M119K (Blue) for 60min or 10 μ M U73122 (yellow) for 60 min. Then CCPA was added to the apical surface to a final concentration of 500nM and the capacitance was measured for 300 min. B) The tissue was pretreated with 10nM PMA (blue) on the mucosal surface or pretreated with 500nM Calphostin C for 30 min and then treated with 500nM CCPA (Green). C) The tissue was pretreated with 15 μ M Tapi-2 for 90 min (red) or 1 μ M AG1478 for 30 min and then treated with 10nM PMA. The PMA alone data was reproduced from figure 5 B. Data are presented as mean \pm SEM. Statistically significant values are marked with an * ($n \geq 3$, $p < 0.05$).

To explore how PKC may act to stimulate ADAM17 activity we scanned its amino acid sequence using the proteomics tool Scansite and identified a canonical PKC phosphorylation motif (X-R/K-X-X-S/T-X-R/K-X) (318,319) in the cytoplasmic tail of the protein centered at Ser₈₁₁ (Figure 23 A). To our knowledge, this potential phosphorylation site has not been explored previously. To test its possible role in CCPA-mediated exocytosis, we silenced endogenous ADAM17 using shRNA and then expressed an shRNA-resistant variant of wild-type ADAM17 HA-tagged at its C-terminus (ADAM17^r-HA) or mutants in which Ser 811 was mutated to an Ala residue (ADAM17^{r/S811A}-HA) or a potentially “phosphomimetic” mutant in which Ser₈₁₁ was mutated to an Asp residue (ADAM17^{r/S811D}-HA) (Figure 23 A). The exogenous expression of ADAM17-HA^r restored CCPA-induced hGH secretion in the shRNA background (Figure 23 B). The levels of hGH release were slightly higher than that observed for the endogenous protein (compare Figure 23 C with Figure 21 H). This could be due to the exogenous expression of the ADAM17 protein. Remarkably, expression of ADAM17^{r/S811A}-HA caused a significant reduction in the exocytosis of hGH by ~80% indicating a critical role for the specific amino acid in the A₁AR-mediated activation of ADAM17. Importantly, ADAM17^{r/S811A}-HA was expressed at >70% of the umbrella cells and was localized to the apical pole, indicating that the mutation did not impair the trafficking ability of the protein. (Figure 23 D). However, ADAM17^{r/S811D}-HA did not significantly stimulate exocytosis above the wild-type protein (Figure 23 B-C).

Together, these results indicate that adenosine-mediated increase in apical exocytosis are dependent on activation of PKC and that one possible target of this kinase is Ser811 in the cytoplasmic domain of ADAM17, a residue that may exert its effect in response to phosphorylation.

Figure 23 Ser811 in the c-tail of ADAM17 is required for A₁AR-mediated apical exocytosis



A) Schematic showing the different domains of ADAM17. The consensus PKC phosphorylation motif (Ser811) has been highlighted, and the conserved motif with the basic amino acids at the -3 and +2 sites marked by the arrows. The point mutations performed are depicted in the lower panels. B) hGH assay: in the top panel, equal volumes of buffer concentrate from the various treatments were resolved in 4-15% SDS PAGE and the western blots were probed with rabbit-anti human growth hormone antibody. In the second panel, equal quantity of proteins from the uroepithelial lysates corresponding to the treatment groups of the top panel were resolved in 4-15% SDS PAGE and the western blots were probed with rabbit-anti human growth hormone antibody. In the bottom panel equal quantities of proteins of the same lysates used in the middle panel were resolved in 4-15% SDS PAGE and the western blots were probed with rabbit-anti ADAM17 antibody. C) Quantification of B. Data is represented as mean band density \pm SEM of the released hGH as a ratio to the total gGH expressed in the tissue. D) Rat uroepithelium expressing ADAM17 shRNA + ADAM17^{r/S811A}-HA is stained with ADAM17 (red), Actin (green) and nuclei (blue). A cell where expression of ADAM17 is knocked out neighboring another cell where ADAM17^{r/S811A}-HA is expressed is marked with the *. The cell junctions are marked by white arrows.

3.4 DISCUSSION

The urinary bladder undergoes continuous cycles of filling and voiding, subjecting the bladder mucosa to constant mechanical stress. The uroepithelium has evolved numerous specializations to cope including: (1) the mucosal surface of the bladder is highly folded and is reversibly unfurled during bladder filling; (2) the umbrella cells maintain a robust tight junction barrier that can expand and contract with the bladder cycle; (3) the pre-existing population of umbrella cell DFVs undergo apical exocytosis, which when accompanied by cell-shape changes in the umbrella cell increases the luminal volume. There is however a fourth mechanism, which we call the late-phase exocytic response. It is triggered by stress (e.g. excess stretch), it ensures incorporation of additional apical membrane, and is characteristically dependent on EGFR transactivation, protein synthesis, and protein secretion. Currently, there is little information about which stimuli promote the late-phase response or how these events trigger EGFR transactivation. Our current results show that (1) adenosine, like stretch, also stimulates exocytosis via EGFR transactivation, that (2) ADAM17 is the relevant metalloproteinase (at least in rats), that (3) an $A_1AR \rightarrow G_{\alpha i} \rightarrow G_{\beta \gamma} \rightarrow PLC \rightarrow PKC$ signaling cascade acts upstream of ADAM17 to promote HB-EGF cleavage, and that (4) the C-terminal tail of ADAM17 contains residues critical for its function.

3.4.1 Adenosine, like stretch, stimulates apical exocytosis via EGFR transactivation

We previously showed that the late-phase exocytic response is triggered downstream of EGFR transactivation when uroepithelial tissue (mounted in an Ussing chamber) is maximally bowed outwards – akin to what the tissue experiences in a full bladder (43). In this case, EGFR transactivation functions to alleviate luminal stress by increasing apical surface area via exocytosis. Because adenosine also stimulates apical exocytosis in umbrella cells (53), because it is released from both surfaces of the epithelium in response to a full bladder (306), and because adenosine is reported to act as a stress-relieving hormone (104,320,321), we asked whether adenosine also stimulated EGFR transactivation. We found that like maximal stretch, adenosine stimulates a slow and gradual increase in apical exocytosis, which is dependent on the activity of a metalloproteinase that cleaves HB-EGF, resulting in EGFR transactivation. Furthermore, both responses require the downstream stimulation of ERK1/2 and both have a requirement for protein synthesis and secretion. Two studies have previously reported adenosine-mediated EGFR transactivation, but they did not identify metalloproteinase involved, nor did they dissect the signaling pathway that linked A₁AR to EGFR activation (322,323).

While stretch and adenosine both stimulate exocytosis by way of EGFR transactivation, the pathways employed are not necessarily identical and there may be species differences. For example, in rabbit tissue the ADAM17 inhibitor Tapi-2 and the PKC inhibitor calphostin C impair adenosine-stimulated exocytosis, but have no apparent effect on the stretch-induced late-phase response. Thus, in rabbit uroepithelium, stretch and adenosine likely utilize distinct upstream signaling pathways and metalloproteinases. This conclusion is further supported by our previous observation in rabbit tissue that the late-phase exocytic response is potentiated by adenosine, but not dependent on it (53). Physiologically, these additive events would allow the

umbrella cells to respond to stimuli generated in its immediate environment (e.g. stretch) but also to external stimuli such as adenosine, which can be produced locally or from other tissues in the lower or upper urinary tract (324).

3.4.2 ADAM17 mediates adenosine-dependent EGFR transactivation

We detected message for ADAM-9, -10, -15 and -17 in the uroepithelium, but focused our studies on ADAM17 because of the abundance of studies demonstrating the physiological relevance of this ADAM family member, including the observation that ADAM17 is the physiological convertase for several EGFR ligands including HB-EGF (221,245,250) . Several pieces of data support a critical role for ADAM17 function in late-phase exocytosis. First, we find that in umbrella cells ADAM17 is localized to UP3a-positive discoidal/fusiform vesicles, the major apically directed vesicle population in these cells. Second, we observe that ADAM17 is expressed at or near the apical surface of the umbrella cells, which we previously showed is a primary site for EGFR and HB-EGF-dependent receptor transactivation (43). Third, we find that the ADAM17 inhibitor Tapi2 impairs exocytosis. Finally, we adapted our previously described *in situ* adenoviral transduction approach to express ADAM17-specific interfering RNAs. This technique resulted in an ~ 90% knockdown of ADAM17 expression in the uroepithelium and caused a >85% decrease in CCPA-induced hGH release. While we cannot rule out a role for other ADAMs in this process, the knockout of ADAM17 was sufficient to block the majority of A₁AR-stimulated exocytosis in the uroepithelium. However, as noted above a different ADAM isoform is likely required for stretch-induced transactivation in rabbits.

3.4.3 A $G_i \rightarrow G_{\beta\gamma} \rightarrow PLC \rightarrow DAG \rightarrow PKC$ pathway promotes ADAM17 activation

An important question is the upstream signaling events that lead to ADAM17 activation, as many studies employ non-physiological stimuli such as treatment with TPA and PMA. Work to date has shown roles for ERK, p38 MAPK, and several classical PKC isoforms (166,167,230,303,304). For example, in lung cells, PKC ϵ -mediated ADAM17 activation has been shown to be necessary for premalignant changes post exposure to tobacco smoke (315), while in glioblastoma cells, migration was initiated by PKC α -mediated activation and membrane translocation of ADAM10 and the subsequent cleavage of N-cadherin (325). Furthermore, in African green monkey kidney cells (Vero-H cells), PKC δ was found to directly bind and activate ADAM9, leading to cleavage of HB-EGF (326). Our current data show that A₁AR-mediated apical exocytosis requires G_i and $G_{\beta\gamma}$, confirming that the activation of ADAM17 occurs downstream of a *bona fide* A₁AR, G_i -protein signaling event. Furthermore, we observe a requirement for PLC, which is known to generate IP₃ and diacylglycerol, a well-known activator of PKC. Finally we have shown a requirement for PKC in apical exocytosis, noting that the selective PKC inhibitor calphostin C inhibits adenosine-stimulated exocytosis, while TPA stimulates it. Importantly, we can show that these effects occur upstream of EGFR transactivation. While we do not know if there are additional effectors in the pathway, our results are consistent with the hypothesis that a $G_i \rightarrow G_{\beta\gamma} \rightarrow PLC \rightarrow DAG \rightarrow PKC$ cascade promotes ADAM17 activation.

PKC may promote apical exocytosis by phosphorylation of Ser811 in the cytoplasmic domain of ADAM17

An important but unresolved question in the field is how stimuli such as PMA promote ADAM-dependent shedding of EGFR ligands. PMA is reported to act, in part, by enhancing

membrane traffic of ADAMs to the cell surface (201); however, other reports indicate that the surface distribution of ADAM17 is not significantly altered by this treatment (215,327,328). Alternatively, the ligands themselves that may show enhanced traffic. An alternative hypothesis is that stimuli such as PMA promote ADAM17 function by altering its dimer-monomer equilibrium and association with tissue inhibitor of metalloproteinases (TIMP) 3 (244); however, the lack of TIMP3 expression was previously reported to be without effect on ADAM activity (238). Still yet, PMA is proposed to change the redox potential of extracellular protein disulfide isomerase, which may then alter ADAM17 activity by rearrangements of its disulfide bonds (305). Finally, PMA, acting through PKC, may function by promoting ADAM17 phosphorylation. Current evidence indicates that PMA may activate ERK or p38 MAPK, both of which are reported to phosphorylate Thr735 in the cytoplasmic domain of ADAM17 (201,202). Furthermore, phosphorylation of Ser791 or Ser819 (by unknown kinases) is also reported (210,303), but Ser791 is apparently phosphorylated in the resting state, and mutations of Ser819 do not appear to impact ADAM17 activity (210). Finally, there are several reports that ADAM17 lacking its cytoplasmic domain can still trigger EGFR transactivation (238,327-329), a finding at odds with any role for phosphorylation in ADAM17 activation.

We identified a canonical PKC phosphorylation site in the cytoplasmic domain of ADAM17, centered at Ser811. Mutation of this residue to an Ala residue almost completely blocked CCPA-induced hGH release, consistent with the possibility that this residue is critical for ADAM17-dependent EGFR transactivation in the umbrella cell. While we hypothesize that this residues function is modulated by phosphorylation, mutation of Ser811 to a nominally phosphomimetic Asp residue was without effect. However, it is worth noting that phosphorylation is not always mimicked by substitutions with Glu or Asp residues (330-332). Thus, we will need

to perform additional experiments to confirm whether Ser811 is indeed phosphorylated and whether this event correlates with ADAM17 function in umbrella cells. In either case, our result does indicate a critical role for the cytoplasmic domain of ADAM17 in the regulation of its activity, and is inconsistent with the hypothesis that ADAM17 functions independently of this domain.

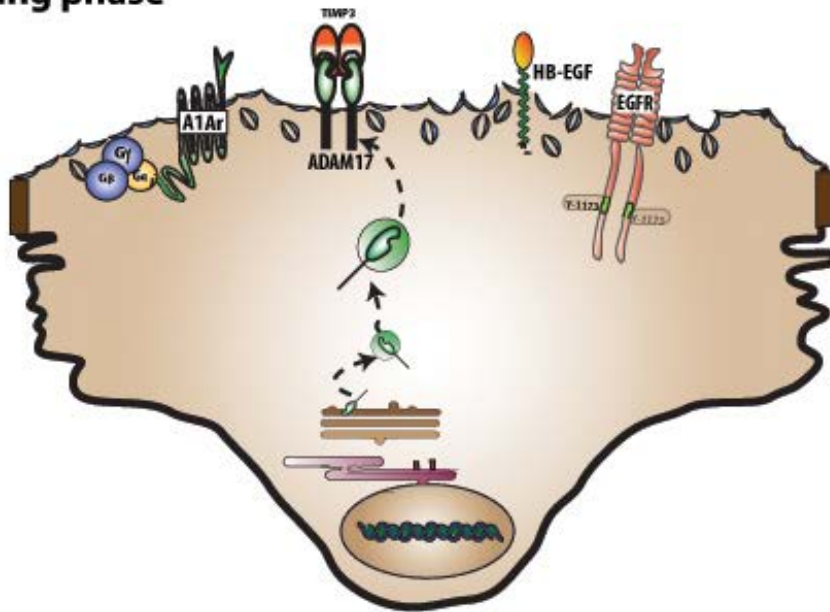
Assuming that Ser811 is phosphorylated, how might it act? One possibility is that phosphorylation of this residue alters the conformation of ADAM17, thus promoting its activity. If true, then this would represent a form of inside-out signaling. This could be a direct effect on ADAM17 or might be indirect, e.g. it could act by modifying the association of the proteinase with TIMP3 (243,244,333). An additional possibility is that phosphorylation of Ser811 forms a docking site for other proteins to bind and trigger ADAM17 activation and or association with its substrates. Potential interacting proteins include MAD-2, a component of mitotic spindle assembly (233), the protein tyrosine phosphatase-H1 (PTPH-1) and SAP9, both of which interact with the COOH-terminal of ADAM17 and negatively regulate its function (234,334), Eve-1 (235), or the N-arginine dibasic convertase (nardilysin) that interacts with both HB-EGF and ADAM17 and regulates cleavage of the latter (335). Obviously, additional work is needed to understand the mechanisms by which ADAM17 activity is regulated.

In summary we propose the following model of how ADAM17 activity is regulated in the umbrella cells: In the quiescent state, when the uroepithelium is not activated by adenosine stimulation, ADAM17 at the apical surface is kept in an inactive dimer state by the inhibitory effect of TIMP3 (Figure 24 A). On activation of A₁AR, a G_i→G_{βγ}→PLC→PKC pathway is initiated leading to the activation of ADAM17, possibly by phosphorylation at Ser811 in the cytoplasmic tail. Active ADAM17 breaks away from the dimer conformation and loses TIMP3

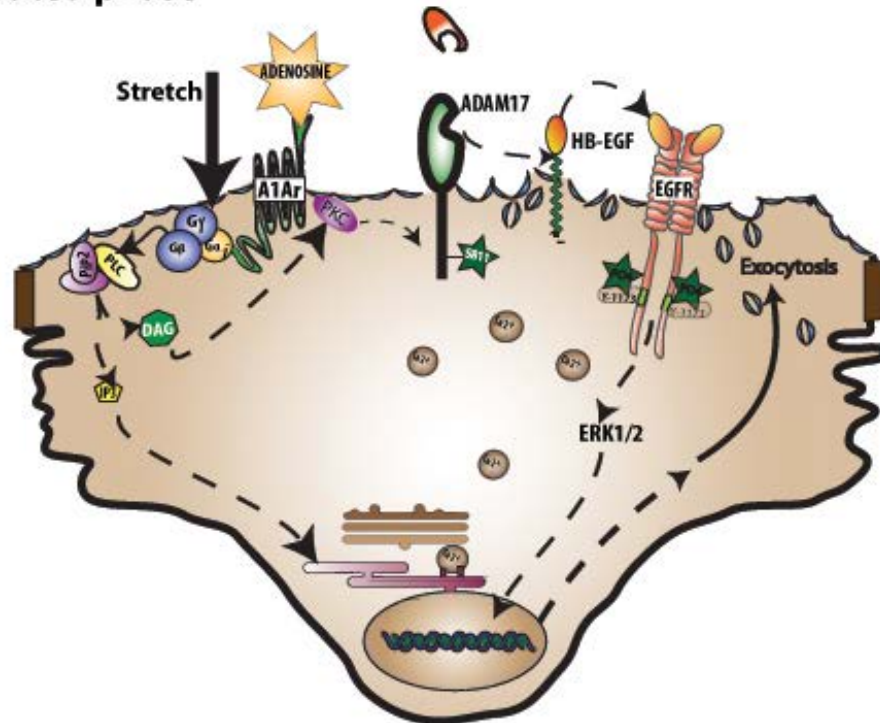
inhibition. It cleaves and releases HB-EGF. Released HB-EGF binds and activates EGFR by phosphorylation at Tyr1173 leading to downstream ERK1/2 MAPK pathway, protein synthesis and exocytosis (Figure 24 B). While stretch-mediated apical exocytosis in rats also requires ADAM17 activity, the signaling pathway that activates the protein or the upstream-mechanosensors that are triggered were not investigated in this study.

Figure 24 Schematic of A₁AR-mediated EGFR transactivation

A Resting phase



B Activated phase



A. In the quiescent bladder where A_1AR is not activated, ADAM17 is kept dormant by the inhibitory action of TIMP 3, HB-EGF is not cleaved and EGFR is not activated. B. In the bladder stimulated by adenosine, A_1AR is activated which in turn triggers a $G_i \rightarrow G_{\beta\gamma} \rightarrow PLC \rightarrow PKC$ pathway that leads to the activation of ADAM 17 (by phosphorylation of Ser811). Activated ADAM17 is released from the inhibitory action of TIMP3 and in-turn cleaves and releases HB-EGF which binds and transactivates EGFR. Active EGFR, by means of Y-1173 phosphorylation in its cytoplasmic tail establishes an ERK1/2 signaling cascade that results in protein synthesis and exocytosis.

4.0 CONCLUSION

4.1 INTRODUCTION

The bladder mucosa is constantly exposed to physiological stress induced by cyclical changes in bladder volume and constituents of the urine. I undertook this study to understand the various cellular mechanisms employed by the umbrella cells to cope with the stress. I focused my studies on the impact of adenosine and adenosine-mediated signaling because it is one of the most well-known stress response hormones in the body (320,336). For example, during ischemic episodes in the heart adenosine protects by decreasing the metabolic load of the myocardium and by increasing the coronary blood flow by vasodilation (337). Further, the role of adenosine as an organ protective agent during hypoxia and numerous other pathological conditions has been studied (81,276). Not surprisingly then, I found that adenosine is released from the bladder mucosa when the uroepithelium is under stress. Further, my studies revealed that activation of A₁AR lead to a decrease in the threshold pressure of bladder-voiding, and at the cellular level triggered EGFR transactivation and membrane trafficking. As my dissertation comes to an end, my research paves the way for future studies that will better our understanding of the uroepithelium and sensory transduction by epithelial cells in general. I first briefly summarize my findings and then put forth some ideas for areas of research that warrant further investigation.

4.2 SUMMARY OF RESULTS

4.2.1 Impact of adenosine on bladder function

While there are many studies that focus on ATP-mediated bladder regulation, it is well-known that ATP is actively converted to adenosine by CD39 and CD73 in the extracellular space (324,338). Further, we have evidence that all four adenosine receptors are expressed in the uroepithelium and especially A₁AR is expressed on the apical surface of umbrella cells (53). Therefore, I studied the turnover of adenosine in the bladder lumen and the impact of activating apical A₁AR on bladder function (Chapter 2). My studies revealed that extracellular adenosine levels significantly increased when the bladder was subjected to stretch-induced stress. While, the mucosal adenosine levels were regulated by the function of adenosine deaminases and ENTs, the serosal adenosine levels were maintained by adenosine kinase and nucleoside transporters. To understand the role of this increased adenosine level on the function of the organ, I performed CMG on anesthetized rats. Adenosine or the A₁AR agonist CCPA was intravesically instilled and the intraluminal pressure monitored. Remarkably, activation of the A₁AR with CCPA or enriching luminal adenosine by blocking its routes of turnover caused lowering of the threshold pressure of bladder voiding. This could be a mechanism through which adenosine relieves interluminal stress in the bladder, by allowing the bladder to void from a lower threshold pressure.

While adenosine plays protective role during normal physiological processes, stresses such as ischemia, hypoxia, bacterial cystitis in the bladder, intestinal infection, and diseases such as asthma leads to an increase in extracellular adenosine which worsens the condition. This could

be because of activating A_{2A} and A₃ receptors on the NK cells, mast cells and neutrophils and triggering the release of inflammatory mediators such as TNF α , IL-12 and INF γ (137-141,158).

The results of my studies align with these other reports on adenosine receptor signaling in inflamed organs (134,276). I studied the impact of adenosine on pathologic bladders. I artificially induced bladder cystitis by treatment with cyclophosphamide, and studied the impact of adenosine on it. Intriguingly, adenosine exacerbated the bladder pathology by causing increased detrusor activity and reducing the time between successive voids.

Adenosine protects at the organ level by reducing threshold pressure of voiding and relieving interluminal stress. However, the umbrella cells are also subjected to stress when incomplete voiding on outlet obstruction leads to over full bladder. We lack information on how adenosine impacts these cells and whether it modulates membrane trafficking events in the cells to relieve stress. Therefore, in the second part of my dissertation, I studied the impact of adenosine at the cellular level on the umbrella cells.

4.2.2 The network of signals that coordinate umbrella cell function

I report that activating apically localized A₁AR trigger a late phase-like exocytosis response that is dependent on protein synthesis and is sensitive to BFA treatment. Furthermore, A₁AR triggered apical exocytosis occurs via a pathway that depends on apical HB-EGF-mediated EGFR transactivation and downstream ERK1/2 activation. Interestingly, kinetics of exocytosis and the EGFR transactivation were similar to stretch-mediated late phase exocytosis. This indicates that multiple stimuli, perhaps related to stress can activate these pathways. I next sought to understand how the A₁AR triggered the response. I identified the cellular pathway that links A₁AR to EGFR and report that an A₁AR \rightarrow G_i \rightarrow G _{$\beta\gamma$} \rightarrow PLC \rightarrow PKC pathway is involved. PKC

lead to the activation of ADAM17 which in-turn cleaved HB-EGF and resulted in EGFR activation.

Importantly, I used a previously described method for *in situ* transduction to express shRNAs, allowing me to knockdown the expression of ADAM17 specifically in the umbrella cells. This tool is particularly exciting because it allows us to specifically target proteins in the umbrella cells and knock them down. A₁AR- and stretch-mediated EGFR transactivation and apical exocytosis was blocked on ADAM17 knockdown.

Finally, to determine how PKC activates ADAM17, I studied a previously unexplored canonical PKC phosphorylation motif in the cytoplasmic tail of ADAM17. I performed point mutations where the serine residue at site 811 was converted to Ala or Asp. The Ser811Ala mutation impaired A₁AR-mediated apical exocytosis. Whether this serine residue is directly phosphorylated by PKC has yet to be investigated. But my studies revealed the importance of the cytoplasmic domain of the protein and is inconsistent with the whereby ADAM17-mediated substrate cleavage is not dependent on this domain.

4.2.3 Conclusion of my studies

The results of my two studies indicate that adenosine-mediated signaling plays a beneficial role in the bladder both at the organ and at the cellular levels. Adenosine is actively released during bladder stress and is constantly turned over. While at the organ level luminal adenosine, acting on A₁AR lowered the threshold pressure of bladder voiding thus relieving stress, at the cellular level, adenosine has an additional role of promoting exocytosis in umbrella cells. The exocytosis leads to increase in the apical surface area of umbrella cells, thereby resulting in the increase in bladder volume. Thus the role of adenosine in the bladder can be summarized as: *a protective*

agent that, during stressful conditions promotes bladder voiding by lowering the threshold pressure and also increases the apical surface of umbrella cells to mitigate the stress induced by mechanical stretching of the cells. While the results of my studies help to better understand the role of adenosine in bladder function, it has raised few important questions that warrant further study. I have addressed some of the questions in the following section.

4.3 FUTURE DIRECTIONS

The role of the cytoplasmic domain of ADAM17

The role of the metalloproteinase in other organ systems including the heart, kidney, brain, and embryonic development has been well studied (339-341). However, its role in bladder function is only now beginning to become clear. My data suggests that a PKC-mediated inside-out signaling is essential for ADAM17 function. However, this is in contradiction to studies which showed that the cytoplasmic tail was not required for the function of the enzyme (238,329). However, many of these studies were performed in immortalized cell lines where ADAM17 was exogenously expressed and artificially activated. The activity of ADAM17 in the physiological system might work differently and might require its cytoplasmic tail for its function. In conversations with other scientist working on ADAM17 signaling, I gathered that the role of cytoplasmic tail of ADAM17 is more essential for the trafficking of the protein than its catalytic activity. While the function of the metalloproteinase domain can be regulated differently, the role of the cytoplasmic tail could be to regulate surface expression of the protein.

Perhaps, the cytoplasmic tail, and its various interacting proteins adds another level of regulation by modulating surface expression. More studies are warranted especially in dissecting the regulation of its catalytic function from its trafficking pattern within the cell.

Most importantly, I identified a canonical PKC phosphorylation site in the cytoplasmic domain of ADAM17 that has not been explored before. Point mutations where the critical serine residue (Ser811) was converted to alanine had a big impact on A₁AR-mediated apical exocytosis. However, at this point, we still do not know if the serine residue is phosphorylated and if so, whether PKC directly phosphorylates it. More experiments are required to determine whether the residue is phosphorylated. Mass spectrometry analysis has proved to be challenging because of the proximity of the residue to trypsin cleavage sites (mass spectrometry is done post trypsin-mediated cleavage of the protein), hence an alternative strategy has to be employed. Immunoprecipitation of activated ADAM17, followed by immunoblotting with phosphor-serine antibodies is another approach. However, the presence of other serine residues in the cytoplasmic tail that are phosphorylated (Ser791 and Ser 819) might complicate the results.

I also identified mRNA message for ADAM10 in the uroepithelium. ADAM10 is the closest relative to ADAM17. The role of ADAM10 in the bladder was not elucidated in this study and warrants further research.

How does adenosine lower threshold pressure?

My studies using CMG revealed that activation of luminal A₁AR relieved bladder pressure by lowering the threshold pressure of voiding. How might this happen? It is possible that activating apically localized A₁AR on the umbrella cells triggers the release of factors from the basolateral surface. Subjacent to the umbrella cells are afferent nerve processes (A δ fibers and C-fibers). As mentioned earlier, the A δ fibers sense bladder fullness and interluminal stress

and could be a direct target of factors released from the basolateral surface of the umbrella cells. Furthermore, the intermediate cells could act as amplifiers of the signals received from the umbrella cells, thus enhancing the stress signals received from the umbrella cells (342,343).

In support of my view that activation of apical adenosine can activate afferent neurons, numerous studies have shown that mechanical stretching of the bladder triggers firing of afferent nerves (290,344). My studies showed that stress induced by mechanical stretching cause release of adenosine from the uroepithelium. Taken together, these data indicate that stress-induced release of adenosine binds apical A₁AR and triggers release of factors from the uroepithelium that could have a direct impact on the neuronal circuitry of the bladder.

What could these factors be? Numerous studies have shown that neuro-modulatory effectors such as Ach, ATP and NO are released from the uroepithelium (71,73,75,345-347). Furthermore, I report that adenosine is also released from the serosal surface of the uroepithelium under stress. These are the likely factors to be released from the uroepithelium on adenosine-mediate signaling. The released factors might bind and activate the afferent nerve process, which have been reported to carry the receptors for these factors.

However, the challenging task would be to study the factors released from the serosal surface of the uroepithelium in real time as bladder fills and its impact on the afferent nerves and muscles. The Ussing chamber apparatus is a good setup to collect factors released from the serosal surface. Apical A₁AR can be activated and the factors released from the serosal surface can be determined by sampling the buffer bathing the serosal chamber at different time points and analyzing the sample for the presence of the candidate factors such as Ach, NO, and ATP.

Another method of identifying the mediators released from the uroepithelium on A₁AR activation is by specifically knocking down enzymes and proteins involved in the synthesis of

the factors. For example, choline acetyltransferase can be knockdown specifically in the umbrella cells by using the shRNA-mediated knockdown technique that I used in this dissertation, and synthesis of Ach can be blocked. CMGs can be performed in the knockdown rat, and CCPA can be intravesically instilled to determine whether Ach is involved in A₁AR-mediated bladder modulation. Similar approaches can be used to study NO or ATP involvement in A₁AR-mediated bladder regulation.

Does transactivation lead to lowering of threshold pressure of bladder voiding?

From my studies on the umbrella cells, I found that activation of A₁AR lead to EGFR transactivation. Could this pathway be how A₁AR triggers lowering of threshold pressure and could this be a central pathway via which the bladder relieves luminal stress?

This could be tested in CMG studies where EGFR is blocked by intravesicle administration of AG1478. In addition, CMG can also be performed on rats where ADAM17 is knocked out (as ADAM17^{-/-} mice are not viable). These experiments would reveal the importance of EGFR transactivation in modulating bladder function.

The adenoviral-mediated *in situ* knockdown technique that I have used to study the role of ADAM17 in my dissertation is a powerful tool to study specific pathways and the role of specific proteins in bladder regulation. Performing CMG on rats where specific proteins in the transactivation pathway such as EGFR, HB-EGF or PKC are knocked down will provide valuable, real-time information on the role of proteins in bladder regulation.

How does EGFR transactivation promote exocytosis?

Adenosine stimulates exocytosis at the apical surface of umbrella cells via EGFR transactivation. My data indicates that protein synthesis is required for the exocytosis. However, the identity of the protein(s) synthesized is unknown. The protein synthesis could result in the manufacture of fresh vesicles and the machinery required to export them to the apical surface or could result in the expression of a yet to be identified protein that triggers the exocytosis of pre-existing vesicles.

The proteins synthesized downstream of EGFR transactivation and how it impacts late phase exocytosis definitely warrants further studies. It will be interesting to perform a microarray analysis of all the genes transcribed as result of adenosine- and stretch-mediated EGFR transactivation. The analysis would provide very valuable information regarding why myriad signaling pathways converge onto EGFR transactivation in umbrella cells and what genes are activated/ down regulated, leading to late phase exocytosis.

Furthermore, we still don't know if the early- and late-phase exocytic pathways lead to the exocytosis of distinct DFV populations. There is a possibility that there are two distinct population of DFVs, the Rab11a and the Rab27 positive vesicles (24). It will be interesting to know what are the deciding factors within the cell that determine which population of vesicles will be exocytosed.

To delineate between the roles of Rab11a positive DFVs and Rab27 positive DFVs the adenoviral-mediated knockdown strategy can be employed. By knocking down either Rab11a or Rab27 and activating A₁AR or stretch in Ussing chamber apparatus, the protein involved in two phase of exocytosis can be ascertained.

4.4 CLOSING COMMENTS

This dissertation has furthered our understanding of the role of adenosine on bladder function both at the organ level and at the cellular level. From a clinical perspective, the discovery that adenosine regulates bladder function by lowering the threshold pressure has therapeutic potential in treating urinary bladder stress-related disorders. From a cell biology perspective, the discovery that A₁AR transactivates EGFR in the umbrella cells, and that the pathway involves ADAM17 are key findings that open many new avenues of research in umbrella cell biology. Finally, while this work has answered few questions, has given rise to many more critical questions. Further investigation is required to better understand the sensory function of the umbrella cells and the other polarized epithelial cells of our body.

5.0 MATERIALS AND METHODS

5.1 CHAPTER 2 MATERIALS AND METHODS

5.1.1 Reagents

Unless otherwise specified, all chemicals were obtained from Sigma (St. Louis, MO) and were of reagent grade or better. Adenosine, adenosine agonists, and modulators of adenosine turnover were freshly prepared as stocks in the following diluents: a 10 mM stock of CCPA was made in DMSO, 25 mg/ml of cyclophosphamide was prepared in distilled H₂O, a 10 mM stock solution of *S*-(4-nitrobenzyl)-6-thioinosine (NBTI) was prepared in DMSO, 100 μ M 5-iodotubericidin (IDT; Tocris, Ellisville, MO), 10mM stock of *erythro*-9-(2-hydroxy-3-nonyl)adenine hydrochloride (EHNA; Tocris) was made in DMSO, and a 10 mM stock of 1,3-dipropyl-8-cyclopentylxanthine (DPCPX) made in DMSO. Adenosine was freshly prepared and dissolved in Krebs buffer (110 mM NaCl, 5.8 mM KCl, 25 NaHCO₃, 1.2 mM KH₂PO₄, 2.0 mM CaCl₂, 1.2 mM MgSO₄, 11.1 mM glucose, pH 7.4). Beuthanasia-D and butorphanol (Torbugesic-SA) were purchased from Butler Schein (Dublin, OH). Lidocaine (LMX4) and isoflurane were purchased from Webster Veterinary (Webster, NY). The polyclonal anti-A₁ receptor rabbit antibody was obtained from Abcam (ab82477; Cambridge, MA), fluorophore- or HRP-conjugated secondary

antibodies were purchased from Jackson ImmunoResearch (West Grove, PA), and TRITC-labeled phalloidin and To-Pro3 were procured from Molecular Probes/Invitrogen (Grand Island, NY).

5.1.2 Animals

Animals used in this study were female New Zealand white rabbits (3–4 kg; Myrtle's Rabbitry, Thompson Station, TN) and female Sprague-Dawley rats (250–300 g; Harlan Laboratories). Rabbits were euthanized by intravenous injection of 300 mg of pentobarbital sodium (Buthensia D) into the ear vein after the area was numbed using topical lidocaine ointment. After euthanasia the bladders were rapidly excised and processed as described below. Rats were sedated by inhalation of isoflurane and then 1.2 g/kg urethane dissolved in H₂O was injected subcutaneously. After 2 h, the rats were prepared for adenosine measurements or cystometry as detailed below. At the end of the experiments, the rats were euthanized by inhalation of 100% CO₂, and a thoracotomy was performed to verify death. All animal studies were carried out with the approval of the University of Pittsburgh Animal Care and Use Committee.

5.1.3 Mounting the uroepithelium in Ussing stretch chambers

Mounting of tissue in Ussing stretch chambers was performed as described previously (28). Briefly, excised rabbit bladders were cut open longitudinally, washed with Krebs buffer, and then mounted on custom-made Teflon racks, mucosal side down. The smooth muscle layers were removed with sharp scissors and forceps. The remaining mucosal tissue, containing the

uroepithelium, was mounted on the pins of a plastic ring with a 2-cm² opening. The ring, with tissue, was sandwiched between two halves of a modified Ussing stretch chamber. Each hemichamber (mucosal and serosal) was filled with 12.5 ml of Krebs solution and the serosal hemichamber was bubbled with gas containing 5% (vol/vol) CO₂ and 95% (vol/vol) air. The tissue was equilibrated for 30 min before the start of the experiment.

5.1.4 Measurement of adenosine, AMP, and inosine

After mounting and equilibration, rabbit tissue was isovolumetrically washed three times with 60 ml of Krebs buffer. After a 60-min incubation, the tissue was gradually stretched by infusing Krebs solution into the enclosed mucosal chamber at a rate of 100 µL/min until the chamber was filled (2 ml). Afterwards, the Luer ports providing access to the mucosal hemichamber were sealed and an additional 500 µL of buffer was pumped into the mucosal hemichamber, causing the uroepithelial tissue to completely bow outwards. The fully distended tissue was incubated for an additional 60 min. Samples, taken with replacement from the serosal or mucosal hemichambers at the designated time points, were heat inactivated, flash frozen in liquid nitrogen, and stored at -80°C.

For *in vivo* studies, rats were anesthetized and two-h post urethane administration, a toe/tail pinch was used to confirm that the animals had reached an appropriate anesthetic depth. Anesthetized rats were placed on their backs and the hind legs secured to the table to provide easier access to the abdomen. The fur around the urethral opening and along the caudal midline was removed with a surgical grade trimmer (Oster, McMinnville, TN). The hairless area was wiped with 70% ethanol and a 1.5 -cm incision was made just to the left of the midline. The

subcutaneous fat and muscle layer were incised and the bladder was then located and exteriorized. The ureters were located, tied off using a 6-0 silk suture (Covidien, Mansfield, MA), and then cut to prevent urine from entering the bladder. The bladder was placed back in the body cavity and the incision sutured close. A 22g I.V. catheter was trimmed to a length of 1.5 cm, inserted through the urethra, and then residual urine was removed by gently pressing the abdomen to promote voiding. The bladder was then filled with sterile phosphate buffered saline containing 0.9 mM CaCl_2 and 1.0 mM MgCl_2 (PBS+) and the bladder voided. This was repeated two additional times. The bladder was then slowly filled for 60 min with PBS+ at a rate of 6 $\mu\text{l}/\text{min}$. At the end of this incubation, the bladders were voided and the intravesicle fluid collected for analysis. Subsequently the bladder was again slow filled for 60 min, and then maintained in its filled state for an additional 60 min. At the end of the treatment the bladder was voided and fluid was then collected. Samples were treated and stored at -80°C as described above.

Adenosine, AMP, and inosine concentrations in the samples were determined using a triple quadrupole mass spectrometer (TSQ Quantum-Ultra, ThermoFisher Scientific, San Jose, CA) as previously described (348).

5.1.5 Cystometry analysis

Rats were anesthetized and their bladder exposed as described above. Upon being exteriorized, the bladder was held in position by placing a plastic dowel behind the bladder. The bladder was moistened with normal saline and shallow purse string sutures were made around the dome using a 6-0 silk suture material. Care was taken to not puncture the bladder. The area within the boundary of the sutures was punctured with an 18 G needle, and a flame-flanged PE50 tube was

inserted into the hole. The suture was tightened around the tubing and the tube was gently retracted until the flange was flush with the mucosa. The bladder was returned to the peritoneal cavity, and the surgical incision was closed around the PE50 tubing in two layers using 6-0 silk suture.

The PE50 tubing was connected to a 3 way port: one branch led to a pressure transducer, while the other two were connected to syringes containing buffered urine substitute (BUS) \pm drug. BUS, made in accordance with the published composition of Sprague-Dawley rat urine (349), had the following composition: 26 mM $(\text{NH}_4)_2\text{SO}_4$, 149 mM NaCl, 267 mM KCl, 3 mM CaCl_2 , and 0.4% (w/v) MgPO_4 . The solution was titrated with NaOH until a pH of 6.5 was measured. The pressure transducer was connected to a Quad Bridge Amplifier and Powerlab 4/30 (ADInstruments; Castle Hill, Australia), which was interfaced with an iMac computer (Apple; Cupertino, CA) running the Chart 5.0 program (ADInstruments; castle Hill, Australia). The syringes containing the buffers were placed in a syringe pump (New Era Syringe Pump Systems, Farmingdale, NY) and BUS was infused into the bladder at a rate of 50 $\mu\text{l}/\text{min}$ for 45 min, until uniform peaks were obtained. BUS (\pm drugs) was then infused for 60-90 minutes. The effluent was collected and the volume was measured to determine the fluid recovery.

The cystometrograms (CMGs) were recorded using the Chart program (ADInstruments). Following a 45-min period of equilibration, data for 8-12 successive bladder cycles were collected and for each animal the average values for the following parameters were entered in an Excel spread sheet (MS Office, Microsoft, Redmond, WA): 1) the basal pressure was the lowest pressure point recorded immediately following a void; 2) the threshold pressure was the pressure point recorded just before the spike in pressure was observed as the bladder began to void; 3) the peak pressure was the maximum pressure recorded during voiding; 4) the intercontraction

interval (ICI) was the time between two consecutive peak pressures; 5) the percent fluid recovery was the ratio of the volume of fluid released versus that infused into the bladder. The mean and SEM were calculated for each similarly treated experimental group and the data analyzed for statistical significance using the techniques described below.

5.1.6 Cyclophosphamide treatment

An acute cyclophosphamide-induced cystitis was induced as described previously (284,350). In brief, rats were sedated with isoflurane and administered 1mg/kg butorphenol subcutaneously and 150 mg/kg cyclophosphamide intraperitoneally. Two h after these injections the rats were given 1.2 g/kg urethane subcutaneously, and then 2 h later the CMG analysis was performed as detailed above.

5.1.7 Immunofluorescence labeling and image acquisition

Bladder tissue was fixed and processed as described previously (49)

. Images were captured using a 63X 1.2 NA glycerol objective and the appropriate laser lines of a Leica TCS SP5 CW-STED confocal microscope (in normal confocal mode). The photomultipliers were set at 900-1200 and images collected using an average of six line scans. Serial 0.25 μm z-sections were acquired. The images were imported into Volocity 4-D software (Perkin Elmers; Waltham, MA) and following image reconstruction and contrast correction

exported as TIFF files. The exported images were opened in Adobe Photoshop CS5, converted to JPEG format, and the composite images prepared in Adobe Illustrator CS5.

5.1.8 Western blot analysis

Lysates of uroepithelial cells and western blotting was performed as described previously (43).

5.1.9 Statistical analysis

Statistical significance between means was determined by Student's *t*-test or in the case of multiple comparisons by analysis of variance (ANOVA). If a significant difference in the means was detected by ANOVA, multiple comparisons were performed using Dunnett's post-test correction. Statistical analyses were performed using Prism 5 software (GraphPad, La Jolla, CA)

5.2 CHAPTER 3 MATERIALS AND METHODS

5.2.1 Reagents and antibodies

Unless otherwise specified, all chemicals were obtained from Sigma (St. Louis, MO) and were of reagent grade or better. Adenosine was freshly prepared and dissolved in Krebs buffer (110 mM NaCl, 5.8 mM KCl, 25 NaHCO₃, 1.2 mM KH₂PO₄, 2.0 mM CaCl₂, 1.2 mM MgSO₄, 11.1 mM glucose, pH 7.4). The following stock solutions were prepared in DMSO: AG1478 (10 mM), calphostin-C (250 µM), 2-Chloro-N⁶-Cyclopentyladenosine (CCPA) (10 mM), GM6001 (15 mM), Tapi-2 (15 mM, Tocris, Bristol, U.K) and U0126 (10 mM). A 10mM stock of phorbol myristate acetate (PMA) was prepared in ethanol, and the following stocks were prepared in molecular biology grade water: pertussis toxin (100 µg/ml), CRM197 (25 ng/ml), and M119K (10 mM, purchased from the National Cancer Institute, Bethesda, MD). WGA-FITC was purchased from Vector labs (Burlingame, CA) Beuthanasia-D was purchased from Butler Schein (Dublin, OH). Lidocaine (LMX4) and isoflurane were purchased from Webster Veterinary (Webster, NY). The polyclonal anti-A₁AR rabbit antibody was obtained from Abcam (ab82477; Cambridge, MA), anti-ADAM17 rabbit polyclonal antibody from EMD-Millipore (Billerica, MA), anti-EGFR and anti-EGFR-phospho-Y-1173 rabbit polyclonal antibodies from Cell Signaling Technology (Danvers, MA) fluorophore- or HRP-conjugated secondary antibodies were purchased from Jackson ImmunoResearch (West Grove, PA), and TRITC-labeled phalloidin and To-Pro3 were procured from Molecular Probes/Invitrogen (Grand Island, NY).

5.2.2 Animals

Animals used in this study were female New Zealand white rabbits (3–4 kg; Covance, Princeton, NJ) and female Sprague-Dawley rats (250–300 g; Harlan Laboratories, Indianapolis, IN). Rabbits were euthanized by intravenous injection of 300 mg of Buthesia D into the ear vein after the area was numbed using topical lidocaine ointment. After euthanasia, the bladders were rapidly excised and processed as described below. Rats were sedated by inhalation of isoflurane and kept under sedation during the adenoviral infection procedure (see description below) by constant inhalation of isoflurane. At the end of the procedure, the rats were allowed to revive. Twenty-four h after infection, the rats were euthanized by inhalation of 100% CO₂, a thoracotomy was performed, and the bladder was excised. All animal studies were carried out with the approval of the University of Pittsburgh Animal Care and Use Committee.

5.2.3 Cell Culture

293A cells (Invitrogen) were used to prepare ADAM17- or scrambled-shRNA viruses. The cells were grown in DMEM purchased from Corning Cellgro (Corning, NY) supplemented with 10% v/v fetal bovine serum (Thermo scientific, Logan, UT), 1% v/v MEM non-essential amino acids (Life Technologies, Grand Island, NY), 2mM glutamate (Sigma), and 1% v/v penicillin/streptomycin (Lonza, Walkersville, MD). cre8 cells were grown in DMEM purchased from Sigma supplemented with 10% v/v defined fetal bovine serum (Thermo scientific) and 1% v/v penicillin/streptomycin. HEK293 cells were grown in DMEM supplemented with 10% v/v fetal bovine serum and 1% v/v penicillin/streptomycin. When producing viruses, cells were grown in their respective media, but without penicillin/streptomycin.

5.2.4 Immunofluorescence labeling and image acquisition

Bladder tissue was fixed and processed as described previously. Briefly, tissues fixed with 4% PFA fixative (4% paraformaldehyde in 100 mM $(\text{CH}_3)_2\text{AsO}_2\text{Na} \cdot 3\text{H}_2\text{O}$) were embedded in OCT-based cryo-blocks. 4 μm sections cryosections were obtained using a Leica CM1950 cryostat on the hydrophobic surface of glass slides. The sections were washed three times 5 min each with PBS and the fixative was quenched with quench buffer (20mM Glycine, 75mM NH_4Cl) for 10 min. When staining for ADAM17, the sections were quenched for 7 min and were subsequently quenched with quench buffer supplemented with 0.05% w/v SDS for an additional 3 min. The tissue was then washed with PBS and blocked with block buffer (7% w/v Fish gelatin, 0.25% saponin v/v and 0.05% NaN_3 w/v made in PBS) for 1-h at room temp. 1:200 dilution of the antibodies where made in the block buffer, applied on the section and incubated at room temp for 2 hr in the case of ADAM17 or overnight at 4°C for A_1AR or UP3a. The primary antibody was washed away with PBS and detected using either Alexa488- or Cy3-labelled secondary antibodies. Actin and nuclei were stained with either rhodamine or fluorescein phalloidin and TOPRO-3 respectively. The sections were post-fixed for 10 min with 4% PFA fixative, mounting buffer (1% w/v phenyldiamine, 20mM Tris, 90% v/v glycerol, pH 8.0) was applied on the section and covered with a glass cover slip. The slide and coverslip assembly was sealed with nail polish. Images were captured using a 63 X 1.2 NA glycerol objective and the appropriate laser lines of a Leica TCS SP5 CW-STED confocal microscope (in normal confocal mode). The photomultipliers were set at 900-1200 V and images collected using an average of six line scans. Serial 0.25 μm Z-sections were acquired. The images were imported into Volocity 4-D software (Perkin Elmers; Waltham, MA) and following image reconstruction and contrast

correction exported as TIFF files. The exported images were opened in Adobe Photoshop CS5, converted to JPEG format, and the composite images prepared in Adobe Illustrator CS5.

5.2.5 Mounting rabbit uroepithelium or rat bladders in Ussing stretch chambers

Isolation of rabbit uroepithelium from the underlying muscle layers and mounting in Ussing stretch chambers were performed as described earlier. Briefly, rabbit bladder was excised, slit open vertically along one of the lateral veins and spread on a custom made Teflon rack with the uroepithelium facing down. The muscles were carefully removed with the pair of tweezers and sharp scissors. The remaining tissue containing the intact uroepithelium was mounted on the pins at the outer edges of a plastic ring with an opening of 2 cm². The rings were locked between two Ussing stretch hemichambers, which were clamped into position on a Teflon base. Warm Krebs buffer was simultaneously added to the mucosal (apical facing) and serosal (muscle facing) chambers. The tissue was gassed with 95% air/5% CO₂ during a 30-45 min equilibration period and treated with the indicated drug added to the mucosal and serosal hemichambers bathing the tissue. However, CCPA, CRM197, or PMA were added only to the mucosal hemichamber. The tissue capacitance (C_T) and transepithelial resistance were measured for a period up to 300 min.

Rat bladder tissue was processed as described earlier. Briefly, the bladder was excised, cut open along one of the lateral veins and then carefully spread and pinned out on rubber dissection mats. The dissected bladders were then mounted on the pins of a plastic ring with an opening of 0.75 cm² and the rings clamped between two Ussing stretch hemichambers. The chambers were filled with Krebs buffer and equilibrated. To stretch the tissue, buffer was added to the mucosal hemichamber chamber via Luer ports at a rate of 35 μ l/min using a syringe pump

(New Era pump systems, Farmingdale, NY). Once the chamber was filled, an additional 250 μ l was then pumped into the chamber to stretch the tissue

5.2.6 Western blot analysis

To prepare lysates, bladder tissue was placed on a rubber dissection mat with the mucosal surface facing up. The tissue was held in place by pinning it at the four corners using 20G $\frac{3}{4}$ " needles (BD Biosciences). An aliquot (35-50 μ l) of SDS lysis buffer (50mM Triethanolamine, pH 8.6, 100 mM NaCl, 5mM EDTA, 0.2% w/v NaN_3 , 0.5% w/v SDS) containing a protease and phosphatase inhibitor cocktail (Cell Signaling Technologies, Boston, MA) was added to the mucosal surface and the uroepithelium recovered by gently scraping the cells using an rubber cell scraper (Sarstedt, Newton, NC). The cell lysate was transferred to a 1.6 ml Eppendorf tube, vortex-mixed at 4°C for 10 min using a model 5432 mixer (Eppendorf, Hauppauge, NY) and centrifuged at 13,000 rpm for 10 min at 4° in a table top model 5415D microcentrifuge (Eppendorf). The clear supernatant was collected, flash frozen, and stored at -80°C. The protein concentration was quantified using the BCA assay (Pierce, Rockford, IL). Equal amounts of protein from the bladder lysates was resolved by electrophoresis on 4-15% polyacrylamide gradient gels (BioRad, Hercules, CA) at 200 V and constant current for 30 min. For ADAM17 and hGH, proteins were transferred to Immobilon P membranes (Millipore) at 375 mA constant current using a 100 mM CAPS, pH 11.0 running buffer. In the case of the EGFR, proteins were transferred to nitrocellulose membranes (GE healthcare) at 375 mA constant current using a Tris-glycine running buffer (25mM Tris, 190mM Glycine) for 2 hr. The membrane was blocked for 30 min with 5% w/v non-fat milk made in TBST buffer (TBS + 0.1% Tween 20). Following the

blocking step, the membrane was incubated with primary antibodies overnight at 4°C. After adequate washes with TBST, the membrane was incubated with goat-anti rabbit-HRP or goat-anti mouse-HRP secondary antibodies for 1h at room temp and washed with TBST. The bands were detected by incubating the membrane with ECL chemiluminescence solution for 2 min (Pierce, Rockford, IL), followed by film capture on Carestream Kodak Biomax films (Carestream, Rochester, NY). Data were quantified using QuantityOne quantification software (Biorad)

5.2.7 Reverse transcriptase PCR

Total RNA was isolated using the RNAqueous kit (Invitrogen) according to the vendor protocol. Briefly, excised rat bladders were slit open along the lateral veins using a scalpel and the bladder pinned out as described above. Cell lysis buffer (50µl) was added to the mucosal surface and the surface was gently scrapped with a rubber cell scraper to lyse the uroepithelium. The lysate was collected, mixed with the provided 64% ethanol buffer, filtered through the included filter cartridges, and total mRNA eluted using the elution buffer provided with the kit. The isolated RNA was treated with DNase (Turbo DNA, Ambion) to deplete any residual genomic DNA. The purified total RNA was used to generate cDNA using the Retroscript first strand synthesis kit (Life technologies) with random decamer oligos provided with the kit according to the vendor's protocol. The cDNA was used as a PCR template and amplification of ADAMs and β -Actin were performed using standard PCR protocol and rat specific sequence primers as follows: target, forward 5'-primer, 3' reverse primer:

ADAM9: AATTGTCACTGTGAAGATGGCTGGGCTCC, GCAGCCGCAACCAGGGGGATGATTAGG

ADAM10: CAAGTGTGCATTGGGCAATGTGCAGG, TGTTCCTGCAAAGAGCCTGTACTGG

ADAM12: AGGATCATGCAACATGTACCAATAGCAGCC, AGGATGTTAGGCTGACCATCATTGCTTGG
ADAM15: CTCCTCAGCCTCCTGTTGTTATTGGTCC, GGGTACTGGAAAGCTGACATTAGCTTGC
ADAM17: GAAGTTTCTGGCAGACAACATCGTTGGG, GGAACGGCTTGATAATGCGAACAGATGC
 β Actin: TCCATCATGAAGTGTGACGTTGACATCC, GGAGCAATGATCTTGATCTTCATGGTGC.

The PCR products were resolved using gel electrophoresis in a 1% agarose gel. The image was captured using a GelDoc image capture system (BioRad).

5.2.8 Generation of adenoviruses encoding ADAM17 shRNA

The iRNAi software (Nucleobytes.com) was used to search the Rat ADAM17 cDNA (Pubmed accession number NM_020306) for optimal sequences containing the sequence AA(N19). Four shRNA sequences were selected. The top and the bottom strands were individually synthesized (IDT, Coralville, IA) and annealed by mixing the two strands in equal concentrations, heating to 94°C and cooling gradually to room temperature. The annealed shRNA sequences were then ligated into the linearized pU6/ENTR vector (Life Technologies). The ability of the different shRNA sequences to silence ADAM17 was determined by co-transfecting HEK293ft cells with shRNA-pU6/ENTR vectors and ADAM17 cDNA. Twenty-four h later, cells were lysed, the proteins were resolved by SDS-PAGE, and ADAM17 detected by western blotting using the techniques described above. Of the four, the sequence that had maximum silencing efficiency (>80%; 5'- GGATTAGCTTACGTTGGTTCT-3') was selected and recombined into the pBLOCKiT Adenovirus System vector (Invitrogen) using an *in vitro* clonase-mediated recombination reaction according to vendor's protocol. The recombined pBLOCKiT vector was linearized by PacI restriction digestion, and transfected into 293A cells using Lipofectamine 2000 reagent (Life Technologies). Eleven days post transfection, when the cytopathic effect was

greater than 75%, the cells in this first P1 generation were harvested by titration, and lysed by freezing the cells at -70°C and thawing them for 5-10 min in a 37°C waterbath. Three freeze-thaw cycles were typically sufficient to lyse the cells. The lysate, containing released virus, was used to infect a new round of cells (P2), a process that was repeated one additional time (P3). The P3 viruses were produced by infecting ten 15-cm petri dishes (BD Falcon San Jose, CA) of 293A cells with virus-containing lysate from P2. On the third day, when the cells showed more than 85% cytopathic effect, they were recovered by titration, pooled, centrifuged at 3500g (Eppendorf 5810 R) for 14 min at 4°C , and mixed in 7 ml of re-suspension buffer (100 mM Tris, pH 7.4, 10 mM EDTA). The concentrated cell suspension was lysed by repeated freeze-thaw cycles as described above. The lysate was separated from the cell debris by centrifuging at $5000 \times g$ (Eppendorf 5810 R) for 15 min at 4°C . The supernatant was carefully removed and applied to the top of a step gradient containing 2.5 ml of 1.25 g/ml CsCl solution, which was layered on top of 2.5 ml of 1.4 g/ml CsCl loaded into clear 13 ml PET ultracentrifugation tube (Thermo Scientific). The sample was centrifuged at 35,000 rpm for 1hr at 4°C using a Beckman Coulter (Brea, CA) using SW-41 swinging bucket rotor. The concentrated virus, which appeared as an off-white band at the interface of the two CsCl layers, was collected by piercing the side wall of the tube with an 18G needle and aspiration into a connected 5 cc syringe (BD Biosciences). The viruses were further purified by passage through a PE10 gel filtration column (GE Healthcare) equilibrated with virus suspension buffer (PBS containing 10% v/v glycerol). The virus-containing fractions were detected by monitoring the A_{260} , pooled, and stored at -70°C in small aliquots, which were thawed in a 37°C water bath just prior to use.

5.2.9 In situ adenoviral transduction and detection of human growth hormone (hGH) release

In situ transduction of rat bladder uroepithelium and measurement of hGH release was performed as described earlier (22). Briefly, rats were sedated with isoflurane and a Jelco IV catheter (Smith Medicals, Southington, CT) was introduced into the bladder via the urethra. The bladder was rinsed with PBS, and filled with 400 μ l of 0.1% w/v dodecyl- β -D-maltoside dissolved in PBS. The urethra was clamped, and after 5 min unclamped to allow the detergent to void. The latter step was facilitated by applying slight pressure to the lower abdomen. The bladder was filled with 400 μ l PBS containing adenoviruses expressing hGH alone or with adenoviruses encoding scrambled-shRNA, ADAM17-shRNA, or the ADAM17-HA constructs described below (2.5×10^8 infectious virus particles, typically in a volume of 2-10 μ l). The bladder was then clamped. After 30 min the clamp was removed and the virus solution was allowed to void. The bladder was rinsed with PBS, anesthesia was discontinued, and the rats were allowed to revive. Thirty-h post infection, the animals were sacrificed by inhalation of CO₂ and the bladder was immediately excised, slit open, and mounted on tissue rings as described above. After 90 min of equilibration, the buffer bathing the apical surface was isovolumetrically replaced with fresh buffer and treated \pm 500nM CCPA. Sixty-min later the apical buffer was removed and concentrated using 10K molecular weight cutoff Amicon Centricon (Millipore) to a volume of 250 μ L. The corresponding tissue was unmounted from its tissue ring and a lysate was prepared prior to Western blot analysis to detect hGH.

5.2.10 WGA-FITC labeling experiment

Rat bladders were mounted in Ussing chambers, and after equilibration were incubated with 25 µg/ml WGA-FITC for 2-h ± 500 nM CCPA added to the mucosal hemichamber. The tissues were then unmounted from the chambers, washed with ice cold 100 mM N-Acetyl D-glucosamine for 4 times, 20 min each and then through washed with ice cold PBS for 3 times 15 min each and fixed with 4% PFA fixative for 30 min at 37°C. The tissue was stained and the images were captured and processed as described above.

5.2.11 Generation of shRNA resistant-ADAM17 and S811A and S811D point mutants

ADAM17 cDNA (from Addgene plasmid 19141(351)) was cloned into pADLOX vector and cDNA encoding HA was added in-frame to the C-terminus of ADAM17 after a gap of two amino acids. A silent mutation was engineered into the ADAM17 sequence (5' GGATTAGCGTACGTTGGTTCT) using the QuickChange XL mutagenesis kit (Agilent), making the construct resistant to the ADAM17 shRNA described above. This resulting construct, called pADLOX-ADAM17^R-HA, was further mutagenized to convert serine at position 811 to an alanine or aspartate residue, generating pADLOX-ADAM17^{R/S811A}-HA (TCA to GCC) and pADLOX-ADAM17^{R/S811D}-HA (TCA to GAC). The constructs (3 µg) were preincubated with Lipofectamine 2000 Opti-MEM media for 30 min, mixed with 3 µg Ψ5 adenoviral genomic DNA (Ad5 strain), and added to Cre8 cells (22,352). Preparation of the adnoviruses and *in situ* transduction were performed as described above.

5.2.12 Statistical analysis

Statistical significance between means was determined by Student's *t*-test or in the case of multiple comparisons by analysis of variance (ANOVA). If a significant difference in the means was detected by ANOVA, multiple comparisons were performed using Dunnett's post-test correction. Statistical analyses were performed using Prism 5 software (GraphPad, La Jolla, CA)

5.3 ADDITIONAL MATERIALS AND METHODS

5.3.1 Generation of lentiviral vectors encoding A₁AR shRNA

iRNAi software was used to design the shRNA sequences. Rat A₁AR cDNA sequence (Pubmed accession number NM64299.1) was analyzed using the software and the shRNA sequences were searched using the 19 (AA) parameter used for ADAM17 shRNAs. Four sequences were selected and the shRNAs were synthesized with CTCGAG loop sequence. An XbaI site was engineered at the 3' end of the sequence, for quick determination of success of cloning. The sequences were cloned into the AgeI-EcoRI site of pLKO.1.GFP.AgeI(-). The clones were verified by sequencing and used to determine which sequence had the best knockdown efficiency. The selected sequence was then used to make the lentivirus using the following protocol:

HEK293ft cells were grown in a 10cm plate in DMEM with 10%FBS and 500mg/ml Geneticin. When the cells reached 85-90% confluence, the media was removed and 5ml Optimem supplemented with 5% FBS was added. 9 μ L of Virapower cocktail (Invitrogen) + 3 μ G of pLKO.1.GFP.Age(-).A₁ARshRNA plasmid were transfected into the cell using Lipofectamine2000. 24-h post transfection, the Optimem was removed and 10ml of DMEM + 10% FBS was added to the cells. 72-h post transfection, the media containing the virus was removed and filtered through a 0.44 μ M PVDF filter. 1ml viral aliquots were stored in -80°C.

5.3.2 DNA and plasmids

Rat A₁AR cDNA in pcDNA3.1 vector (pcDNA.ratA₁ARcDNA) was a kind gift from Dr. Joel Linden. pLKO.1.GFP was a kind gift from Dr. Elaine Fuchs. However, the vector had an additional AgeI site within the hist2h2be-eGFP cassette that impaired cloning of the shRNA sequences as the cloning sites were AgeI-EcoRI. Therefore, the extra AgeI site was removed using site directed mutagenesis and the cloning competent plasmid was called pLKO.1.GFP.Age(-).

5.3.3 Procedure

5.3.3.1 Lentiviral infection in HEK293 cells

HEK293 cells were grown in 6 well plates and rat pcDNA.ratA₁AR cDNA was transfected into the cells using Lipofectamine. 24-h post transfection 10 μ L of lentivirus was added to each well. 24- and 48-h post addition the cells were harvested and lysed.

5.3.3.2 Lentiviral infection in rats

Lentiviral infection in rats were performed as explained in section 5.2.9.

5.3.4 Western blot

Western blots were performed as explained in section 5.2.6. Rabbit anti-A₁AR antibody was purchased from Abcam and used at a concentration of 1:2000.

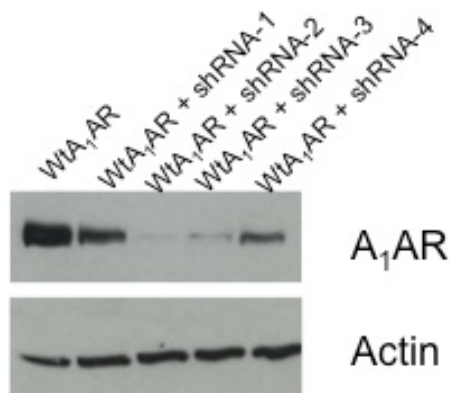
APPENDIX A

KNOCKDOWN OF A₁AR USING LENTIVIRAL-BASED SHRNA VECTORS

A₁AR was the cornerstone of my project. Therefore, I initiated a pilot project to determine the impact of knocking down A₁AR in umbrella cells. The scope of the project was twofold. 1) To determine the impact of umbrella cell-specific A₁AR knockdown on the function of the bladder and 2) To develop a novel *in situ* lentiviral-based shRNA-knockdown technique that can be used to study other proteins in that are involved in membrane trafficking in umbrella cells. The GFP-tagged pLKO.1 vector was a kind gift from Dr. Elaine Fuchs. The vector was designed on a pLKO.1 backbone, where a hist2h2be-eGFP gene was engineered in the place of the puromycin gene cassette. The shRNA expression was driven by a U6 RNA promoter which was upstream to an EcoR1-Age1 cloning site (353). A₁AR shRNA was designed using the iRNAi shRNA software using the AA(19) parameter used for ADAM17 shRNA design and cloned into the lentiviral vector. The sequences were tested in HEK293 cells where A₁AR was exogenously expressed using a pcDNA A₁AR plasmid construct (a kind gift from Dr. Joel Linden). Of the four sequences tested, A₁AR-shRNA sequence 2 (5'- GATCCCTCTCCGGTACAAG-3') was effective in completely knocking down A₁AR expression (Figure 25). The constructs were used to prepare lentiviruses and tested on umbrella cells.

Unfortunately, the transduction efficiency of lentiviruses in the umbrella cells was very poor. This could be because the lentivirus particles were pseudotyped to express vesicular stomatitis virus- glycoprotein G (VSV-G) on their surface for enhancing their tropism. However, VSV-G requires clathrin machinery for uptake. Because endocytosis mechanism in umbrella cells does not occur via clathrin coated pits, this might have hampered entry of the lentiviral particles into the umbrella cell (42).

Figure 25 A₁AR knockdown using lentiviral vectors



HEK293 cells expressing either wild type A₁AR or wild type A₁AR + one of the shRNA sequences were harvested 24-h post transfection. Equal quantities of the protein were loaded and the western blots were probed with either rabbit anti-A₁AR antibody or rabbit anti-actin antibody. Sequence 2 showed maximum knockdown of A₁AR.

APPENDIX B

A RAB11A-RAB8A-MYO5B NETWORK PROMOTES STRETCH-REGULATED EXOCYTOSIS IN BLADDER UMBRELLA CELLS

As a pilot project, I worked in collaboration with Dr. Khandelwal to determine the role of myosin5B actin motor protein in stretch-mediated apical exocytosis in rats. The work completed my dissertation project as it furthered our understanding of how the network of Rabs and their interplay with the cortical actin cytoskeleton regulates apical exocytosis in umbrella cells.

The work was published in MBoC in February 2013. I have presented an abstract of the work here. The complete work can be accessed from pubmed (PMID: 23389633)

Multiple Rabs are associated with secretory granules/vesicles, but how these GTPases are coordinated to promote regulated exocytosis is not well understood. In bladder umbrella cells a subapical pool of discoidal/fusiform-shaped vesicles (DFVs) undergoes Rab11a-dependent regulated exocytosis in response to bladder filling. We show that Rab11a-associated vesicles are enmeshed in an apical cytokeratin meshwork and that Rab11a likely acts upstream of Rab8a to promote exocytosis. Surprisingly, expression of Rabin8, a previously described Rab11a effector and guanine nucleotide exchange factor for Rab8, stimulates stretch-induced exocytosis in a manner that is independent of its catalytic activity. Additional studies demonstrate that the

unconventional motor protein myosin5B motor (Myo5B) works in association with the Rab8a-Rab11a module to promote exocytosis, possibly by ensuring transit of DFVs through a subapical, cortical actin cytoskeleton before fusion. Our results indicate that Rab11a, Rab8a, and Myo5B function as part of a network to promote stretch-induced exocytosis, and we predict that similarly organized Rab networks will be common to other regulated secretory pathways

APPENDIX C

BLADDER FILLING AND VOIDING AFFECT UMBRELLA CELL TIGHT JUNCTION ORGANIZATION AND FUNCTION

I worked on another project with Dr. Marcelo to understand the effect of bladder filling and voiding on the organization of the tight junctional complex of the umbrella cells. The study furthered our understanding of how stress impacts the tight junctions. Though not a part of my study, it will be interesting to investigate the impact of A₁AR signaling on the tight junction complex too.

The work was published in AJP-Renal Physiology in July 2013. I have presented an abstract of the work here. The complete work can be accessed from pubmed (PMID: 23884145)

Epithelial cells are continuously exposed to mechanical forces including shear stress and stretch, though the impact these forces have on tight junction (TJ) organization and function are poorly understood. Umbrella cells form the outermost layer of the stratified uroepithelium and undergo large cell shape and surface area changes during the bladder cycle. Here we investigated the effects of bladder filling and voiding on the umbrella cell TJ. We found that bladder filling promoted a significant increase in the length of the TJ ring, which was quickly reversed within 5 min of voiding. Interestingly, when isolated uroepithelial tissue was mounted in Ussing

chambers and exposed to physiological stretch, we observed a tenfold drop in both transepithelial electrical resistance (TER) and the umbrella cell junctional resistance. The effects of stretch on TER were reversible and dependent on the applied force. Furthermore, the integrity of the umbrella cell TJ was maintained in the stretched uroepithelium, as suggested by the limited permeability of biotin, fluorescein, and ruthenium red. Finally, we found that depletion of extracellular Ca^{2+} by EGTA completely disrupted the TER of unstretched, but not of stretched uroepithelium. Taken together our studies indicate that the umbrella cell TJ undergoes major structural and functional reorganization during the bladder cycle. The impact of these changes on bladder function is discussed.

BIBLIOGRAPHY

1. Apodaca, G. (2004) *Traffic* **5**, 117-128
2. Negrete, H. O., Lavelle, J. P., Berg, J., Lewis, S. A., and Zeidel, M. L. (1996) *The American journal of physiology* **271**, F886-894
3. Hu, P., Meyers, S., Liang, F. X., Deng, F. M., Kachar, B., Zeidel, M. L., and Sun, T. T. (2002) *American journal of physiology. Renal physiology* **283**, F1200-1207
4. Khandelwal, P., Abraham, S. N., and Apodaca, G. (2009) *American journal of physiology. Renal physiology* **297**, F1477-1501
5. Hicks, R. M. (1965) *The Journal of cell biology* **26**, 25-48
6. Porter, K. R., Kenyon, K., and Badenhausen, S. (1967) *Protoplasma* **63**, 262-274
7. Walz, T., Haner, M., Wu, X. R., Henn, C., Engel, A., Sun, T. T., and Aebi, U. (1995) *Journal of molecular biology* **248**, 887-900
8. Wu, X. R., Lin, J. H., Walz, T., Haner, M., Yu, J., Aebi, U., and Sun, T. T. (1994) *The Journal of biological chemistry* **269**, 13716-13724
9. Hicks, R. M., Ketterer, B., and Warren, R. C. (1974) *Philosophical transactions of the Royal Society of London. Series B, Biological sciences* **268**, 23-38
10. Kachar, B., Liang, F., Lins, U., Ding, M., Wu, X. R., Stoffler, D., Aebi, U., and Sun, T. T. (1999) *Journal of molecular biology* **285**, 595-608
11. Hu, P., Deng, F. M., Liang, F. X., Hu, C. M., Auerbach, A. B., Shapiro, E., Wu, X. R., Kachar, B., and Sun, T. T. (2000) *The Journal of cell biology* **151**, 961-972
12. Simons, K., and Eehalt, R. (2002) *The Journal of clinical investigation* **110**, 597-603
13. Acharya, P., Beckel, J., Ruiz, W. G., Wang, E., Rojas, R., Birder, L., and Apodaca, G. (2004) *American journal of physiology. Renal physiology* **287**, F305-318
14. Lewis, S. A., Eaton, D. C., and Diamond, J. M. (1976) *The Journal of membrane biology* **28**, 41-70
15. Lewis, S. A., and Diamond, J. M. (1976) *The Journal of membrane biology* **28**, 1-40
16. Walker, S. R., Callahan, H. J., Fritz, R., and Mulholland, S. G. (1989) *Urology* **33**, 127-130
17. Grist, M., and Chakraborty, J. (1994) *Urology* **44**, 26-33
18. Staehelin, L. A., Chlapowski, F. J., and Bonneville, M. A. (1972) *The Journal of cell biology* **53**, 73-91
19. Deng, F. M., Ding, M., Lavker, R. M., and Sun, T. T. (2001) *Proceedings of the National Academy of Sciences of the United States of America* **98**, 154-159
20. Truschel, S. T., Ruiz, W. G., Shulman, T., Pilewski, J., Sun, T. T., Zeidel, M. L., and Apodaca, G. (1999) *The Journal of biological chemistry* **274**, 15020-15029
21. Kerr, D. E., Liang, F., Bondioli, K. R., Zhao, H., Kreibich, G., Wall, R. J., and Sun, T. T. (1998) *Nature biotechnology* **16**, 75-79

22. Khandelwal, P., Ruiz, W. G., Balestreire-Hawryluk, E., Weisz, O. A., Goldenring, J. R., and Apodaca, G. (2008) *Proceedings of the National Academy of Sciences of the United States of America* **105**, 15773-15778
23. Wang, E. C., Lee, J. M., Ruiz, W. G., Balestreire, E. M., von Bodungen, M., Barrick, S., Cockayne, D. A., Birder, L. A., and Apodaca, G. (2005) *The Journal of clinical investigation* **115**, 2412-2422
24. Khandelwal, P., Prakasam, H. S., Clayton, D. R., Ruiz, W. G., Gallo, L., van Roekel, D., Lukianov, S., Peranen, J., Goldenring, J. R., and Apodaca, G. (2013) *Molecular biology of the cell*
25. Lewis, S. A., and de Moura, J. L. (1984) *The Journal of membrane biology* **82**, 123-136
26. Lewis, S. A., and de Moura, J. L. (1982) *Nature* **297**, 685-688
27. Truschel, S. T., Wang, E., Ruiz, W. G., Leung, S. M., Rojas, R., Lavelle, J., Zeidel, M., Stoffer, D., and Apodaca, G. (2002) *Molecular biology of the cell* **13**, 830-846
28. Wang, E., Truschel, S., and Apodaca, G. (2003) *Methods* **30**, 207-217
29. Wang, E. C., Lee, J. M., Johnson, J. P., Kleyman, T. R., Bridges, R., and Apodaca, G. (2003) *American journal of physiology. Renal physiology* **285**, F651-663
30. Lewis, S. A., and Hanrahan, J. W. (1990) *Methods in enzymology* **192**, 632-650
31. N. Sperelakis, i. (1998), 1061-1075
32. Anderson, J. M., and Van Itallie, C. M. (2009) *Cold Spring Harbor perspectives in biology* **1**, a002584
33. Stetson, D. L., Lewis, S. A., Alles, W., and Wade, J. B. (1982) *Biochimica et biophysica acta* **689**, 267-274
34. Lewis, S. A., and Wills, N. K. (1982) *The Journal of membrane biology* **67**, 45-53
35. Davies, R. J., Joseph, R., Kaplan, D., Juncosa, R. D., Pempinello, C., Asbun, H., and Sedwitz, M. M. (1987) *Biophysical journal* **52**, 783-790
36. Clausen, C., Lewis, S. A., and Diamond, J. M. (1979) *Biophysical journal* **26**, 291-317
37. Gogelein, H., and Van Driessche, W. (1981) *Pflugers Archiv : European journal of physiology* **389**, 105-113
38. Minsky, B. D., and Chlapowski, F. J. (1978) *The Journal of cell biology* **77**, 685-697
39. Apodaca, G. (2002) *American journal of physiology. Renal physiology* **282**, F179-190
40. Amano, O., Kataoka, S., and Yamamoto, T. Y. (1988) *The Tohoku journal of experimental medicine* **156**, 417-418
41. Yu, W., Khandelwal, P., and Apodaca, G. (2009) *Molecular biology of the cell* **20**, 282-295
42. Khandelwal, P., Ruiz, W. G., and Apodaca, G. (2010) *The EMBO journal* **29**, 1961-1975
43. Balestreire, E. M., and Apodaca, G. (2007) *Molecular biology of the cell* **18**, 1312-1323
44. Valentijn, K., Valentijn, J. A., and Jamieson, J. D. (1999) *Biochemical and biophysical research communications* **266**, 652-661
45. Sandy, J. R., Meghji, S., Farndale, R. W., and Meikle, M. C. (1989) *Biochimica et biophysica acta* **1010**, 265-269
46. Watson, P. A., Haneda, T., and Morgan, H. E. (1989) *The American journal of physiology* **256**, C1257-1261
47. Sudhof, T. C., and Rothman, J. E. (2009) *Science* **323**, 474-477
48. Born, M., Pahner, I., Ahnert-Hilger, G., and Jons, T. (2003) *European journal of cell biology* **82**, 343-350

49. Khandelwal, P., Prakasam, H. S., Clayton, D. R., Ruiz, W. G., Gallo, L. I., van Roekel, D., Lukianov, S., Peranen, J., Goldenring, J. R., and Apodaca, G. (2013) *Molecular biology of the cell* **24**, 1007-1019
50. Zhou, G., Liang, F. X., Romih, R., Wang, Z., Liao, Y., Ghiso, J., Luque-Garcia, J. L., Neubert, T. A., Kreibich, G., Alonso, M. A., Schaeren-Wiemers, N., and Sun, T. T. (2012) *Molecular biology of the cell* **23**, 1354-1366
51. Barg, S., and Machado, J. D. (2008) *Acta Physiol (Oxf)* **192**, 195-201
52. Tsuboi, T., McMahon, H. T., and Rutter, G. A. (2004) *The Journal of biological chemistry* **279**, 47115-47124
53. Yu, W., Zacharia, L. C., Jackson, E. K., and Apodaca, G. (2006) *American journal of physiology. Cell physiology* **291**, C254-265
54. Beckel, J. M., and Holstege, G. (2011) *Handbook of experimental pharmacology*, 99-116
55. Birder, L. A., De Groat, W. C., and Apodaca, G. (2008) Physiology of the urothelium. in *Textbook of the neurogenic bladder* (Corcos, J., and Schick, E. eds.), 2 Ed., Martin Dunitz, London ; New York. pp 19-39
56. Blok, B. F., and Holstege, G. (1997) *Neuroscience letters* **222**, 195-198
57. Sugaya, K., Matsuyama, K., Takakusaki, K., and Mori, S. (1987) *Neuroscience letters* **80**, 197-201
58. Holstege, G., and Mouton, L. J. (2003) *International review of neurobiology* **56**, 123-145
59. Blok, B. F., de Weerd, H., and Holstege, G. (1997) *Neuroscience letters* **233**, 109-112
60. Birder, L. A., and de Groat, W. C. (2007) *Nature clinical practice. Urology* **4**, 46-54
61. Kanai, A. J. (2011) *Handbook of experimental pharmacology*, 171-205
62. Birder, L. A., Nakamura, Y., Kiss, S., Nealen, M. L., Barrick, S., Kanai, A. J., Wang, E., Ruiz, G., De Groat, W. C., Apodaca, G., Watkins, S., and Caterina, M. J. (2002) *Nature neuroscience* **5**, 856-860
63. Birder, L. A., Kanai, A. J., de Groat, W. C., Kiss, S., Nealen, M. L., Burke, N. E., Dineley, K. E., Watkins, S., Reynolds, I. J., and Caterina, M. J. (2001) *Proceedings of the National Academy of Sciences of the United States of America* **98**, 13396-13401
64. Floyd, K., Hick, V. E., and Morrison, J. F. (1982) *The Journal of physiology* **323**, 65-75
65. Vial, C., and Evans, R. J. (2000) *British journal of pharmacology* **131**, 1489-1495
66. Tempest, H. V., Dixon, A. K., Turner, W. H., Elneil, S., Sellers, L. A., and Ferguson, D. R. (2004) *BJU international* **93**, 1344-1348
67. Lee, H. Y., Bardini, M., and Burnstock, G. (2000) *The Journal of urology* **163**, 2002-2007
68. Chess-Williams, R. (2002) *Autonomic & autacoid pharmacology* **22**, 133-145
69. Yamanishi, T., Chapple, C. R., Yasuda, K., Yoshida, K., and Chess-Williams, R. (2002) *The Journal of urology* **168**, 2706-2710
70. Chopra, B., Barrick, S. R., Meyers, S., Beckel, J. M., Zeidel, M. L., Ford, A. P., de Groat, W. C., and Birder, L. A. (2005) *The Journal of physiology* **562**, 859-871
71. Apodaca, G., Balestreire, E., and Birder, L. A. (2007) *Kidney international* **72**, 1057-1064
72. Grandaliano, G., Gesualdo, L., Bartoli, F., Ranieri, E., Monno, R., Leggio, A., Paradies, G., Caldarulo, E., Infante, B., and Schena, F. P. (2000) *Kidney international* **58**, 182-192
73. Birder, L. A. *Handbook of experimental pharmacology*, 207-231
74. Maggi, C. A. (1990) *Ciba Foundation symposium* **151**, 77-83; discussion 83-90

75. Birder, L. A., Apodaca, G., De Groat, W. C., and Kanai, A. J. (1998) *The American journal of physiology* **275**, F226-229
76. Zenser, T. V., Thomas, D. J., Jacob, A. K., and Davis, B. B. (1992) *Journal of cellular physiology* **150**, 214-219
77. Birder, L. A., Ruan, H. Z., Chopra, B., Xiang, Z., Barrick, S., Buffington, C. A., Roppolo, J. R., Ford, A. P., de Groat, W. C., and Burnstock, G. (2004) *American journal of physiology. Renal physiology* **287**, F1084-1091
78. Pandita, R. K., Mizusawa, H., and Andersson, K. E. (2000) *The Journal of urology* **164**, 545-550
79. Templeman, L., Chapple, C. R., and Chess-Williams, R. (2002) *The Journal of urology* **167**, 742-745
80. Bekar, L., Libionka, W., Tian, G. F., Xu, Q., Torres, A., Wang, X., Lovatt, D., Williams, E., Takano, T., Schnermann, J., Bakos, R., and Nedergaard, M. (2008) *Nature medicine* **14**, 75-80
81. Dougherty, C., Barucha, J., Schofield, P. R., Jacobson, K. A., and Liang, B. T. (1998) *FASEB journal : official publication of the Federation of American Societies for Experimental Biology* **12**, 1785-1792
82. Drury, A. N., and Szent-Gyorgyi, A. (1929) *The Journal of physiology* **68**, 213-237
83. Eltzschig, H. K. (2013) *J Mol Med (Berl)* **91**, 141-146
84. Delacretaz, E. (2006) *The New England journal of medicine* **354**, 1039-1051
85. Funaya, H., Kitakaze, M., Node, K., Minamino, T., Komamura, K., and Hori, M. (1997) *Circulation* **95**, 1363-1365
86. Porkka-Heiskanen, T., Strecker, R. E., and McCarley, R. W. (2000) *Neuroscience* **99**, 507-517
87. Gray, J. H., Owen, R. P., and Giacomini, K. M. (2004) *Pflugers Archiv : European journal of physiology* **447**, 728-734
88. Young, J. D., Yao, S. Y., Sun, L., Cass, C. E., and Baldwin, S. A. (2008) *Xenobiotica; the fate of foreign compounds in biological systems* **38**, 995-1021
89. Baldwin, S. A., Beal, P. R., Yao, S. Y., King, A. E., Cass, C. E., and Young, J. D. (2004) *Pflugers Archiv : European journal of physiology* **447**, 735-743
90. Robson, S. C., Sevigny, J., and Zimmermann, H. (2006) *Purinergic signalling* **2**, 409-430
91. Alberts, B. (2008) *Molecular biology of the cell*, 5th ed., Garland Science, New York
92. Klaasse, E. C., Ijzerman, A. P., de Grip, W. J., and Beukers, M. W. (2008) *Purinergic signalling* **4**, 21-37
93. Oldham, W. M., and Hamm, H. E. (2008) *Nature reviews. Molecular cell biology* **9**, 60-71
94. Hermans, E. (2003) *Pharmacology & therapeutics* **99**, 25-44
95. Fredholm, B. B., AP, I. J., Jacobson, K. A., Klotz, K. N., and Linden, J. (2001) *Pharmacological reviews* **53**, 527-552
96. Hasko, G., Linden, J., Cronstein, B., and Pacher, P. (2008) *Nat Rev Drug Discov* **7**, 759-770
97. Ryzhov, S., Novitskiy, S. V., Zaynagetdinov, R., Goldstein, A. E., Carbone, D. P., Biaggioni, I., Dikov, M. M., and Feoktistov, I. (2008) *Neoplasia* **10**, 987-995
98. Akaiwa, K., Akashi, H., Harada, H., Sakashita, H., Hiromatsu, S., Kano, T., and Aoyagi, S. (2006) *Brain research* **1122**, 47-55
99. Cohen, M. V., and Downey, J. M. (2008) *Basic Res Cardiol* **103**, 203-215

100. Liang, B. T., and Jacobson, K. A. (1998) *Proceedings of the National Academy of Sciences of the United States of America* **95**, 6995-6999
101. Chen, Y., Corriden, R., Inoue, Y., Yip, L., Hashiguchi, N., Zinkernagel, A., Nizet, V., Insel, P. A., and Junger, W. G. (2006) *Science* **314**, 1792-1795
102. Martin, P. L., Wysocki, R. J., Jr., Barrett, R. J., May, J. M., and Linden, J. (1996) *The Journal of pharmacology and experimental therapeutics* **276**, 490-499
103. Ohta, A., and Sitkovsky, M. (2001) *Nature* **414**, 916-920
104. Jacobson, K. A. (2009) *Handbook of experimental pharmacology*, 1-24
105. Siddiqi, S. M., Pearlstein, R. A., Sanders, L. H., and Jacobson, K. A. (1995) *Bioorganic & medicinal chemistry* **3**, 1331-1343
106. Jacobson, K. A., and Gao, Z. G. (2006) *Nat Rev Drug Discov* **5**, 247-264
107. Yan, L., Burbiel, J. C., Maass, A., and Muller, C. E. (2003) *Expert opinion on emerging drugs* **8**, 537-576
108. Smith, R. G., Griffin, P. R., Xu, Y., Smith, A. G., Liu, K., Calacay, J., Feighner, S. D., Pong, C., Leong, D., Pomes, A., Cheng, K., Van der Ploeg, L. H., Howard, A. D., Schaeffer, J., and Leonard, R. J. (2000) *Biochemical and biophysical research communications* **276**, 1306-1313
109. Korbonits, M., and Grossman, A. B. (2004) *European journal of endocrinology / European Federation of Endocrine Societies* **151 Suppl 1**, S67-70
110. Biber, K., Klotz, K. N., Berger, M., Gebicke-Harter, P. J., and van Calker, D. (1997) *The Journal of neuroscience : the official journal of the Society for Neuroscience* **17**, 4956-4964
111. Tomura, H., Itoh, H., Sho, K., Sato, K., Nagao, M., Ui, M., Kondo, Y., and Okajima, F. (1997) *The Journal of biological chemistry* **272**, 23130-23137
112. Wen, J., Grenz, A., Zhang, Y., Dai, Y., Kellems, R. E., Blackburn, M. R., Eltzschig, H. K., and Xia, Y. (2011) *FASEB journal : official publication of the Federation of American Societies for Experimental Biology* **25**, 2823-2830
113. Schulte, G., and Fredholm, B. B. (2003) *Cellular signalling* **15**, 813-827
114. Ribeiro, J. A., and Sebastiao, A. M. (2010) *Journal of Alzheimer's disease : JAD* **20 Suppl 1**, S3-15
115. Ochiishi, T., Chen, L., Yukawa, A., Saitoh, Y., Sekino, Y., Arai, T., Nakata, H., and Miyamoto, H. (1999) *The Journal of comparative neurology* **411**, 301-316
116. Ochiishi, T., Saitoh, Y., Yukawa, A., Saji, M., Ren, Y., Shirao, T., Miyamoto, H., Nakata, H., and Sekino, Y. (1999) *Neuroscience* **93**, 955-967
117. Stone, T. W., Ceruti, S., and Abbracchio, M. P. (2009) *Handbook of experimental pharmacology*, 535-587
118. Fredholm, B. B., and Dunwiddie, T. V. (1988) *Trends in pharmacological sciences* **9**, 130-134
119. Olsson, R. A. (1970) *Circulation research* **26**, 301-306
120. Berne, R. M. (1980) *Circulation research* **47**, 807-813
121. Tune, J. D., Gorman, M. W., and Feigl, E. O. (2004) *J Appl Physiol* **97**, 404-415
122. Tawfik, H. E., Teng, B., Morrison, R. R., Schnermann, J., and Mustafa, S. J. (2006) *American journal of physiology. Heart and circulatory physiology* **291**, H467-472
123. Liang, B. T., and Gross, G. J. (1999) *Circulation research* **84**, 1396-1400

124. Matherne, G. P., Linden, J., Byford, A. M., Gauthier, N. S., and Headrick, J. P. (1997) *Proceedings of the National Academy of Sciences of the United States of America* **94**, 6541-6546
125. Hansen, P. B., Castrop, H., Briggs, J., and Schnermann, J. (2003) *Journal of the American Society of Nephrology : JASN* **14**, 2457-2465
126. Vallon, V., and Osswald, H. (2009) *Handbook of experimental pharmacology*, 443-470
127. Hoenderop, J. G., Hartog, A., Willems, P. H., and Bindels, R. J. (1998) *The American journal of physiology* **274**, F736-743
128. Kang, H. S., Kerstan, D., Dai, L. J., Ritchie, G., and Quamme, G. A. (2001) *American journal of physiology. Renal physiology* **281**, F1141-1147
129. Bjorck, T., Gustafsson, L. E., and Dahlen, S. E. (1992) *The American review of respiratory disease* **145**, 1087-1091
130. Brown, R. A., Clarke, G. W., Ledbetter, C. L., Hurle, M. J., Denyer, J. C., Simcock, D. E., Coote, J. E., Savage, T. J., Murdoch, R. D., Page, C. P., Spina, D., and O'Connor, B. J. (2008) *The European respiratory journal* **31**, 311-319
131. Wilson, C. N., Nadeem, A., Spina, D., Brown, R., Page, C. P., and Mustafa, S. J. (2009) *Handbook of experimental pharmacology*, 329-362
132. Trost, T., and Schwabe, U. (1981) *Molecular pharmacology* **19**, 228-235
133. Ukena, D., Furler, R., Lohse, M. J., Engel, G., and Schwabe, U. (1984) *Naunyn-Schmiedeberg's archives of pharmacology* **326**, 233-240
134. Aronsson, P., Johnsson, M., Vesela, R., Winder, M., and Tobin, G. (2012) *Autonomic neuroscience : basic & clinical* **171**, 49-57
135. Kalk, P., Eggert, B., Relle, K., Godes, M., Heiden, S., Sharkovska, Y., Fischer, Y., Ziegler, D., Bielenberg, G. W., and Hocher, B. (2007) *British journal of pharmacology* **151**, 1025-1032
136. Cristalli, G., Muller, C. E., and Volpini, R. (2009) *Handbook of experimental pharmacology*, 59-98
137. Hasko, G., Csoka, B., Nemeth, Z. H., Vizi, E. S., and Pacher, P. (2009) *Trends in immunology* **30**, 263-270
138. Lappas, C. M., Sullivan, G. W., and Linden, J. (2005) *Expert opinion on investigational drugs* **14**, 797-806
139. Thiel, M., Caldwell, C. C., and Sitkovsky, M. V. (2003) *Microbes and infection / Institut Pasteur* **5**, 515-526
140. Hasko, G., Kuhel, D. G., Chen, J. F., Schwarzschild, M. A., Deitch, E. A., Mabley, J. G., Marton, A., and Szabo, C. (2000) *FASEB journal : official publication of the Federation of American Societies for Experimental Biology* **14**, 2065-2074
141. Lappas, C. M., Rieger, J. M., and Linden, J. (2005) *J Immunol* **174**, 1073-1080
142. Visser, S. S., Theron, A. J., Ramafi, G., Ker, J. A., and Anderson, R. (2000) *Biochemical pharmacology* **60**, 993-999
143. Nadeem, A., Fan, M., Ansari, H. R., Ledent, C., and Jamal Mustafa, S. (2007) *American journal of physiology. Lung cellular and molecular physiology* **292**, L1335-1344
144. Feoktistov, I., Goldstein, A. E., and Biaggioni, I. (1999) *Molecular pharmacology* **55**, 726-734
145. Ryzhov, S., Goldstein, A. E., Matafonov, A., Zeng, D., Biaggioni, I., and Feoktistov, I. (2004) *J Immunol* **172**, 7726-7733
146. Jarvis, M. F., and Williams, M. (1989) *European journal of pharmacology* **168**, 243-246

147. Cunha, R. A., Johansson, B., van der Ploeg, I., Sebastiao, A. M., Ribeiro, J. A., and Fredholm, B. B. (1994) *Brain research* **649**, 208-216
148. Dixon, A. K., Gubitz, A. K., Sirinathsinghji, D. J., Richardson, P. J., and Freeman, T. C. (1996) *British journal of pharmacology* **118**, 1461-1468
149. Morelli, M., Di Paolo, T., Wardas, J., Calon, F., Xiao, D., and Schwarzschild, M. A. (2007) *Progress in neurobiology* **83**, 293-309
150. Ohta, A., Gorelik, E., Prasad, S. J., Ronchese, F., Lukashev, D., Wong, M. K., Huang, X., Caldwell, S., Liu, K., Smith, P., Chen, J. F., Jackson, E. K., Apasov, S., Abrams, S., and Sitkovsky, M. (2006) *Proceedings of the National Academy of Sciences of the United States of America* **103**, 13132-13137
151. Meyerhof, W., Muller-Brechlin, R., and Richter, D. (1991) *FEBS letters* **284**, 155-160
152. Borea, P. A., Gessi, S., Bar-Yehuda, S., and Fishman, P. (2009) *Handbook of experimental pharmacology*, 297-327
153. Fozard, J. R., Pfannkuche, H. J., and Schuurman, H. J. (1996) *European journal of pharmacology* **298**, 293-297
154. Auchampach, J. A., Jin, X., Wan, T. C., Caughey, G. H., and Linden, J. (1997) *Molecular pharmacology* **52**, 846-860
155. Feoktistov, I., and Biaggioni, I. (1995) *The Journal of clinical investigation* **96**, 1979-1986
156. Young, H. W., Molina, J. G., Dimina, D., Zhong, H., Jacobson, M., Chan, L. N., Chan, T. S., Lee, J. J., and Blackburn, M. R. (2004) *J Immunol* **173**, 1380-1389
157. Lee, H. T., Kim, M., Joo, J. D., Gallos, G., Chen, J. F., and Emala, C. W. (2006) *Am J Physiol Regul Integr Comp Physiol* **291**, R959-969
158. Hasko, G., Nemeth, Z. H., Vizi, E. S., Salzman, A. L., and Szabo, C. (1998) *European journal of pharmacology* **358**, 261-268
159. Inoue, Y., Chen, Y., Hirsh, M. I., Yip, L., and Junger, W. G. (2008) *Shock* **30**, 173-177
160. Zheng, J., Wang, R., Zambraski, E., Wu, D., Jacobson, K. A., and Liang, B. T. (2007) *American journal of physiology. Heart and circulatory physiology* **293**, H3685-3691
161. Lee, H. T., and Emala, C. W. (2000) *American journal of physiology. Renal physiology* **278**, F380-387
162. Avila, M. Y., Stone, R. A., and Civan, M. M. (2002) *Investigative ophthalmology & visual science* **43**, 3021-3026
163. Trevethick, M. A., Mantell, S. J., Stuart, E. F., Barnard, A., Wright, K. N., and Yeadon, M. (2008) *British journal of pharmacology* **155**, 463-474
164. Varani, K., Padovan, M., Vincenzi, F., Targa, M., Trotta, F., Govoni, M., and Borea, P. A. (2011) *Arthritis research & therapy* **13**, R197
165. Henry, P., Demolombe, S., Puceat, M., and Escande, D. (1996) *Circulation research* **78**, 161-165
166. Dang, M., Armbruster, N., Miller, M. A., Cermenio, E., Hartmann, M., Bell, G. W., Root, D. E., Lauffenburger, D. A., Lodish, H. F., and Herrlich, A. (2013) *Proceedings of the National Academy of Sciences of the United States of America* **110**, 9776-9781
167. Dang, M., Dubbin, K., D'Aiello, A., Hartmann, M., Lodish, H., and Herrlich, A. (2011) *The Journal of biological chemistry* **286**, 17704-17713
168. Mifune, M., Ohtsu, H., Suzuki, H., Nakashima, H., Brailoiu, E., Dun, N. J., Frank, G. D., Inagami, T., Higashiyama, S., Thomas, W. G., Eckhart, A. D., Dempsey, P. J., and Eguchi, S. (2005) *The Journal of biological chemistry* **280**, 26592-26599

169. Ohtsu, H., Dempsey, P. J., and Eguchi, S. (2006) *American journal of physiology. Cell physiology* **291**, C1-10
170. Casas-Gonzalez, P., Ruiz-Martinez, A., and Garcia-Sainz, J. A. (2003) *Biochimica et biophysica acta* **1633**, 75-83
171. Daub, H., Wallasch, C., Lankenau, A., Herrlich, A., and Ullrich, A. (1997) *The EMBO journal* **16**, 7032-7044
172. Dey, M., Baldys, A., Sumter, D. B., Gooz, P., Luttrell, L. M., Raymond, J. R., and Gooz, M. (2010) *The Journal of pharmacology and experimental therapeutics* **334**, 775-783
173. Eguchi, S., Iwasaki, H., Hirata, Y., Frank, G. D., Motley, E. D., Yamakawa, T., Numaguchi, K., and Inagami, T. (1999) *European journal of pharmacology* **376**, 203-206
174. Fischer, O. M., Hart, S., Gschwind, A., and Ullrich, A. (2003) *Biochemical Society transactions* **31**, 1203-1208
175. Kakiashvili, E., Dan, Q., Vandermeer, M., Zhang, Y., Waheed, F., Pham, M., and Szaszi, K. (2011) *The Journal of biological chemistry* **286**, 9268-9279
176. Kanno, H., Horikawa, Y., Hodges, R. R., Zoukhri, D., Shatos, M. A., Rios, J. D., and Dartt, D. A. (2003) *American journal of physiology. Cell physiology* **284**, C988-998
177. Higashiyama, S., Iwabuki, H., Morimoto, C., Hieda, M., Inoue, H., and Matsushita, N. (2008) *Cancer science* **99**, 214-220
178. Iwasaki, H., Eguchi, S., Ueno, H., Marumo, F., and Hirata, Y. (1999) *Endocrinology* **140**, 4659-4668
179. Rodland, K. D., Bollinger, N., Ippolito, D., Opresko, L. K., Coffey, R. J., Zangar, R., and Wiley, H. S. (2008) *The Journal of biological chemistry* **283**, 31477-31487
180. Swanson, K. V., Griffiss, J. M., Edwards, V. L., Stein, D. C., and Song, W. (2011) *Cellular microbiology* **13**, 1078-1090
181. Tsai, W., Morielli, A. D., and Peralta, E. G. (1997) *The EMBO journal* **16**, 4597-4605
182. Prigent, S. A., and Lemoine, N. R. (1992) *Progress in growth factor research* **4**, 1-24
183. Todaro, G. J., Rose, T. M., Spooner, C. E., Shoyab, M., and Plowman, G. D. (1990) *Seminars in cancer biology* **1**, 257-263
184. Rajkumar, T., and Gullick, W. J. (1994) *Breast cancer research and treatment* **29**, 3-9
185. Hunter, T. (1998) *Philosophical transactions of the Royal Society of London. Series B, Biological sciences* **353**, 583-605
186. Schlessinger, J. (2000) *Cell* **103**, 211-225
187. Schlessinger, J. (1988) *Trends in biochemical sciences* **13**, 443-447
188. Pawson, T., and Schlessingert, J. (1993) *Current biology : CB* **3**, 434-442
189. Yarden, Y., and Sliwkowski, M. X. (2001) *Nature reviews. Molecular cell biology* **2**, 127-137
190. Rodrigues, G. A., Falasca, M., Zhang, Z., Ong, S. H., and Schlessinger, J. (2000) *Molecular and cellular biology* **20**, 1448-1459
191. Daub, H., Weiss, F. U., Wallasch, C., and Ullrich, A. (1996) *Nature* **379**, 557-560
192. Keates, S., Keates, A. C., Nath, S., Peek, R. M., Jr., and Kelly, C. P. (2005) *Gut* **54**, 1363-1369
193. Pinkas-Kramarski, R., Alroy, I., and Yarden, Y. (1997) *Journal of mammary gland biology and neoplasia* **2**, 97-107
194. Normanno, N., Bianco, C., Strizzi, L., Mancino, M., Maiello, M. R., De Luca, A., Caponigro, F., and Salomon, D. S. (2005) *Current drug targets* **6**, 243-257

195. Zwick, E., Daub, H., Aoki, N., Yamaguchi-Aoki, Y., Tinhofer, I., Maly, K., and Ullrich, A. (1997) *The Journal of biological chemistry* **272**, 24767-24770
196. Eguchi, S., Numaguchi, K., Iwasaki, H., Matsumoto, T., Yamakawa, T., Utsunomiya, H., Motley, E. D., Kawakatsu, H., Owada, K. M., Hirata, Y., Marumo, F., and Inagami, T. (1998) *The Journal of biological chemistry* **273**, 8890-8896
197. Murasawa, S., Mori, Y., Nozawa, Y., Gotoh, N., Shibuya, M., Masaki, H., Maruyama, K., Tsutsumi, Y., Moriguchi, Y., Shibazaki, Y., Tanaka, Y., Iwasaka, T., Inada, M., and Matsubara, H. (1998) *Circulation research* **82**, 1338-1348
198. Grosse, R., Roelle, S., Herrlich, A., Hohn, J., and Gudermann, T. (2000) *The Journal of biological chemistry* **275**, 12251-12260
199. Li, X., Lee, J. W., Graves, L. M., and Earp, H. S. (1998) *The EMBO journal* **17**, 2574-2583
200. Gschwind, A., Zwick, E., Prenzel, N., Leserer, M., and Ullrich, A. (2001) *Oncogene* **20**, 1594-1600
201. Soond, S. M., Everson, B., Riches, D. W., and Murphy, G. (2005) *Journal of cell science* **118**, 2371-2380
202. Xu, P., and Derynck, R. (2010) *Molecular cell* **37**, 551-566
203. Gomis-Ruth, F. X. (2003) *Molecular biotechnology* **24**, 157-202
204. Edwards, D. R., Handsley, M. M., and Pennington, C. J. (2008) *Molecular aspects of medicine* **29**, 258-289
205. Gooz, M. (2010) *Critical reviews in biochemistry and molecular biology* **45**, 146-169
206. Wewer, U. M., Morgelin, M., Holck, P., Jacobsen, J., Lydolph, M. C., Johnsen, A. H., Kveiborg, M., and Albrechtsen, R. (2006) *The Journal of biological chemistry* **281**, 9418-9422
207. Mazzocca, A., Coppari, R., De Franco, R., Cho, J. Y., Libermann, T. A., Pinzani, M., and Toker, A. (2005) *Cancer research* **65**, 4728-4738
208. Katagiri, T., Harada, Y., Emi, M., and Nakamura, Y. (1995) *Cytogenetics and cell genetics* **68**, 39-44
209. Kleino, I., Ortiz, R. M., and Huovila, A. P. (2007) *BMC molecular biology* **8**, 90
210. Fan, H., Turck, C. W., and Derynck, R. (2003) *The Journal of biological chemistry* **278**, 18617-18627
211. Weskamp, G., Schlondorff, J., Lum, L., Becherer, J. D., Kim, T. W., Saftig, P., Hartmann, D., Murphy, G., and Blobel, C. P. (2004) *The Journal of biological chemistry* **279**, 4241-4249
212. Boutet, P., Aguera-Gonzalez, S., Atkinson, S., Pennington, C. J., Edwards, D. R., Murphy, G., Reyburn, H. T., and Vales-Gomez, M. (2009) *J Immunol* **182**, 49-53
213. Skovronsky, D. M., Moore, D. B., Milla, M. E., Doms, R. W., and Lee, V. M. (2000) *The Journal of biological chemistry* **275**, 2568-2575
214. Shirakabe, K., Wakatsuki, S., Kurisaki, T., and Fujisawa-Sehara, A. (2001) *The Journal of biological chemistry* **276**, 9352-9358
215. Black, R. A., Rauch, C. T., Kozlosky, C. J., Peschon, J. J., Slack, J. L., Wolfson, M. F., Castner, B. J., Stocking, K. L., Reddy, P., Srinivasan, S., Nelson, N., Boiani, N., Schooley, K. A., Gerhart, M., Davis, R., Fitzner, J. N., Johnson, R. S., Paxton, R. J., March, C. J., and Cerretti, D. P. (1997) *Nature* **385**, 729-733
216. Moss, M. L., Jin, S. L., Milla, M. E., Bickett, D. M., Burkhart, W., Carter, H. L., Chen, W. J., Clay, W. C., Didsbury, J. R., Hassler, D., Hoffman, C. R., Kost, T. A., Lambert,

- M. H., Leesnitzer, M. A., McCauley, P., McGeehan, G., Mitchell, J., Moyer, M., Pahel, G., Rocque, W., Overton, L. K., Schoenen, F., Seaton, T., Su, J. L., Becherer, J. D., and et al. (1997) *Nature* **385**, 733-736
217. Murphy, G. (2008) *Nature reviews. Cancer* **8**, 929-941
 218. Niewiarowski, S., McLane, M. A., Kloczewiak, M., and Stewart, G. J. (1994) *Seminars in hematology* **31**, 289-300
 219. Smith, K. M., Gaultier, A., Cousin, H., Alfandari, D., White, J. M., and DeSimone, D. W. (2002) *The Journal of cell biology* **159**, 893-902
 220. Reddy, P., Slack, J. L., Davis, R., Cerretti, D. P., Kozlosky, C. J., Blanton, R. A., Shows, D., Peschon, J. J., and Black, R. A. (2000) *The Journal of biological chemistry* **275**, 14608-14614
 221. Blobel, C. P. (2005) *Nature reviews. Molecular cell biology* **6**, 32-43
 222. Wang, Y., Zhang, A. C., Ni, Z., Herrera, A., and Walcheck, B. (2010) *J Immunol* **184**, 4447-4454
 223. Gonzales, P. E., Galli, J. D., and Milla, M. E. (2008) *Biochemistry* **47**, 9911-9919
 224. Buckley, C. A., Rouhani, F. N., Kaler, M., Adamik, B., Hawari, F. I., and Levine, S. J. (2005) *American journal of physiology. Lung cellular and molecular physiology* **288**, L1132-1138
 225. Schlondorff, J., Becherer, J. D., and Blobel, C. P. (2000) *The Biochemical journal* **347 Pt 1**, 131-138
 226. Wang, X., He, K., Gerhart, M., Huang, Y., Jiang, J., Paxton, R. J., Yang, S., Lu, C., Menon, R. K., Black, R. A., Baumann, G., and Frank, S. J. (2002) *The Journal of biological chemistry* **277**, 50510-50519
 227. Leonard, J. D., Lin, F., and Milla, M. E. (2005) *The Biochemical journal* **387**, 797-805
 228. Gonzales, P. E., Solomon, A., Miller, A. B., Leesnitzer, M. A., Sagi, I., and Milla, M. E. (2004) *The Journal of biological chemistry* **279**, 31638-31645
 229. Kriegler, M., Perez, C., DeFay, K., Albert, I., and Lu, S. D. (1988) *Cell* **53**, 45-53
 230. Bell, H. L., and Gooz, M. (2010) *The American journal of the medical sciences* **339**, 105-107
 231. Zhang, Q., Thomas, S. M., Lui, V. W., Xi, S., Siegfried, J. M., Fan, H., Smithgall, T. E., Mills, G. B., and Grandis, J. R. (2006) *Proceedings of the National Academy of Sciences of the United States of America* **103**, 6901-6906
 232. Niu, A., Wen, Y., Liu, H., Zhan, M., Jin, B., and Li, Y. P. (2013) *Journal of cell science*
 233. Nelson, K. K., Schlondorff, J., and Blobel, C. P. (1999) *The Biochemical journal* **343 Pt 3**, 673-680
 234. Peiretti, F., Deprez-Beauclair, P., Bonardo, B., Aubert, H., Juhan-Vague, I., and Nalbone, G. (2003) *Journal of cell science* **116**, 1949-1957
 235. Tanaka, M., Nanba, D., Mori, S., Shiba, F., Ishiguro, H., Yoshino, K., Matsuura, N., and Higashiyama, S. (2004) *The Journal of biological chemistry* **279**, 41950-41959
 236. Canault, M., Tellier, E., Bonardo, B., Mas, E., Aumailley, M., Juhan-Vague, I., Nalbone, G., and Peiretti, F. (2006) *Journal of cellular physiology* **208**, 363-372
 237. Jia, H. P., Look, D. C., Tan, P., Shi, L., Hickey, M., Gakhar, L., Chappell, M. C., Wohlford-Lenane, C., and McCray, P. B., Jr. (2009) *American journal of physiology. Lung cellular and molecular physiology* **297**, L84-96
 238. Le Gall, S. M., Maretzky, T., Issuree, P. D., Niu, X. D., Reiss, K., Saftig, P., Khokha, R., Lundell, D., and Blobel, C. P. (2010) *Journal of cell science* **123**, 3913-3922

239. Horiuchi, K., Le Gall, S., Schulte, M., Yamaguchi, T., Reiss, K., Murphy, G., Toyama, Y., Hartmann, D., Saftig, P., and Blobel, C. P. (2007) *Molecular biology of the cell* **18**, 176-188
240. Solomon, A., Akabayov, B., Frenkel, A., Milla, M. E., and Sagi, I. (2007) *Proceedings of the National Academy of Sciences of the United States of America* **104**, 4931-4936
241. Wang, Y., Herrera, A. H., Li, Y., Belani, K. K., and Walcheck, B. (2009) *J Immunol* **182**, 2449-2457
242. Wisniewska, M., Goettig, P., Maskos, K., Belouski, E., Winters, D., Hecht, R., Black, R., and Bode, W. (2008) *Journal of molecular biology* **381**, 1307-1319
243. Kwak, H. I., Mendoza, E. A., and Bayless, K. J. (2009) *Matrix biology : journal of the International Society for Matrix Biology* **28**, 470-479
244. Xu, P., Liu, J., Sakaki-Yumoto, M., and Derynck, R. (2012) *Science signaling* **5**, ra34
245. Sahin, U., Weskamp, G., Kelly, K., Zhou, H. M., Higashiyama, S., Peschon, J., Hartmann, D., Saftig, P., and Blobel, C. P. (2004) *The Journal of cell biology* **164**, 769-779
246. Sahin, U., and Blobel, C. P. (2007) *FEBS letters* **581**, 41-44
247. Peschon, J. J., Slack, J. L., Reddy, P., Stocking, K. L., Sunnarborg, S. W., Lee, D. C., Russell, W. E., Castner, B. J., Johnson, R. S., Fitzner, J. N., Boyce, R. W., Nelson, N., Kozlosky, C. J., Wolfson, M. F., Rauch, C. T., Cerretti, D. P., Paxton, R. J., March, C. J., and Black, R. A. (1998) *Science* **282**, 1281-1284
248. Mann, G. B., Fowler, K. J., Gabriel, A., Nice, E. C., Williams, R. L., and Dunn, A. R. (1993) *Cell* **73**, 249-261
249. Luetkeke, N. C., Qiu, T. H., Peiffer, R. L., Oliver, P., Smithies, O., and Lee, D. C. (1993) *Cell* **73**, 263-278
250. Hassemer, E. L., Le Gall, S. M., Liegel, R., McNally, M., Chang, B., Zeiss, C. J., Dubielzig, R. D., Horiuchi, K., Kimura, T., Okada, Y., Blobel, C. P., and Sidjanin, D. J. (2010) *Genetics* **185**, 245-255
251. Horiuchi, K., Zhou, H. M., Kelly, K., Manova, K., and Blobel, C. P. (2005) *Developmental biology* **283**, 459-471
252. Merlos-Suarez, A., Ruiz-Paz, S., Baselga, J., and Arribas, J. (2001) *The Journal of biological chemistry* **276**, 48510-48517
253. Yano, S., Macleod, R. J., Chattopadhyay, N., Tfelt-Hansen, J., Kifor, O., Butters, R. R., and Brown, E. M. (2004) *Bone* **35**, 664-672
254. Das, R., Mahabeleshwar, G. H., and Kundu, G. C. (2004) *The Journal of biological chemistry* **279**, 11051-11064
255. Zhao, Y., He, D., Saatian, B., Watkins, T., Spannhake, E. W., Pyne, N. J., and Natarajan, V. (2006) *The Journal of biological chemistry* **281**, 19501-19511
256. Ancha, H. R., Kurella, R. R., Stewart, C. A., Damera, G., Ceresa, B. P., and Harty, R. F. (2007) *The international journal of biochemistry & cell biology* **39**, 2143-2152
257. Su, T., Bryant, D. M., Luton, F., Verges, M., Ulrich, S. M., Hansen, K. C., Datta, A., Eastburn, D. J., Burlingame, A. L., Shokat, K. M., and Mostov, K. E. (2010) *Nature cell biology* **12**, 1143-1153
258. Rieg, T., and Vallon, V. (2009) *Am J Physiol Regul Integr Comp Physiol* **296**, R419-427
259. Wei, C. J., Li, W., and Chen, J. F. *Biochimica et biophysica acta* **1808**, 1358-1379
260. Picher, M., Burch, L. H., Hirsh, A. J., Spsychala, J., and Boucher, R. C. (2003) *The Journal of biological chemistry* **278**, 13468-13479

261. Picher, M., Burch, L. H., and Boucher, R. C. (2004) *The Journal of biological chemistry* **279**, 20234-20241
262. Hirsh, A. J., Stonebraker, J. R., van Heusden, C. A., Lazarowski, E. R., Boucher, R. C., and Picher, M. (2007) *Biochemistry* **46**, 10373-10383
263. Law, W. R., Conlon, B. A., and Ross, J. D. (2007) *Shock* **28**, 259-264
264. Van Linden, A., and Eltzschig, H. K. (2007) *Expert Opin Biol Ther* **7**, 1437-1447
265. Deussen, A. (2000) *Naunyn-Schmiedeberg's archives of pharmacology* **362**, 351-363
266. Lloyd, H. G., and Fredholm, B. B. (1995) *Neurochem Int* **26**, 387-395
267. Mubagwa, K., and Flameng, W. (2001) *Cardiovascular research* **52**, 25-39
268. Gorlach, A. (2005) *Circulation research* **97**, 1-3
269. Fields, R. D., and Burnstock, G. (2006) *Nat Rev Neurosci* **7**, 423-436
270. Kudo, M., Wang, Y., Xu, M., Ayub, A., and Ashraf, M. (2002) *American journal of physiology. Heart and circulatory physiology* **283**, H296-301
271. Parratt, J. R. (1994) *Trends in pharmacological sciences* **15**, 19-25
272. Caruso, M., Holgate, S. T., and Polosa, R. (2006) *Curr Opin Pharmacol* **6**, 251-256
273. Liang, B. T. (1998) *The Biochemical journal* **336** (Pt 2), 337-343
274. Heurteaux, C., Lauritzen, I., Widmann, C., and Lazdunski, M. (1995) *Proceedings of the National Academy of Sciences of the United States of America* **92**, 4666-4670
275. Sitaraman, S. V., Merlin, D., Wang, L., Wong, M., Gewirtz, A. T., Si-Tahar, M., and Madara, J. L. (2001) *The Journal of clinical investigation* **107**, 861-869
276. Estrela, A. B., and Abraham, W. R. *Curr Med Chem* **18**, 2791-2815
277. Phillis, J. W., and Smith-Barbour, M. (1993) *Life Sci* **53**, 497-502
278. Dhalla, A. K., Dodam, J. R., Jones, A. W., and Rubin, L. J. (2001) *Journal of molecular and cellular cardiology* **33**, 1143-1152
279. de Groat, W. C. (2004) *Urology* **64**, 7-11
280. Aronsson, P., Andersson, M., Ericsson, T., and Giglio, D. *Basic Clin Pharmacol Toxicol* **107**, 603-613
281. Maggi, C. A., Conte, B., Furio, M., Santicioli, P., Giuliani, S., and Meli, A. (1989) *Gen Pharmacol* **20**, 833-838
282. Lohse, M. J., Klotz, K. N., Schwabe, U., Cristalli, G., Vittori, S., and Grifantini, M. (1988) *Naunyn-Schmiedeberg's archives of pharmacology* **337**, 687-689
283. Schaddelee, M. P., Read, K. D., Cleypool, C. G., Ijzerman, A. P., Danhof, M., and de Boer, A. G. (2005) *Eur J Pharm Sci* **24**, 59-66
284. Dang, K., Lamb, K., Cohen, M., Bielefeldt, K., and Gebhart, G. F. (2008) *J Neurophysiol* **99**, 49-59
285. Zhou, Y., Murthy, J. N., Zeng, D., Belardinelli, L., and Blackburn, M. R. *PloS one* **5**, e9224
286. Jackson, E. K., Ren, J., Cheng, D., and Mi, Z. *American journal of physiology. Renal physiology* **301**, F565-573
287. Naydenova, Z., Rose, J. B., and Coe, I. R. (2008) *American journal of physiology. Heart and circulatory physiology* **294**, H2687-2692
288. Loffler, M., Morote-Garcia, J. C., Eltzschig, S. A., Coe, I. R., and Eltzschig, H. K. (2007) *Arteriosclerosis, thrombosis, and vascular biology* **27**, 1004-1013
289. McCloskey, K. D. *Neurourol Urodyn* **29**, 82-87
290. Janig, W., and Morrison, J. F. (1986) *Prog Brain Res* **67**, 87-114
291. Yoshimura, N., and de Groat, W. C. (1997) *Int J Urol* **4**, 111-125

292. Drake, M. J., and Turner, W. H. (2004) Physiology of the smooth muscles of the bladder and urethra. in *Text book of the Neurogenic bladder : adults and children*, Martin Dunitz, London ; New York. pp xviii, 779 p.
293. Pinna, C., Eberini, I., Puglisi, L., and Burnstock, G. (1999) *European journal of pharmacology* **367**, 85-89
294. Hayashi, Y., Takimoto, K., Chancellor, M. B., Erickson, K. A., Erickson, V. L., Kirimoto, T., Nakano, K., de Groat, W. C., and Yoshimura, N. (2009) *Am J Physiol Regul Integr Comp Physiol* **296**, R1661-1670
295. Cronstein, B. N., Levin, R. I., Philips, M., Hirschhorn, R., Abramson, S. B., and Weissmann, G. (1992) *J Immunol* **148**, 2201-2206
296. Anvari, F., Sharma, A. K., Fernandez, L. G., Hranjec, T., Ravid, K., Kron, I. L., and Laubach, V. E. *The Journal of thoracic and cardiovascular surgery* **140**, 871-877
297. Hofer, S., Ivarsson, L., Stoitzner, P., Auffinger, M., Rainer, C., Romani, N., and Heufler, C. (2003) *J Invest Dermatol* **121**, 300-307
298. Reiss, K., and Saftig, P. (2009) *Seminars in cell & developmental biology* **20**, 126-137
299. Luo, X., Prior, M., He, W., Hu, X., Tang, X., Shen, W., Yadav, S., Kiryu-Seo, S., Miller, R., Trapp, B. D., and Yan, R. (2011) *The Journal of biological chemistry* **286**, 23967-23974
300. Jackson, L. F., Qiu, T. H., Sunnarborg, S. W., Chang, A., Zhang, C., Patterson, C., and Lee, D. C. (2003) *The EMBO journal* **22**, 2704-2716
301. Sternlicht, M. D., Sunnarborg, S. W., Kouros-Mehr, H., Yu, Y., Lee, D. C., and Werb, Z. (2005) *Development* **132**, 3923-3933
302. Le Gall, S. M., Bobe, P., Reiss, K., Horiuchi, K., Niu, X. D., Lundell, D., Gibb, D. R., Conrad, D., Saftig, P., and Blobel, C. P. (2009) *Molecular biology of the cell* **20**, 1785-1794
303. Hall, K. C., and Blobel, C. P. (2012) *PloS one* **7**, e31600
304. Killock, D. J., and Ivetic, A. (2010) *The Biochemical journal* **428**, 293-304
305. Willems, S. H., Tape, C. J., Stanley, P. L., Taylor, N. A., Mills, I. G., Neal, D. E., McCafferty, J., and Murphy, G. (2010) *The Biochemical journal* **428**, 439-450
306. Prakasam, H. S., Herrington, H., Roppolo, J. R., Jackson, E. K., and Apodaca, G. (2012) *American journal of physiology. Renal physiology* **303**, F279-292
307. Yu, W., Hill, W. G., Apodaca, G., and Zeidel, M. L. (2011) *American journal of physiology. Renal physiology* **300**, F49-59
308. Manjunath, S., and Sakhare, P. M. (2009) *Indian journal of pharmacology* **41**, 97-105
309. Uchida, T., Pappenheimer, A. M., Jr., and Harper, A. A. (1973) *The Journal of biological chemistry* **248**, 3851-3854
310. Chalaris, A., Adam, N., Sina, C., Rosenstiel, P., Lehmann-Koch, J., Schirmacher, P., Hartmann, D., Cichy, J., Gavrilova, O., Schreiber, S., Jostock, T., Matthews, V., Hasler, R., Becker, C., Neurath, M. F., Reiss, K., Saftig, P., Scheller, J., and Rose-John, S. (2010) *The Journal of experimental medicine* **207**, 1617-1624
311. Kveiborg, M., Instrell, R., Rowlands, C., Howell, M., and Parker, P. J. (2011) *PloS one* **6**, e17168
312. Bucheimer, R. E., and Linden, J. (2004) *The Journal of physiology* **555**, 311-321
313. Chang, S. J., Tzeng, C. R., Lee, Y. H., and Tai, C. J. (2008) *Cellular signalling* **20**, 1248-1255

314. Freund, S., Ungerer, M., and Lohse, M. J. (1994) *Naunyn-Schmiedeberg's archives of pharmacology* **350**, 49-56
315. Lemjabbar-Alaoui, H., Sidhu, S. S., Mengistab, A., Gallup, M., and Basbaum, C. (2011) *PloS one* **6**, e17489
316. Kirui, J. K., Xie, Y., Wolff, D. W., Jiang, H., Abel, P. W., and Tu, Y. (2010) *The Journal of pharmacology and experimental therapeutics* **333**, 393-403
317. Nishizuka, Y. (1992) *Science* **258**, 607-614
318. Nishikawa, K., Toker, A., Johannes, F. J., Songyang, Z., and Cantley, L. C. (1997) *The Journal of biological chemistry* **272**, 952-960
319. Pearson, R. B., and Kemp, B. E. (1991) *Methods in enzymology* **200**, 62-81
320. Chen, Y., and Bache, R. J. (2003) *Circulation research* **93**, 691-693
321. Headrick, J. P., Peart, J. N., Reichelt, M. E., and Haseler, L. J. (2011) *Biochimica et biophysica acta* **1808**, 1413-1428
322. Williams-Pritchard, G., Knight, M., Hoe, L. S., Headrick, J. P., and Peart, J. N. (2011) *American journal of physiology. Heart and circulatory physiology* **300**, H2161-2168
323. Xie, K. Q., Zhang, L. M., Cao, Y., Zhu, J., and Feng, L. Y. (2009) *Acta pharmacologica Sinica* **30**, 889-898
324. Jackson, E. K., Mi, Z., Zhu, C., and Dubey, R. K. (2003) *The Journal of pharmacology and experimental therapeutics* **307**, 888-896
325. Kohutek, Z. A., diPierro, C. G., Redpath, G. T., and Hussaini, I. M. (2009) *The Journal of neuroscience : the official journal of the Society for Neuroscience* **29**, 4605-4615
326. Izumi, Y., Hirata, M., Hasuwa, H., Iwamoto, R., Umata, T., Miyado, K., Tamai, Y., Kurisaki, T., Sehara-Fujisawa, A., Ohno, S., and Mekada, E. (1998) *The EMBO journal* **17**, 7260-7272
327. Doedens, J. R., Mahimkar, R. M., and Black, R. A. (2003) *Biochemical and biophysical research communications* **308**, 331-338
328. Doedens, J. R., and Black, R. A. (2000) *The Journal of biological chemistry* **275**, 14598-14607
329. Black, R. A., Doedens, J. R., Mahimkar, R., Johnson, R., Guo, L., Wallace, A., Virca, D., Eisenman, J., Slack, J., Castner, B., Sunnarborg, S. W., Lee, D. C., Cowling, R., Jin, G., Charrier, K., Peschon, J. J., and Paxton, R. (2003) *Biochemical Society symposium*, 39-52
330. Paleologou, K. E., Schmid, A. W., Rospigliosi, C. C., Kim, H. Y., Lamberto, G. R., Fredenburg, R. A., Lansbury, P. T., Jr., Fernandez, C. O., Eliezer, D., Zweckstetter, M., and Lashuel, H. A. (2008) *The Journal of biological chemistry* **283**, 16895-16905
331. Corbit, K. C., Trakul, N., Eves, E. M., Diaz, B., Marshall, M., and Rosner, M. R. (2003) *The Journal of biological chemistry* **278**, 13061-13068
332. Tabor, S., and Richardson, C. C. (1985) *Proceedings of the National Academy of Sciences of the United States of America* **82**, 1074-1078
333. Amour, A., Slocombe, P. M., Webster, A., Butler, M., Knight, C. G., Smith, B. J., Stephens, P. E., Shelley, C., Hutton, M., Knauper, V., Docherty, A. J., and Murphy, G. (1998) *FEBS letters* **435**, 39-44
334. Zheng, Y., Schlondorff, J., and Blobel, C. P. (2002) *The Journal of biological chemistry* **277**, 42463-42470
335. Nishi, E., Hiraoka, Y., Yoshida, K., Okawa, K., and Kita, T. (2006) *The Journal of biological chemistry* **281**, 31164-31172
336. Kumar, V., and Sharma, A. (2009) *European journal of pharmacology* **616**, 7-15

337. Ralevic, V., and Burnstock, G. (1998) *Pharmacological reviews* **50**, 413-492
338. Cometti, B., Dubey, R. K., Imthurn, B., Jackson, E. K., and Rosselli, M. (2003) *Biology of reproduction* **69**, 868-875
339. Wilson, C. L., Gough, P. J., Chang, C. A., Chan, C. K., Frey, J. M., Liu, Y., Braun, K. R., Chin, M. T., Wight, T. N., and Raines, E. W. (2013) *Mechanisms of development* **130**, 272-289
340. Fiorentino, L., Cavallera, M., Menini, S., Marchetti, V., Mavilio, M., Fabrizi, M., Conserva, F., Casagrande, V., Menghini, R., Pontrelli, P., Arisi, I., D'Onofrio, M., Lauro, D., Khokha, R., Accili, D., Pugliese, G., Gesualdo, L., Lauro, R., and Federici, M. (2013) *EMBO molecular medicine* **5**, 441-455
341. Gil-Bea, F. J., Gerenu, G., Aisa, B., Kirazov, L. P., Schliebs, R., and Ramirez, M. J. (2012) *Neurobiology of disease* **48**, 439-446
342. Birder, L. A., Ruggieri, M., Takeda, M., van Koevinge, G., Veltkamp, S., Korstanje, C., Parsons, B., and Fry, C. H. (2012) *Neurourol Urodyn* **31**, 293-299
343. Fry, C. H., Sui, G. P., Kanai, A. J., and Wu, C. (2007) *Neurourol Urodyn* **26**, 914-919
344. Zagorodnyuk, V. P., Brookes, S. J., Spencer, N. J., and Gregory, S. (2009) *The Journal of physiology* **587**, 3523-3538
345. Birder, L. A., Barrick, S. R., Roppolo, J. R., Kanai, A. J., de Groat, W. C., Kiss, S., and Buffington, C. A. (2003) *American journal of physiology. Renal physiology* **285**, F423-429
346. Birder, L. A., Nealen, M. L., Kiss, S., de Groat, W. C., Caterina, M. J., Wang, E., Apodaca, G., and Kanai, A. J. (2002) *The Journal of neuroscience : the official journal of the Society for Neuroscience* **22**, 8063-8070
347. Hanna-Mitchell, A. T., Beckel, J. M., Barbadora, S., Kanai, A. J., de Groat, W. C., and Birder, L. A. (2007) *Life Sci* **80**, 2298-2302
348. Jackson, E. K., Ren, J., and Mi, Z. (2009) *The Journal of biological chemistry* **284**, 33097-33106
349. Shevock, P. N., Khan, S. R., and Hackett, R. L. (1993) *Urol Res* **21**, 309-312
350. Lanteri-Minet, M., Bon, K., de Pommery, J., Michiels, J. F., and Menetrey, D. (1995) *Exp Brain Res* **105**, 220-232
351. Lemieux, G. A., Blumenkron, F., Yeung, N., Zhou, P., Williams, J., Grammer, A. C., Petrovich, R., Lipsky, P. E., Moss, M. L., and Werb, Z. (2007) *The Journal of biological chemistry* **282**, 14836-14844
352. Hardy, S., Kitamura, M., Harris-Stansil, T., Dai, Y., and Phipps, M. L. (1997) *Journal of virology* **71**, 1842-1849
353. Beronja, S., Livshits, G., Williams, S., and Fuchs, E. (2010) *Nature medicine* **16**, 821-827